

SPLASHABILITY MODELS OF SOME TROPICAL SOILS



KOFI ANANE-FENIN

2002

UNIVERSITY OF CAPE COAST

SPLASHABILITY MODELS OF SOME TROPICAL SOILS

BY

Kofi Anane-Fenin

A THESIS SUBMITTED

TO THE DEPARTMENT OF PHYSICS, FACULTY OF SCIENCE,
UNIVERSITY OF CAPE COAST, IN PARTIAL FULFILLMENT OF
THE REQUIREMENTS FOR THE AWARD OF DOCTOR OF
PHILOSOPHY
(Ph.D) DEGREE IN PHYSICS

NOVEMBER 2002

ii

| | |
|---------------------------|-------------|
| CLASS NO. | |
| ACCESSION NO. 00219005 | |
| CAT. CHECKED | FINAL CHECK |

DECLARATION

I hereby declare that this thesis is the result of my own original research and that no part of it has been presented for another degree in this University or elsewhere.



.....

Date: 13th November, 2003

Kofi Anane-Fenin

(Candidate)

We hereby declare that the preparation and presentation of this thesis were supervised in accordance with the guidelines on supervision of thesis laid down by the University of Cape Coast.

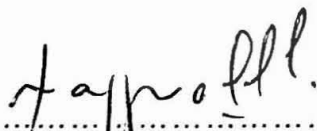


.....

Date: 13th November, 2003

Prof Mensah Bonsu

(Principal Supervisor)



.....

Date: 13th November 2003

Prof Haruna Yakubu

(Supervisor)

DEDICATION

This thesis is dedicated to my wife **Faustina**, my children, **Kwame**, **Ekua** and **Adwoa** and to my brother **Uncle Wae** and his family.



ABSTRACT

Falling raindrops are the major agents responsible for initiating soil erosion. They cause soil detachment from its original position. The collision between dry soil particles and raindrop is essentially a modeled collision between two elastic bodies. Water, of course, has a high volumetric surface tension. It is precisely this tension which forces the falling drop of water to take on a spherical shape which offers strong resistance to deformation. Water from a raindrop acts both as an energy source and wetting agent. The energy is transmitted to the aggregate or soil clod. The detached particles are transported by two mechanisms; displacement caused by physical impact and particle entrainment caused by overland flow. Rain splash has now been recognized as an important erosion agent. Rain splash erosion information from aggregated tropical soils is under-represented in literature.

The splashability of twelve different soils from the Cape Coast area was investigated. The soils are associated with a variety of vegetation types under different cultivated crops and different parent materials.

Undisturbed core samples of the soils were taken carefully using deep steel cylinders. Using artificial rainfall characteristics and soil properties as input we simulated raindrop-induced soil splash rates for these soils. Five of the soil samples used in the study were classified as sandy clay loam, four as sandy loam and the remaining three samples, as sandy clay, loamy sand and clay respectively. The total elemental analysis indicated that the major element in the soils was iron.

A linear plot was used to establish a relationship between soil splashed and rainfall intensity. The relationship was observed to be approximately linear with highly

significant correlation. Aggregate stability and organic content did not correlate with soil splashed, implying that these indices are not reliable for assessing the splashability of the soils in this area. Mechanical ratio, iron content, and kinetic energy of rainfall strongly correlated with soil splashed.

The main physical aspects of soil splash caused by raindrops were modeled. Two physically based models were proposed. The models required input parameter of soil detachment due to the action and interaction of raindrop. The models relate the splashability of soils to specific hydraulic and mechanical properties of the initially undisturbed soil as well as the physical characteristics of the rainfall applied, under given initial and boundary conditions defining the flow system.

The dynamics of the splashability of the soil at the surface are found to be related to the following variables: the rainfall intensity, maximal drop diameter, initial shear strength and water content.

The results show that the proposed models address the main factors affecting soil splashability. It also shows that incorporating intensity effect and kinetic energy of rainfall into the basic soil erosion model can represent raindrop-induced soil detachment processes.

TABLE OF CONTENTS

| | |
|---|-------------|
| TITLE PAGE..... | i |
| DECLARATION..... | iii |
| DEDICATION..... | iv |
| ABSTRACT..... | v |
| TABLE OF CONTENTS | vii |
| LIST OF TABLES..... | xii |
| LIST OF FIGURES..... | xiii |
| LIST OF SYMBOLS..... | xv |
| EXPLANATION Of ACRONYMS..... | xx |
| ACKNOWLEDGEMENT..... | xxi |
| CHAPTER ONE..... | 1 |
| 1.0 INTRODUCTION..... | 1 |
| 1.1 Concepts of Erosion..... | 2 |
| 1.1.1 Soil Detachment Mechanism..... | 3 |
| 1.2 Surface Sealing..... | 6 |
| 1.3 Factors Affecting Erosivity and Erodibility..... | 8 |
| 1.3.1 Intensity..... | 9 |
| 1.3.2 Shape and Size of Raindrops..... | 11 |
| 1.3.3 Terminal Velocity..... | 12 |
| 1.3.4 Kinetic Energy and Momentum..... | 13 |
| 1.3.5 Aggregate Stability and Structure..... | 15 |
| 1.4 Significance of Erosion..... | 17 |

| | | |
|--------------------------|---|-----------|
| 1.5 | Off-farm change of Erosion-effect on Water | |
| | Sources..... | 19 |
| 1.6 | The Purpose of the Research..... | 23 |
| 1.7 | Objective of the Study..... | 25 |
| 1.8 | Hypotheses..... | 25 |
| | | |
| CHAPTER TWO | | 26 |
| 2.0 | THE THEORY OF SOIL-WATER FLOW | 26 |
| 2.1 | The General Water Flow Equation..... | 26 |
| | 2.1.1 Thermodynamic Equilibrium..... | 27 |
| | 2.1.2 Bingham's Law..... | 29 |
| 2.2 | Particular Solution of Moisture Transport | |
| | Equation..... | 31 |
| 2.3 | Hydraulic Conductivity of Two-Phase System..... | 36 |
| | 2.3.1 Kozeny Model..... | 36 |
| 2.4 | Infiltration..... | 40 |
| | 2.4.1 Steady Infiltration..... | 41 |
| | 2.4.2 Analytical and Semi-Analytical | |
| | Procedure..... | 43 |
| | 2.4.3 Approximate Solutions..... | 48 |

| | | |
|----------------------------|---|-----------|
| 2.4.4 | Empirical Equations..... | 50 |
| | | |
| CHAPTER THREE | | 52 |
| 3.0 | MATERIAL AND METHOD | 52 |
| 3.1 | The Research Area..... | 51 |
| 3.1.1 | Adukrom Site... .. | 52 |
| 3.1.2 | Efutu-Esiam and Jukwa Road..... | 52 |
| 3.1.3 | University Farm-Akotokyir Site..... | 55 |
| 3.2 | Particle-Size Analysis and Texture..... | 55 |
| 3.3 | Aggregate Stability and Mechanical Ratio..... | 56 |
| 3.4 | Rainfall Simulation..... | 56 |
| 3.4.1 | Determination of Raindrop Size..... | 57 |
| 3.5 | Splash Erosion..... | 57 |
| 3.6 | Determination of Chemical and Mineralogical Properties | 58 |
| 3.7 | Determination of Organic Matter Content..... | 58 |
| | | |
| CHAPTER FOUR | | 60 |
| 4.0 | EROSION MODELS | 60 |
| 4.1 | Formulation of Splash Erosion Models..... | 60 |
| 4.1.1 | Splashability Coefficient..... | 60 |
| 4.1.2 | A Dynamic Splashability Model..... | 62 |

| | | |
|--------------------------|---|-----------|
| 4.2 | Modeling of Kinetic Energy of Raindrops..... | 70 |
| 4.2.1 | The Fall Velocity of Raindrop..... | 72 |
| 4.2.2 | Numerical Modeling: Runge- Kutta Method..... | 76 |
| CHAPTER FIVE..... | | 81 |
| 5.0 | RESULTS..... | 81 |
| 5.1 | Some Soil Physical Properties..... | 80 |
| 5.1.1 | Soil Texture..... | 81 |
| 5.1.2 | Aggregate Stability and Mechanical Ratio..... | 82 |
| 5.2 | Some Chemical Properties of Soil..... | .82 |
| 5.3 | Relationship between Soil Splashed and Rainfall Intensity..... | 84 |
| 5.4 | Rainfall Kinetic Energy and Intensity Relationship..... | 94 |
| 5.5 | Physical Models..... | 96 |
| 5.5.1 | Relationship between soil Splashed and some soil properties | 99 |
| 5.5.2 | Relationship between soil Splashability indices and soil Splashed and some soil properties..... | 105 |

| | |
|---|------------|
| CHAPTER SIX..... | 116 |
| 6.0 DISCUSSION..... | 116 |
| 6.1 Splashability versus soil properties..... | 116 |
| 6.2 The splashability indices..... | 118 |
| CHAPTER SEVEN..... | 123 |
| 7.0 CONCLUSIONS..... | 123 |
| CHAPTER EIGHT..... | 125 |
| 8.0 RECOMMENDATIONS AND | |
| SUGGESTIONS FOR FURTHER WORK..... | 125 |
| 8.1 Recommendations..... | 125 |
| 8.2 Suggestion for further work..... | 126 |
| REFERENCES..... | 128 |
| APPENDICES | 148 |
| APPENDIX A..... | 148 |
| APPENDIX B..... | 150 |
| APPENDIX C..... | 152 |
| APPENDIX D..... | 153 |
| APPENDIX E..... | 154 |
| APPENDIX F..... | 155 |
| APPENDIX G | 156 |

LIST OF TABLES

| | | |
|-------------|--|----|
| Table 4.0 | Hydrological soil properties classified by texture according to Rawls et al (1982) | 70 |
| Table 5.0 | Soil textural classification | 81 |
| Table 5.1 | Aggregate Stability and Mechanical ratio | 82 |
| Table 5.2 | Chemical properties of the soils | 83 |
| Table 5.3 | Values of some elements in percentages (determined by Atomic Absorption Spectrometer). | 83 |
| Table 5.4 | Intensity of rainfall and soil splashed in g/min | 84 |
| Table 5.5a | Percentage soil splashed | 86 |
| Table 5.5b | Linear regression parameters of intensity and soil splashed | 88 |
| Table 5.5c | Regression parameters of log log relation of Intensity and soil splashed | 91 |
| Table 5.6a | Rainfall intensity and number of drops hitting soil per second | 91 |
| Table 5.6b | Determination of Kinetic energy of raindrop | 92 |
| Table 5.6c | Drop-size, Kinetic energy and soil splashed | 93 |
| Table 5.6d | Drop-size, Kinetic energy and soil splashed | 94 |
| Table 5.7 | Rainfall energy and intensity relationship – Regression parameters | 95 |
| Table 5.8 | Coefficient of splashability Index (k) of soils | 96 |
| Table 5.9a | Determination of Splashability index (ξ) for $k=2.34*10^6 \text{kg m}^{-2}\text{s}^{-2}$ and $d = 0.54 \text{ mm}$ | 97 |
| Table 5.9b | Determination of Splashability index (ξ) for $k=0.96*10^6 \text{kg m}^{-2}\text{s}^{-2}$ and $d = 0.30 \text{ mm}$ | 97 |
| Table 5.10 | Splashability indices of B, k and ξ | 98 |
| Table 5.11a | Coefficient Indices | 98 |
| Table 5.11b | Summary of soil parameters | 99 |

LIST OF FIGURES

| | | |
|-----------------|--|-----|
| Figure 1.0 | Map of research area | 53 |
| Figure 1.1 | A histogram of mean monthly rainfall in Cape Coast | 54 |
| Figure 5.0(a-d) | Plot of soil splashed and rainfall intensity – sample plot | 87 |
| Figure 5.0(e-h) | Plot of soil splashed and rainfall intensity – sample plot | 89 |
| Figure 5.1(a-d) | The log-log plot of soil splashed and rainfall intensity – sample plot | 90 |
| Figure 5.2 | Plot of soil splashed versus Mechanical ratio | 100 |
| Figure 5.3a | Plot of soil splashed against percentage clay content | 101 |
| Figure 5.3b | Plot of percentage soil splashed against sand/(clay+silt) ratio | 102 |
| Figure 5.4 | Plot of soil splashed against percentage iron content | 103 |
| Figure 5.5 | Plot of soil splashed against percentage organic carbon content | 104 |
| Figure 5.6 | Plot of soil splashed against percentage calcium content | 104 |
| Figure 5.7 | Plot of soil splashed versus kinetic energy | 105 |
| Figure 5.8a | Plot of splashability index (k) against soil splashed | 106 |
| Figure 5.8b | Plot of splashability index (k) against Mechanical ratio | 107 |
| Figure 5.8c | Plot of splashability index (k) against clay content | 108 |
| Figure 5.8d | Plot of splashability index (k) against percentage iron content | 109 |
| Figure 5.8e | Plot of splashability index (k) against sand/(clay+silt) ratio | 110 |
| Figure 5.9a | Plot of splashability index (ξ) against soil splashed | 111 |
| Figure 5.9b | Plot of splashability index (ξ) against Mechanical ratio | 112 |
| Figure 5.9c | Plot of splashability index (ξ) against clay content | 113 |

| | | |
|-------------|---|-----|
| Figure 5.9d | Plot of splashability index (ξ) against percentage iron content | 114 |
| Figure 5.10 | Plot of ξ against k | 115 |



LIST OF SYMBOLS

| | |
|----------|--|
| A | Surface area |
| A_m | Specific surface |
| B | Blank titration |
| B_I | Biot criterion |
| C_D | Drag coefficient |
| D_ϕ | Diffusivity of soil moisture |
| D_T | Thermal diffusivity of soil moisture |
| d | Diameter |
| $E(d)$ | Kinetic energy |
| E_I | Kinetic energy of rainfall |
| F | Constant representing the soil-rainfall system |
| F_B | Buoyant force |
| F_D | Drag force |
| F_o | Fourier criterion |
| F_R | Resisting force |
| g | Acceleration due to gravity |
| H_n | Depth of wetting |
| h | Matrix potential head |
| h_o | Pressure head at soil surface |
| I | Intensity |
| I_c | Cumulative infiltration |
| I_h | Head gradient |

| | |
|--------------|--|
| I^* | Dimensionless cumulative infiltration |
| K_s | Saturated hydraulic conductivity |
| k | Splashability index |
| L | Distance between two points of soil |
| L_f | Thickness of soil |
| l | Distance from soil surface to the impervious layer |
| M_{eq} | Equivalent mass of raindrop |
| m | Mass of soil splashed away |
| m_o | Mass of initial soil used |
| Δm_o | Initial mass of soil decreasing with time |
| $\Delta m'$ | Mass of soil after rains |
| N | Number of particles of solvent |
| N_d | Number of raindrops |
| n | Number of particles of solute |
| P_r | Porosity |
| p | Pressure |
| q | Water flux density (Darcian flow rate) |
| q_R | Rain intensity constant |
| R_e | Reynold's number for porous media |
| r | Radius |
| r_{cc} | Coefficient of regression |
| S | Sorptivity |
| S_d | Soil splashed |

| | |
|------------------|---|
| T | Temperature |
| T(d) | Periodic occurrence |
| t | Time |
| t* | Dimensionless time for DBC |
| U | Potential energy of solvent particles |
| U' | Potential energy of solute particles |
| V | Volume |
| V _d | drop volume |
| V _{pot} | External electric potential |
| V _u | Unit volume |
| v | Velocity |
| V _i | Velocity of viscoplastic fluid in capillary systems |
| v _o | Initial velocity |
| v _p | Mean flow rate in capillary |
| v _s | Falling velocity |
| v _T | Terminal velocity |
| W | Moisture volume per unit volume of the system (moisture flux) |
| β | Constant, Coefficient of moisture |
| χ | Function depending on pressure and temperature alone |
| Φ | Thermodynamic potential |
| φ | Moisture potential |
| γ | Coefficient representing the fraction of precipitation that infiltrates |
| η | Constant |

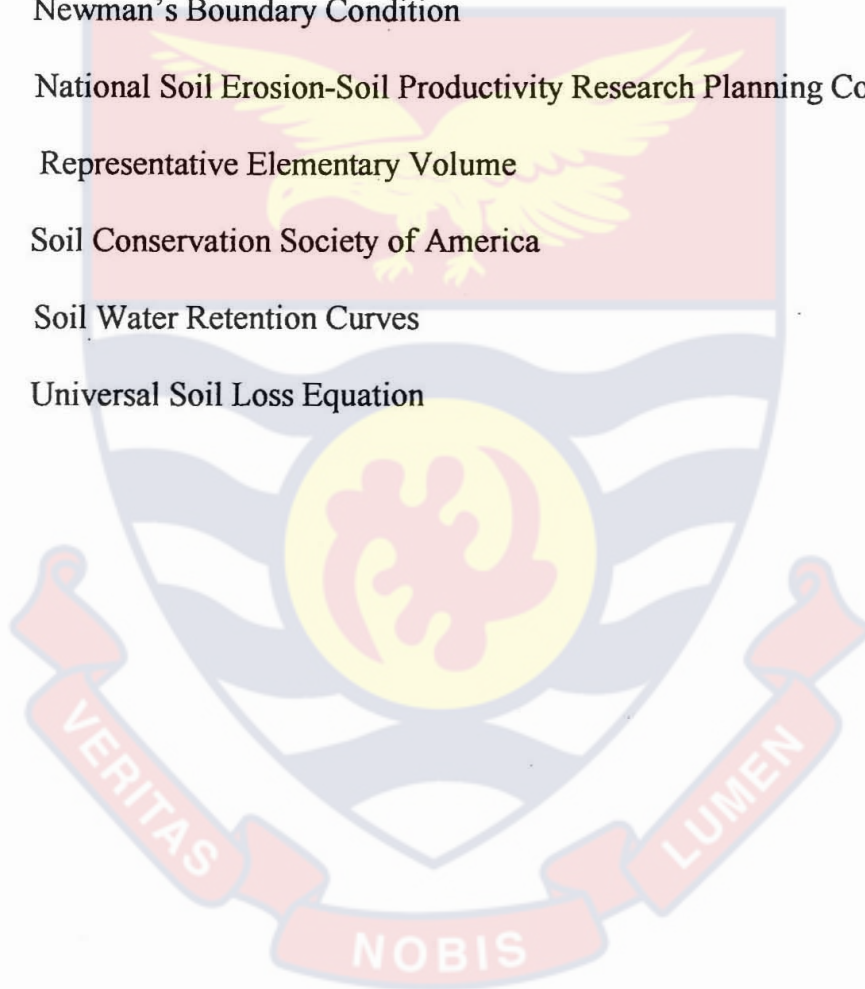
| | |
|-------------|---|
| η_v | Coefficient of viscosity |
| η_d | Dynamic viscosity |
| φ_i | Is one of the following quantities: the capillary potential (ψ), temperature (T), concentration of solutes (c), external electric potential (V_{pot}) or gravity potential(φ). |
| λ | Pore size |
| μ | Constant, chemical potential |
| μ_n | Root of characteristic equilibrium |
| μ_o | Chemical potential of pure solvent |
| θ_i | Initial water content |
| θ_o | Surface water content |
| θ_r | Residual saturation |
| θ_s | Saturated water content |
| ρ_a | Density of air |
| ρ_w | Density of liquid water |
| τ | Shear stress |
| τ^* | Tortuosity |
| τ_o | Ultimate shear stress |
| τ_{o1} | Bulk shear strength |
| ξ | Splashability index |
| ψ | Capillary potential |
| ψ_p | Bubble pressure |

ζ Aggregate stability



EXPLANATION OF ACRONYMS

| | |
|----------|---|
| AS | Aggregate Stability |
| ESP | Exchangeable Sodium Percentage |
| DBC | Dirichlet Boundary Condition |
| GDP | Gross Domestic Product |
| MR | Mechanical Ratio |
| NBC | Newman's Boundary Condition |
| NSESPRPC | National Soil Erosion-Soil Productivity Research Planning Committee |
| REV | Representative Elementary Volume |
| SCSA | Soil Conservation Society of America |
| SWRC | Soil Water Retention Curves |
| USLE | Universal Soil Loss Equation |



ACKNOWLEDGEMENT

I am most grateful to God for granting me the strength and sound mind without which this work would not have been completed.

I extend my sincere gratitude to my Supervisor Prof. Mensah Bonsu of Department of Soil Science University of Cape Coast whose guidance, patience, constructive comments and useful suggestions contributed to the successful compilation of this thesis He was a pillar of support.

My special thanks also go to the former Vice Chancellor, Prof Adjepong for instituting a grant scheme for Academic staff doing the Ph.D. I benefited tremendously from the grant. I am also grateful to Prof A. Ayensu whose invaluable advice, help in the initial planning of this work.

Experimental work can proceed at a slow pace without the assistance of able and knowledgeable technical men who possess the attribute of willingness to lend a helping hand at short notices. In this regard, I wish to mention Messieurs Kwabena Osei-Agyeman of the School of Agriculture and Benjamin Bartels of Department of Chemistry who helped in the analyses of some of the soil samples. I wish to thank my colleagues in the Department of Physics for their moral support. I also extend my sincere thanks to the Head of Department of Physics Prof Yeboah Mensah who contributed in his special and diverse ways to ease my burden so that I could complete this work.

My final vote of thanks goes beyond the immediate confines of academic circles to the family realm, where my dear wife Faustina provided the needed love and understanding during the program.

CHAPTER ONE

1.0 INTRODUCTION

Soil erosion is a surface boundary process and the stability of soil aggregates at the immediate soil surface greatly influences the susceptibility of soil to erosion. Erosion inflicts great damage to agriculture, the water bodies, road and other branches of the national economy and has a detrimental effect on the natural landscape.

Soil erosion by water is potentially a serious problem in the tropics, particularly in West Africa where severe dry weather conditions alternate with high intensity rainfall (Bruce-Okine and Lal, 1975). These adverse conditions, couple with erodible soils, which are often predominantly sandy in the surface layers, make tropical soil more susceptible to erosion (Fournier 1967, Lal 1973).

Water erosion begins with raindrops. The devastating effect of raindrops striking the bare soil was long overlooked but is now recognized as the principal means of detachment of soil particles for water erosion. Ellison (1947) divided the erosion process into detachment and transportation of particles. The detachment process initiates, however, before any water is available at the soil surface for transport. Ellison (1947a, b) also showed that the main detaching agent, falling raindrops, influences soil erosion in three ways: By breaking clods and soil aggregates into individual particles or smaller aggregates, by displacing soils from their original site and by creating turbulence in shallow overland flow. The detachment and airborne movement of small soil particles caused by the impact of raindrops on soils then constitute splash erosion (SCSA1996). The loosened and spattered particles may, or may not be subsequently removed by surface runoff. Depending on their size, cohesive strength, and impact energy, particles

are splashed into the air to various heights and deposited at some distance from their original location. Splashed particles may reach a maximum height of 700mm or more and often move horizontally 1.5 m or more on level surfaces (Ellison, 1944)

1.1 Concepts of splash erosion

The first comprehensive study of splash erosion and the mechanical action of falling raindrop on soil was carried out in 1940 [Laws (1940), Ellison (1944), Ellison (1945)]. Ellison's (1944) assumption of rainfall energy being the driving force of water erosion remained unchallenged and adopted by almost all the researchers and modelers in the field.

Research into mechanics of raindrop impact and soil splash stagnated for nearly 40 years. The main reason for this stagnation was the multitude and complexity of the processes, which take place in a very short period of time following raindrop impact and the elaborate facilities such studies required.

It was only after the application in erosion studies of high-speed photography technique which was capable of slowing down the fast processes of impact and splashed by several thousand times, that some of these complex processes began to be observed and explained.

Photographic studies of raindrop impact of the 1970's and 1980's identified three main processes, which take place concurrently or in quick succession following raindrop impact. They are impact, splash and cratering. Many researchers have since studied impact and splash processes but cratering has not received much attention in soil erosion studies. On the other hand cratering is the only aspect of water drop erosion which researchers in the aerospace and turbine industries are concerned with.

Falling raindrops are the major agents responsible for initiating soil erosion i.e. causing soil detachment from its original position. It was the classical research by Ellison (1944) that indicated the relative importance of falling raindrops vis-à-vis the overland flow in dislodging soil particles. That realization changed the emphasis on minimizing raindrop impact to curtail the source or origin of sediments rather than trying to minimize amount and velocity of overland flow.

Rain splash has now been recognized as an important erosion agent for at least two reasons. When raindrops hit the surface of a bare soil they cause material to splash up and outwards. This is of little effect on flat surfaces but on slopes some of the soil is splashed down slope. Transport of granular solids in overland flow is a fundamental aspect of hill slope erosion (Emmett 1970, Moss and Walker 1978).

A further effect of raindrop impact is that it puddles and seals the soil surface thus reducing infiltration, which leads to accumulation of water layer above the soil surface and eventually to increase run-off. The accumulation of water layer above soil surface may be an important factor influencing splash erosion. A water drop that passes through a thin layer of water is decelerated before striking the soil surface. However it may act as a solid sphere and pick up an added mass as it passes through the water layer increasing the force of impact (Richardson 1950, Palmer 1963). When the water layer is sufficiently thick, the drop may disperse before causing an observable impact on the soil surface.

1.1.1 Soil detachment mechanism

Soil splash occurs in two stages: detachment of soil and transport. The term rainfall detachment is used to describe the removal of soil from the surface by whatever actions that may occur following the impact of raindrops on the soil or on a water layer covering

the soil. Detachment then means the removal of transportable fragments of material from a soil mass by an eroding agent usually raindrops (SC SA 1982).

The process of soil erosion is initiated when the impacting raindrops detach the constituent particles of the aggregate. For aggregate to be destroyed the detaching force of the raindrops must overcome the intrinsic resisting force of the soil aggregates. Therefore, the extent to which a soil erodes, depends on the cohesive forces holding the structural unit together which enables it to resist raindrop impact forces (Meyer 1981)

From our present knowledge the most important factors affecting the raindrop detaching forces are impact velocity of the raindrop, angle of impact, raindrop diameter, shape, surface tension as well as number (or duration) of impact (Nearing and Bradford 1987, Nearing et al 1987, Barry et al., 1991 and Truman et al., 1990)

The soil resistance forces on the other hand refer to the ability of the aggregate to withstand deformation from externally applied forces. It is influenced by the antecedent water content of the aggregate at impact (Cruse and Larson, 1977), the cropping history of the soil, with intensively cultivated soils being less stable than adjacent forest soils (Beare et al., 1994), and the nature and concentration of microbially synthesized aggregate- stabilizing substance like resin and gums (Harris et al., 1966; Lynch and Bragg, 1985).

Also the amount and nature of the organic and inorganic aggregate-stabilizing materials present such as clay particles, humic substances, oxides of iron and aluminum and free CaCO_3 , and amount of silica and polyvalent cations are important (Nearing and Bradford 1985).

The mechanisms, by which these soil physicochemical and biological properties influence aggregate breakdown, have been reviewed in detail by Harris et al (1966), Hamblin and Davies (1977), Oades (1984) and Lynch and Bragg (1985). These studies showed that the dominant soil properties which influence aggregate stability can be grouped into invariant (intrinsic) and dynamic properties and that the manifestation of their effects is related to soil type, season of year and climate. The mechanism of soil detachment by raindrop is therefore complex and involves changes in energy level of the soil-water system.

The collision between dry soil particles and raindrops is essentially a collision between two elastic bodies. Water from a raindrop acts both as an energy source and as a wetting agent. The energy is transmitted to the aggregate or soil clod, but the clod may still retain its shape. The clod progressively gets wet, its soil moisture potential increases, its strength decreases and its particles are detached and spattered about by drops later impacting it. The complex wetting process occurs in three well-defined stages (Yariv 1976): dry soil, soil-water mixture or fluidized soil and soil cum overland flow.

Quick wetting of dry clod affects their detachability in two ways: through the pressure of air entrapped (i.e. pore pressure) and by releasing the heat of wetting. The entrapped air on quick wetting can virtually explode, breaking the clod and spattering soil particles into the air. Energy in the form of air pressure within the soil contributes substantially to detachment at the soil surface. Quirk and Panobokke (1962) reported significant effects of entrapped air on slaking when a dry soil is rapidly immersed in water. Badrashi et al. (1981) showed that entrapped air increased soil detachment by 21 percent.

Depending on their size, cohesive strength and impact energy, soil particles are splashed into the air to various heights and deposited at some distance from their original location. The particles of fine sand are more easily detached than those of clay soil, but the clay particles are more easily transported than sand particles. It is therefore necessary to define the nature of the erosion process when referring to how easily or much the soil is subject to erosion.

The detached particles are transported by two mechanisms: displacement caused by physical impact and particle entrainment caused by overland flow. Moss et al. (1979), Moss and Green (1983) and Moss (1988) showed that soil removed solely by rainfall detachment is transported in shallow surface flow by mechanisms, which they described as “rain flow transportation”. Young and Wiersma (1973) believed drop impact enhanced the ability of the surface flow to transport detached sediment.

1.2 Surface Sealing

During rain, soil aggregates are disintegrated mechanically by the raindrop impact and chemically due to dispersion thus causing surface sealing (Roth and Helming 1992, Le Bissonnais and Singer 1993). However a distinction should be made between a disrupted layer and a seal. A disrupted layer is formed by aggregate slaking and rearrangement of disrupted aggregate with a compacted layer of varying thickness depending on initial aggregates size, formed by the impact action of water drop (Farres 1987, Chiang et al., 1994). This mechanism is physical in nature and is controlled by the kinetic energy of the water drops and the stability of the aggregates (Moldenhauer and Kemper 1969). By contrast, seal formation depends on an additional mechanism: physico-chemical dispersion of soil clays. Dispersed clays then migrate into the soil with infiltrating water,

clog pores immediately beneath the surface and form a layer varying from 0.1 to 0.5 mm thick of very low permeability termed “washed in” zone (Gal et al., 1984, Onofio and Singer 1984, Shainberg et al., 1997). The “washed in” layer has been found to form only in easily dispersed soils (McIntyre 1958).

The physico-chemical mechanism is enhanced by aggregate breakdown and is controlled by concentration and composition of cations in the soil and the applied water (Agassi et al., 1981) and mineralogy of the soil clays (Stein et al., 1991). Aggregate breakdown and sealing have both been related to the cumulative effect of drops energy (Morin and Benyamini, 1977). However aggregate breakdown occurs much faster than seal formation (Shainberg et al., 1992). Shainberg et al. (1997) found that only 9 mm of 3.6 kJm^{-3} rain (i.e. cumulative energy of 32.4 Jm^{-2}) were needed to disintegrate the aggregates, compared with 740 mm of the same rain (cumulative energy $> 144 \text{ Jm}^{-2}$) needed for seal formation. Erosion rates therefore decrease with time during a rain event, due to densification or consolidation and loss of readily transportable sediments (Miller 1987). The importance of raindrop impact has been demonstrated by many experiments. Young and Wiersma (1973) found that when the kinetic energy of simulated rain falling on bare soil was reduced by 89 percent without reducing the intensity of the rain, soil loss was reduced by 90 percent or more in a loam, silt loam and sandy loam.

1.3 Factors affecting Erosivity and Erodibility

The fundamental cause of soil erosion is that rain acts on the soil and the study of erosion can be divided into how it will be affected by different kinds of rain, and how it will vary for different conditions of soil.

The amount of erosion therefore depends on a combination of the power of rain to cause erosion and the ability of the soil to withstand the rain. Rain erosion is therefore considered as a function of the erosivity of the rain and the erodibility of the soil (Kinnell 1973).

Soil erosion, is affected by the character of rainfall, including rain intensity, shape and velocity of raindrops, and the kinetic energy and momentum of rain. Rains in the tropics, particularly those caused by the thunderstorms, have sharp, high-intensity peaks. These intense rains are partly related to the high temperature. The high temperature inhibits the formation of raindrops from ice crystals and permit relatively large quantities of water vapour per unit volume of air. The air masses that are cooled during convection release large quantities of water through condensation. The result is intense downpours, high rate of rainfall per unit time and relatively large drop size.

Soil erodibility is an estimate of the ability of soils to resist erosion based on the physical characteristics of each soil. Generally, soils with faster infiltration rates, higher levels of organic matter and improved soil structure have a greater resistance to erosion. Sand, sandy loam and loamed textured soils tend to be less erodible than silt, very fine soils and certain clay textured soils.

Erodibility is also a measure of soil's susceptibility to detachment and transport by the agents of erosion. But susceptibility is also influenced by many soil properties and their

interaction with climate and management systems. For example soils respond differently to identical kinetic energy or shear stress exerted by moving fluid. These responses depend on their mechanical make up and chemical composition. Because of differences in their inherent properties, soils exhibit different degree of susceptibility to the forces generated by erosion agents. All factors remaining the same, differences in erosion up to 30-fold have been observed due to difference in soil properties (Olson and Wischmeier 1963). Other properties influencing soil's susceptibility to erosion are hydrologic, mineralogical, biological and biochemical as well as the soil profile characteristics. The most important soil physical properties that affect the resistance of a soil to erosion include texture, structure, water retention and transmission properties and unconfined compressive and shear strength. Bryan (1968) reviewed the importance of these properties, in relation to soil erosion. These soil characteristics are dynamic properties. They can be altered overtime and under different land uses and soil surface management systems. As a result, soil erodibility also changes overtime.

1.3.1 Intensity

There is considerable evidence of close association between erosion and rainfall intensity. Many studies have shown that rainfall intensity is more important than rainfall amount (Nichols and Saxton 1932, Tamhane et al., 1959, Meyer and Wischmeier 1969, Foster and Meyer 1975; Foster and Meyer, 1972; Foster et al., 1977 and Meyer 1981).

Soil splash for example is related to intensity. For a given amount of rainfall, high-intensity produces more splash than rain at lower intensity. High erosion rates due to short-term but intense rains have been widely reported in the tropics. (Hutchinson et al., 1958, and Wilkinson 1975). In general, tropical rains fall at higher intensity than

temperate rains. Some tropical rains can attain a 5 – to – 10 minutes intensity of 150 to 200 mm/h.

High intensity over short time intervals is known to cause severe erosion in the tropics. Intensity is important as a potential parameter of erosivity because it is the only feature of rainfall, which in addition to amount, is frequently recorded at conventional meteorological stations. Hudson (1965) proposed an index for measuring erosivity that differs in principle from the normal EI_{30} index. Hudson's index considers only the rainfall kinetic energy that occurs when the rainfall intensity exceeds 25 mm/h. This index was based on the observation that splash erosion of sand surfaces placed under natural rainfall did not occur when the rainfall rate was low. Hudson (1965) also noted that even if a little splash erosion does occur there is usually no run off to carry away the splashed particles when rainfall rate is below 25 mm/h. From his experiments Hudson (1965) concluded that 25 mm/h can be taken as the practical threshold between non-erosive and erosive rain in Zimbabwe. Morgan (1977) also suggested that the threshold should be lowered to 10 mm/h in England.

Several studies (Flanagan et al., 1988, Romkens et al., 1991 and Gimenez et al., 1992) have shown the significance of rainfall intensity and storm pattern on seal characteristics. Other studies have recognized that with increases in raindrop impact energy, the extent of surface seal formation is enhanced, resulting in reduced infiltration rates and increased surface runoff (Agassi et al., 1985, Bradford et al., 1987, Kereen 1990, Bradford and Huang 1991).

1.3.2 Shape and Size of Raindrops.

High rainfall intensity is related to relatively big drop size and the number per unit area per unit time. Raindrops include water particles as large as 7 mm in diameter. The size distribution in a particular storm covers a considerable range and this distribution varies with the rainfall intensity. Not only does the high-intensity storm have more large-diameter raindrops, but it also has a wide range of raindrop diameters. In fact the majority of rainwater comes down in drops between 1 and 4 mm diameter. The upper limit of drops in a natural rainstorm however is about 6 mm (Blanchard 1950). Large raindrops divide in the air, drops over 5 mm in diameter, being generally unstable. The velocity of fall depends on the size of the particle and that large drops fall more rapidly. As the height of fall is increased, the velocity increases, only to a height of about 11 m, the drops then approach a terminal velocity, which varies from about 5 m/s for a 1-mm drop to about 9 m/s for a 5-mm diameter drop.

Since rainstorm has a wide range of drop sizes it is often difficult to characterize the drop size of a rain event. However drop size distribution is an important factor, which affects rainfall erosivity. Attempts have been made to measure drop sizes since 1892 when Lowe reported the first recorded measurement (Hudson 1981). Studies such as Laws and Parsons (1943) also show how the drop size can be measured and hence the drop distribution. A commonly used criterion to express the drop size distribution of rainfall event is to compute its median volume drop diameter or D_{50} . Here D_{50} refers to the raindrop diameter dividing the drop of larger and smaller diameter into groups of equal volume. There is a fairly definite correlation between the intensity of rainfall and the median size (Best 1950). Lal (1987) observed that D_{50} of rainstorms measured at Ibadan

ranges from 2 to 4 mm. The median drop size is affected by many factors such as type of rain (Kowal and Kassam 1976, 1978,) amount of rain, duration of rain, rainfall intensity and wind velocity accompanying the rain.

1.3.3. Terminal velocity

A body falling freely under the force of gravity has two other forces acting on it i.e. the drag and buoyancy forces. The body accelerates until the frictional resistance of air, is equal to the gravitational force.

At equilibrium the body reaches a constant velocity called terminal velocity. The terminal velocity depends upon the size and shape of a body.

Raindrops are not necessarily spherical. Falling raindrops are deformed from spherical shape by unequal pressure as a result of air resistance developing over their surfaces. Most drops attain terminal velocity in about a 10 m fall under gravity. Under natural conditions, the terminal velocity increases with an increase in drop size. Raindrop fall velocities vary from near zero for mist-sized drops to more than 9 m/s for the largest sizes.

A common-sized raindrop of 2 mm falls at velocity of 6 to 7 m/s (Gunn and Kinzer 1949). Hinkle et al., (1987) confirmed the results of Gunn and Kinzer. Measurements of fall velocity have been reported by Wang and Pruppacher (1977) and Roel (1981).

It has been shown experimentally (Park et al., 1982) that soil detachment and splash increase exponentially with increase in impact velocity. Impact velocity is however greatly influenced by wind factor. When rain is accompanied by wind there is an added side-ways component of velocity and the resultant vector may be greater than the still-air velocity. The effect will be greater on small drops falling slowly than on large drops with

higher velocity. There is evidence that with tropical rainfall, highest rates are likely to occur in a relatively still air (Hudson 1964) and this may be connected with the wind patterns around the base of convective thunderstorms.

1.3.4 Kinetic Energy and Momentum

The most important cause of the break-up of clods is the impact of fast-falling raindrops in severe storm, for they possess considerable amount of kinetic energy and momentum. The greater the intensity of the storms, the larger the drops are likely to be and the faster they will fall, and their velocity may even exceed that for free fall because of the effect of air turbulence on the storm.

Hence the more intensive the storm the greater is the shattering effect of the raindrops and the amount of kinetic energy dissipated in this way is very considerable. Raindrops falling in storms of low intensity, e.g. less than 20 or 30 mm/hr do not usually have enough energy to shatter clods. Most of the rains in West Africa during the wet season fall in storms of high intensity. Hence liability to water erosion is conditioned by the frequency of intensive storms.

Evidence relating the kinetic energy and momentum of rain with its power to cause soil erosion is well established (Hudson 1971) and data on the kinetic energy load of rainstorms are basic in studies concerned with soil conservation (Kowal et al., 1973). The action of raindrops on soil particles is most easily understood by considering the momentum of a single raindrop falling on a slope surface. The down slope component of this momentum is transferred in full to the soil surface but only a small proportion of the component normal to the surface is transferred, the remainder being reflected. The transfer of momentum to the soil particles has two effects. First it provides a

consolidating force, compacting the soil and second, it produces a disruptive force as the water rapidly disperses from and returns to the point of impact in laterally flowing jets. The local velocities in these jets are nearly double those of the raindrop impact and are sufficient to impact a velocity of some of the soil particles launching them into the air, entrained within water droplets which are themselves formed by the break up of the raindrop on contact with the ground (Mutchler and Young 1975).

If the size and the terminal velocity of the raindrops are known, it is possible to calculate the kinetic energy and its momentum. However the forces involved are so small that any instrument sufficiently sensitive to record them mechanically is liable to be swamped by wind effects. However, present technological developments have introduced new possibilities, especially in the area of digital electronics for the direct measurement of the kinetic energy of raindrops. Because kinetic energy cannot be routinely measured, many empirical relationships have been established, relating kinetic energy and rainfall intensity (Kinnell 1981). Lal (1987) reported that peak energy load for seasonal distribution of the energy load for sub-humid region of south western Nigeria occurs in June and September, the more erosive months in the year. Studies of kinetic energy required to detach one kilogram of sediment by raindrop impact show that minimal energy is needed for particles of $125\mu\text{m}$ and that particles between 63 and $250\mu\text{m}$ are the most vulnerable to detachment (Poesen 1981, Poesen and Savat 1981). As with the kinetic energy of rains, few data exist for direct measurement of momentum, because it is capital-intensive. More accurate computation of momentum is obtained as a product of the drop mass for each size class with its corresponding velocity.

1.3.5 Aggregate stability and structure

An aggregate is a group of primary particles that cohere to each other more strongly than the other surrounding soil particles. Most adjacent particles adhere to some degree. Therefore disintegration of the soil mass into aggregates requires imposition of a disrupting force. Stability of aggregates is a function of whether the cohesive forces between particles withstand the applied disruptive force.

The importance of aggregate stability to soil physical properties and management relates largely to the voids present between aggregates. The breakdown of unstable aggregates results in pore collapse, which slows infiltration greatly, resulting in runoff and erosion from the surface (Levy and Miller 1997)

Structural stability is the resistance of soil structure to mechanical and physico-chemical destructive forces. The ability of soil to withstand these forces largely depends both on structural stability and on the water content of the soil.

The structural stability varies under natural conditions with the fine sand and silt fraction being weakest as a result of their low content of clay minerals, sesquioxides and humus. Soil rich in Kaolinite clays and iron oxide in the humid tropics may be also weak due to the association of these materials into very small aggregates, which behave like silt and fine sand. Many attempts have been made to assess the erodibility of soil from the instability of its aggregates in water as measured by dispersion.

Aggregate stability influences several aspects of soils physical behaviour. In particular, water infiltration and soil erosion depend strongly on it (Bryan 1968, De Ploey and Poesen, 1985). Emerson and Greenland (1990) in a comprehensive review of soil aggregate formation and stabilization defined two processes of aggregate breakdown;

slaking and dispersion. Other authors more concerned with field observation consider raindrop impact to be the main cause of structural degradation of the soil surface (Nearing and Bradford, 1985).

The main properties influencing aggregate stability and erosion have been well known since the early work of Yoder (1936), Henin (1938), Kemper and Kock (1966), Wischmeier and Mannering (1969). However, some subsequent studies have produced contradictory results (Le Bissonnais, 1996).

Mechanical breakdown of aggregate by raindrop impact usually occurs in combination with other mechanism if the kinetic energy of raindrop is great enough (Al - Durrah and Bradford 1982a, Boiffin, 1984, Nearing et al., 1987, Bradford and Huang, 1992). The importance of this effect is clearly demonstrated by the role of vegetation cover or mulch, which protect the soil surface against such impact.

Mechanical breakdown by raindrops impact plays a dominant role on wet soils because the aggregates are weaker when the soils are wetter. Also under “undrained” conditions the compressive stress of the raindrop impact is transformed into lateral shear that causes the fragments to detach and project (Al-Durrah and Bradford 1982b). Therefore raindrop impact not only detaches but also displaces previously detached fragments. This mechanism is the splash effect (Ellison 1945, Farres 1987).

A discrepancy between aggregate stability and splash measurement under rainfall may be expected because very stable macro aggregates can be moved by splash. However, for many soils aggregate breakdown may occur even without mechanical impact, simply by slaking or dispersion. The fragments resulting from raindrop detachment are generally small being either elementary particles or small micro aggregate ($< 100\mu\text{m}$).

The main properties known to influence aggregate stability and erosion are: soil texture, clay mineralogy, organic matter content, type and concentrations of cations, sesquioxide content and CaCO_3 content, with multiple interactions between these properties that can modify their influence. Emerson and Greenland (1990) gave a complete review of these efforts. Of these soil properties, three play a major role in aggregate stability. They are:

- i) Exchangeable Sodium percentage (ESP) (Emerson, 1967; Kazman et al 1983, Frenkel et al 1978; Shainberg et al 1992). Sodium leads to soil dispersion and reduces soil stability,
- ii) Iron and aluminum oxides and oxyhydroxides that cement aggregates, particularly for tropical and lateritic soils (Romken et al., 1977; Le Bissonnais and Singer 1993), and
- iii) Organic matter, which is a bonding agent between mineral soil particles (Monnier, 1965, Tisdall and Oades 1982; Churchman and Tate 1987; Chenu 1989; Haynes and Swift, 1990), protects the surface against raindrop impact, improves water infiltration and may impact hydrophobic characteristics that reduce wetting rate and slaking (McGhie and Posner 1980; Sullivan 1990; Jouany et al., 1992).

1.4 Significance of Erosion

It is important to distinguish among three interrelated but distinctly different phenomena: Soil erosion, Soil depletion and Soil degradation.

Soil erosion lessens soil productivity through physical loss of topsoil, reduction in rooting depth, removal of plant nutrients and loss of water.

In contrast, soil depletion means loss or decline of soil fertility due to crop removal or removal of nutrients by eluviations from water passing through the soil profile. The soil depletion process is less drastic and can be easily remedied through cultural practices and by adding appropriate soil amendments.

Soil degradation, however is an all encompassing broad term: It implies decline in soil quality through deterioration of the physical, chemical and biological properties of the soil. Accelerated soil erosion is one of the processes that lead to soil degradation. Accelerated soil erosion is a major environmental and economic issue of modern times. Translocation of sediments and sediment borne pollutants to surface waters, have serious ecological and environmental consequences. Worldwide, human- induced accelerated erosion is estimated to be about 2.6 times the natural or geologic erosion e.g. 26 billion tons per year versus 9.9 billion tons per year (Olson et al., 1994).

The loss of productivity due to erosion, though difficult to estimate in precise terms is a major economic set back to the farming community around the world. Soil erosion can reduce crop yields by reducing soil organic matter, water holding capacity and rooting depth: Other erosion-related factors affecting productivity include reduction of plant nutrients, degradation of soil structure and alteration of clay content. Before widespread use of commercial fertilizer, loss of topsoil reduced yields by 50% or more compared to yields from soils with little topsoil loss (NSES PR PC 1981). Thompson et al (1991) found that the yield reduction for corn was 39% and for soya-bean was 24% as topsoil depth was reduced by de-surfacing a Mexico silt loam. It can be inferred that bad farming encourages soil loss. Unfortunately, bad farming and forestry operations in West Africa have encouraged the worst kind of soil erosion. Erosion accelerates when sloping

land is prolonged and when grass is removed from semi-arid land to begin dry land farming. It accelerates whenever hillside forests are felled or cut indiscriminately.

For the farmer and consumer as well, the worst thing about soil erosion is that it reduces crop yields and increases the cost of growing food and fiber.

Thus the first thing erosion does is to reduce the capacity of soil to hold water and its availability to plants. This subjects crops to more frequent and severe water stress.

Secondly erosion contributes to losses of plant nutrients, which wash away with the soil particles. Because sub-soils generally contain fewer nutrients than topsoils, more fertilizer is needed to maintain crop yields. This in turn increases production costs. More over, the addition of fertilizer alone cannot compensate for all the nutrients lost when topsoil erodes.

Thirdly, erosion reduces yield by degrading soil structure, increasing soil erodibility, surface sealing and crusting. Water infiltration is reduced and seedlings have a harder time breaking through the soil crust. Fourthly, erosion reduces productivity because it does not remove topsoil uniformly over the surface of a field. Typically, part of an eroded field still has several centimeters of topsoil left. Other parts may be eroded down to the subsoil. This makes it practically impossible for a farmer to manage the field properly, to apply fertilizers and chemicals uniformly and obtain uniform results. He is also unable to time his planting, since an eroded part of the field may be too wet when the rest of the field is dry and ready for cultivation.

1.5 Off-farm change of erosion – effect on water Resources:

Damage from water erosion is not limited to the loss of productivity on the land and farm level where it occurs. When eroded soil is carried off the farm by run off, it may cause a

variety of damages. Some 60% or more of the soil settles out of the run off before it ever reaches a stream or other water body. Little is known about the fate of this portion of eroded soil and its consequences are not always negative. Some of it, for example may come to rest where the soil already in place is less fertile than the soil deposited. So the productivity of the site is enhanced by deposition. However there appears to be a consensus that the more general effect of the deposited soil is negative. For example an eroded soil from a hillside comes to rest a short distance away at the foot of the slope or lower the flood plain, where it may bury crop or lower the fertility of bottomlands.

A portion of the eroded soil is deposited in local drainage or irrigation ditches or runs into ponds, reservoirs or tributary, streams or rivers. Wherever it is deposited, it is unwelcome. Sediment-filled ditches have to be dug out again, ponds, lakes and reservoirs either have to be dredged out or abandoned there by imposing costs either for clean up or for diminished productivity of the system where deposition occurs. Locally, sediment is an expensive nuisance.

The smaller proportion of the eroded soil that reaches water bodies carried as suspended sediments can cause several different kinds of damage when it is finally deposited.

Turbidity impedes the passage of sunlight through the water, and it decreases the biological productivity of the water. The capacity of the water to support desirable varieties of fish may be reduced correspondingly.

Turbid water is generally less attractive to swimmers and boaters than clean water, so an increase in suspended sediment reduces recreational values of the water.

Turbid water also is heavier than clean water. Turbidity thus increases the cost of pumping a given volume of water from the stream to some other place of intended use.

For many users the turbidity must first be reduced, which of course imposes costs. The cost are highest when the water is for domestic use, because, for that purpose virtually all of the suspended sediment must be removed.

Turbid waters are likely to increase the wear and tear and hence, maintenance cost on the machinery and equipment through which the water is pumped from the stream to its various places of use.

Sedimentation also causes one major problem. This is the accelerated loss of reservoir capacity; whether for flood control, electricity generation, or recreation. Reservoirs are designed to handle some amount of sedimentation and when sedimentation stays within that limit it causes no unexpected problems. However, when such levels are exceeded, a reservoir's life is shortened or the costs of maintaining its design life are increased. Sedimentation of navigable rivers and harbours reduces the traffic handling capacity of these resources or increases the cost of dredging necessary to maintain their capacity. Damage may occur down stream of rivers. Carried along by a river, the sediment is precipitated as the waterway reaches flatter and lower reaches. The sediment deposits raise the level of the riverbed and reduce the capacity of the channel to hold water. Riverbanks overtop more frequently during rainy seasons and flooding may damage productive valuable bottomland. The flooding may also threaten property, human health and public safety. Finally the deposition of sediment may damage or entirely destroy fish-spawning areas, diminishing fish population as a consequence.

In West Africa, especially in the Sahel Region, pressure on the land makes rational use of the soil resource extremely important. For two decades ending 1980, food production has grossly lagged population growth. In sub-Sahara Africa the food staples grew at

1.7% a year, but population increased 3.2% a year (Paulimo 1986). Food production has to be increased substantially to avoid mass starvation in many of these regions. Although the perpetual food deficit in sub-Sahara Africa cannot be entirely attributed to erosion and erosion – induced soil degradation, there is a disturbing degree of correspondence between the areas affected by severe soil erosion and those with proven gross food deficit. The region needs to break this vicious cycle.

The main problem faced by less-developed countries then, is lack of food, which occurs during drought periods. Numerous investigations have dealt with this problem but very few solutions have been suggested. The fact is that there is no easy remedy. However, when speaking in terms of finding a long – term solution to this problem, which undoubtedly will worsen toward the middle of this century, it is essential to create the resources for producing food in the affected areas themselves instead of having recourse to palliative measures such as importing food from the countries having plentiful production. Intensification of agriculture is necessary to increase food production, although this also increases the risk of soil erosion. In the tropics the soil nutrient reserves are often concentrated in the thin surface horizon. This makes much of the exposed subsoil often unsuitable for root growth. It is because of the low productivity of the exposed subsoil coupled with harsh climate that makes erosion more severe in the tropics than in the temperate – zone

Agricultural production in Ghana is still based mainly on seasonal rain fed crops. Such production often creates soil and water conservation problems because of climate, soil and management practices interactions. The total cost of environmental degradation to the Ghanaian economy is estimated to be 4% of the Gross Domestic Product (GDP). If

the broad aim of Ghana Vision 2020 is to be achieved then research into environmental factors ought to be given impetus such that appropriate solutions could be found to minimize the risks and hazard associated with soil-water erosion.

1.6 The purpose of the research

The first scientific investigations of erosion were carried out by a German Scientist (Baver 1939). Apart from this pioneer work, the lead in erosion research has come mainly from United States. Pioneering work in prevention of splash erosion was done in the 1930's by a few individuals, such as Baver, Borst, Woodburn and Musgrave (Baver 1939). This led to the first detailed study of natural rain by Laws (1941). Ellison (1944) was the first soil scientist to analyze the mechanical action of raindrops on soil. However the main features in erosion process were identified and mathematically enumerated into the Universal Soil loss Equation (USLE) by Wischmeier and Mannering (1969). The USLE and its gradual but systematic improvement (Wischmeier and Smith 1958) is a statistical regression model based on soil loss data assembled primarily in the eastern part of humid region of the United States. The factor components represent the influence of climate, soil, topography and land management.

Due to its modest data demands and transparent model structure, the USLE remains the most popular tool for water erosion hazard assessment. However the model has several shortcomings two of which are likely to have prominent implications for the model results. First the mathematical form of the USLE, the multiplication of six factors (i.e. erosivity of the rainfall, erodibility of the soil, the length of slope, the steepness of the slope, cropping management factor and factor

for the practices to control erosion), easily leads to large errors whenever one of the inputs data is misspecified. Second, the USLE has a modest correlation between observed soil losses and model calculation, even with the same data that was used for its calculation. This raises questions about its mathematical model structure and the robustness of the assumed parameter values that are implicitly assigned to the model

In an American study, Wischmeier (1976) reported that measured plot soil losses deviated from computed plot soil losses by an average 12 percent. Van Vliet (1976) calculated potential soil erosion losses in Southern Ontario by means of the USLE. However since the equation was being applied beyond geographic and climatic region for which the equation was generated, no estimate of reliability of the predicted values was available. In the USLE erosion on slopes less than 3 percent was not recognized as significant. But research has identified the seriousness of soil erosion on flatland and the special significance of high rainfall rates for soil erosion on low slope.

Despite the voluminous literature on the global and regional problems of erosion, quantitative and reliable data on the magnitude of the problem are indeed scarce in tropical Africa. There are also few if any checks to verify the validity of available statistics on the magnitude of soil erosion. Most available information especially that from the tropics is based on reconnaissance surveys or on experiments that lack a standardized methodology. Such information base may be of some use in creating public awareness, but it is of little value in developing and implementing strategies to prevent or control erosion. Lack of information on

actual soil erosion and its relationship to cause factors in West Africa has also restricted the adaptation or modification of methods used elsewhere to estimate erosion. As a result environmental consultants and land managers are limited in their efforts to formulate reliable erosion control criteria.

1.7 Objective of the study

The main objective of this work is to find out how rainfall splashability is influenced by rainfall and soil characteristics.

The specific objectives of this research are four fold:

- i) To review the theories of soil-water flow and the mechanisms of splash erosion.
- ii) To discuss the relation between soil properties and soil-water erosion and propose a physically based model that may be used to predict splashability of some tropical soils.
- iii) To provide a clear picture of the fundamental nature and causes of splash erosion in the tropics.
- iv) To propose methodological framework for measuring splash erosion.

1.8 Hypotheses.

This study is based on the following formulated hypotheses.

- i) The extent of soil splashability depends on its nature.
- ii) The fundamental equation based on rainfall energy can be used to estimate soil splashability.
- iii) Vulnerability of soil to rainfall splash and aggregate stability are related.

CHAPTER TWO

2.0 THE THEORY OF SOIL-WATER FLOW

2.1 The general water flow equation

Erosion is a factor of the rainfall that enters the soil and the portion that runs off. Therefore infiltration comes into play in most erosion modeling. Infiltration also depends on the ability of the soil to transmit water. As fast as the water enters the soil and transmitted below the rainfall acceptance of the soil continues to increase. So once the soil has reached its steady state infiltrability, and no more rainfall can be accepted by the soil, then runoff begins and erosion starts.

In this chapter the theories of soil-water flow and infiltration are presented. In one portion of this study soil conductivity constant would be applied to estimate erosion and this constant from the water-flow equation based on the Darcy's law would not be measured but estimated from soil texture. Therefore presenting soil-moisture theory as a prelude to this study is to provide a clear insight into the physics of soil water movement.

Soil in general is a multiphase system of solid, liquid and gaseous components. In a system as complex as soil one cannot determine accurately the space occupied by water or all the forces acting on it. Fluid flow in a disperse system like soils is determined by the geometry of the space occupied by the fluid, its mechanical properties (viscosity, plastic resistance to shear) and the external forces acting on it.

The present state of the transport theory for energy and mass in disperse systems enables us to tackle the problem of forecasting the water regime of soils and develop ways and means of controlling it, including automatic control.

The theory of energy and mass transport in disperse systems developed into two directions.

- i) Determining why thermodynamic equilibrium is violated and investigating how to restore it.
- ii) Developing methods for solving the equations of energy and mass transport, in particular with the aid of digital and analog computers.

2.1.1 Thermodynamic Equilibrium

The conditions of phase equilibrium are $\mu = \text{constant}$ and $T = \text{constant}$

Where μ is the chemical potential, and T is the temperature. The thermodynamic equilibrium of a body in an external field (i.e. Temperature, gravitational and capillary potentials) is possible only when the temperature and chemical potential are equal at every point of the body. In soils these conditions are usually not observed, since continuous transport of heat, aqueous solution and gas takes place, due to the changing boundary conditions. This process usually implies the absence of thermodynamic equilibrium in the soil along the vertical axis. Here we consider solutions to moisture transport problems in soils in a temperature field, a gravitational field and capillary potentials. When thermodynamic equilibrium is upset, the intensity of the energy and mass flux directed at restoring equilibrium depends on the degree to which equilibrium

has been upset. A second factor determining the flux intensity is the property of the system.

The thermodynamic potential of a dilute solution in the presence of external fields (e.g. gravity and electric fields) is.

$$\Phi = N \mu_o (P, T) + n k T \ln \frac{n}{N} + n \chi (P, T) + N U (x, y, z) + n U' (x, y, z) \quad (2.1)$$

where N and n are, respectively, the numbers of particles of the solvent and solute, μ_o is the chemical potential of the pure solvent; $\chi (P, T)$ is a function depending on the pressure and temperature alone; $U (x, y, z)$ and $U' (x, y, z)$ are the potential energies, respectively of the solvent and solute particle in the external fields.

The chemical potential of the solvent in a solution is:

$$\mu = \frac{\partial \Phi}{\partial N} = \mu_o (P, T) - k T \frac{n}{N} + U (x, y, z) \quad (2.2)$$

and the chemical potential of the solute is:

$$\mu' = \frac{\partial \Phi}{\partial n} = k T \ln \frac{n}{N} + \chi (P, T) + U' (x, y, z) \quad (2.3)$$

From the above it follows that the intensity of the mass or energy flux depends on the gradient of such parameters as temperature, pressure, concentration of solutes and potential of the external fields.

The rate of flux for given gradients of the above parameters is affected by the following characteristics of disperse system.

- a) The geometry of the space occupied by phases within the system. This geometry usually depends on the ratio of the phase volumes, the specific surface and inter

phase surfaces, and the distribution of the phase space and over their characteristic dimensions.

- b) The distribution of solutes, electric charges and enthalpy along the normal to the inter phase surfaces.
- c) The liquid viscosity, shear strength, and plastic resistance to shear, which is independent of the flow-velocity derivative along its normal.
- d) The diffusion coefficient of the dissolved particles, the gas molecules and the self-diffusion of the solvent molecules.
- e) The thermal and electric phase characteristics.

2.1.2 Bingham's Law

When liquids percolate in soils, there is usually no turbulent momentum transfer across the flow. As a result the shear stresses are completely absorbed by the resistance which is generally determined not by Newton's fluid friction law, but by Bingham's law.

$$\tau = \tau_o + \eta_v \frac{dv}{dy} \quad (2.4)$$

τ_o is the ultimate shear stress of the viscosity, $\frac{dv}{dy}$ is the velocity derivative along its normal and η_v is the coefficient of viscosity.

In this case the following general expression for flow velocity v_i follows from the theory of viscoplastic fluid flow in capillary systems.

$$v_i = -k_i \text{ grad } \phi_i \quad (2.5)$$

Where ϕ_i can represent the capillary potential, the temperature, the concentration of solutes, the external electric potential or the gravity potential and k_i is a constant.

Consider the case, when the liquid motion determines the flow, and the shear stresses τ in it satisfy.

$$\tau_{o2} \gg \tau \gg \tau_{o1}, \quad (2.6)$$

where τ_{o1} is the bulk shear strength, appearing in the motion as plastic resistances which are independent of the velocity derivative along its normal.

τ_{o2} is the analogous parameter for the boundary layers surrounding solid particles.

One may here assume approximately that the shear stresses are incorporated in the viscous resistance, such that

$$\tau = \tau_o + \eta_v \frac{dv}{dy} \approx \eta_v \frac{dv}{dy} \quad (2.7)$$

Under these conditions k_i is independent of grad φ_i , and the total flow is given by

$$v = - \sum k_i \text{grad } \varphi_i \quad (2.8)$$

Substituting equation (2.8) in the continuity equation

$$\frac{\partial W}{\partial t} = - \text{div } v \quad (2.9)$$

$$\partial W / \partial t = \text{div} (\sum k_i \text{grad } \varphi_i) \quad (2.10)$$

For the one – dimensional case this takes the form.

$$\partial W / \partial t = \partial / \partial x (k_\Phi \partial \Phi / \partial x) + \partial / \partial x (k_V \partial V_{\text{pot}} / \partial x) + \partial / \partial x (k_T \partial T / \partial x) + \partial / \partial x (k_c \partial c / \partial x) \quad (2.11)$$

where Φ is the moisture potential (the sum of capillary and gravitational potentials),

V_{pot} the external electric potential, T the temperature and c the concentration of solutes.

If condition (2.6) is replaced by $\tau \ll \tau_{o2}$, and the orders of τ_{o1} and τ are close to each other, equation (2.8) no longer holds. In this case, Nerpin (1970) suggests replacing the equation $v = -\sum k_i (\varphi_i \text{ grad } \varphi_i)$ by

$$v = -\sum k_i (\varphi_i, \text{ grad } \varphi_i) \text{ grad } \varphi_i \quad (2.12)$$

For example, when varying moisture potential, Φ (the sum of the capillary and gravitational potentials) induces a one-dimensional horizontal flow, equation (2.11) has the form.

$$\frac{\partial W}{\partial t} = k \frac{\partial^2 \Phi}{\partial x^2} + \frac{\partial k}{\partial \Phi} \left(\frac{\partial \Phi}{\partial x} \right)^2 + \frac{\partial k}{\partial (\partial \Phi / \partial x)} \frac{\partial^2 \Phi}{\partial x^2} \frac{\partial \Phi}{\partial x} \quad (2.13)$$

Where W is the flux or the moisture volume per unit volume of the system, t is the time; x is the coordinate along which the moisture flux is considered.

Equations (2.11) and (2.13) are boundary – value problems. Rubin (1967) has shown that equations of this type are only valid for nearly steady – state processes.

2.2 Particular solutions of Moisture Transport Equations.

The problem can be considered under conditions of no external electric field, and constant solute concentrations along the flow. Flows due to a temperature gradient are not considered, but the effect of a temperature variation along the flow on the capillary potential, and consequently on the potential Φ too, is taken into account.

Under these assumptions equation (2.13) becomes

$$\begin{aligned} \frac{\partial W(x,t)}{\partial t} &= \frac{\partial}{\partial x} \left[k_\Phi(W) \frac{\partial \Phi(W,T)}{\partial x} \right] = \frac{\partial}{\partial x} \left[k_\Phi(W) \left(\frac{\partial \Phi}{\partial W} \frac{\partial W}{\partial x} + \frac{\partial \Phi}{\partial T} \frac{\partial T}{\partial x} \right) \right] \\ &= \frac{\partial}{\partial x} \left(D_\Phi \frac{\partial W}{\partial x} + D_T \frac{\partial T}{\partial x} \right) \end{aligned} \quad (2.14)$$

where $D_{\Phi} = k_{\Phi} \frac{\partial \Phi}{\partial W}$ is the diffusivity of soil moisture.

and $D_T = k_{\Phi} \frac{\partial \Phi}{\partial T}$ is the thermal diffusivity of soil moisture

The boundary – value problem is considerably simpler if the soil is assumed vertically homogeneous, and that within a small time interval (from several days to month, depending on the soil type) D_{Φ} and D_T are constant both in time and over the soil depth (linearization of the initial boundary – value problem).

A further simplification is achieved by determining experimentally (from meteorological data) the temperature as a function of a linear coordinate and the time (Nerpin, 1970).

Under these conditions (2.14) reduces to

$$\frac{\partial W}{\partial t} = D_{\Phi} \frac{\partial^2 W}{\partial x^2} + D_T \frac{\partial^2 T}{\partial x^2} \quad (2.15)$$

Now the Boundary conditions:

The initial condition: the moisture is distributed over some soil depth at time

$$t = 0, \quad W(x, 0) = f_H(x) \quad (2.16)$$

The first boundary condition: the moisture content of the lower soil boundary ($x = 0$), which coincides with the upper boundary of the ground-water zone; is maximum W_{\max} .

In this case

$$W(0, t) = W_{\max} = \text{Const} \quad (2.17)$$

and

$$W_{\max} = \text{Const} \text{ (which coincides with the upper boundary of ground-water zone)} \quad (2.18)$$

The second boundary condition: All the moisture arriving at the soil-air boundary evaporates. This condition has the form,

$$D_{\phi} = \frac{\partial W(l,t)}{\partial x} - D_T \frac{\partial T(l,t)}{\partial x} = \beta [W(l,t) - W_{eq}] \quad (2.19)$$

where β is the coefficient of moisture exchange l is the distance from ground-water level to the soil surface and W_{eq} is the soil moisture content in equilibrium. The simplified boundary – value problem described by equations (2.13) – (2.19), has a particular solution only when

$$W_{max} = W_{eq} - \frac{D_T}{\beta} \frac{\partial T(l,t)}{\partial x} \quad (2.20)$$

Equation (2.20) hardly ever holds, and therefore artificial methods must be sought to solve the problem. One of these consists in replacing the condition of constant maximum moisture content of the lower soil surface by the condition that at the initial moment a lower soil layer of some thickness has moisture content equal to the maximum and overlies an impervious layer.

The first boundary condition should reflect the fact that water cannot penetrate through the impervious bounding surface and equation (2.17) therefore becomes

$$\frac{\partial W(0,t)}{\partial x} = 0 \quad (2.21)$$

The variable $W(x,t)$ is now replaced by a new one, $\varpi(x,t)$ where

$$\varpi(x,t) = W(x,t) - W_{eq} + \frac{D_T}{\beta} \frac{\partial T(l,t)}{\partial x} \quad (2.22)$$

and $\varpi(x,t)$ is known for all x and t .

Using expression (2.22) and the above assumptions, the transformed boundary-value problem is

$$\frac{\partial \varpi(x,t)}{\partial t} = D_{\Phi} \frac{\partial^2 \varpi(x,t)}{\partial x^2} + f(x,t) \quad (2.23)$$

$$\varpi(x,0) = f_H(x) - W_{eq} + \frac{D_T}{\beta} \frac{\partial T(l,0)}{\partial x} = f_o(x) \quad (2.24)$$

$$\frac{\partial \varpi(o,t)}{\partial x} = 0 \quad (2.25)$$

$$-D_{\Phi} \frac{\partial \varpi(l,T)}{\partial x} = \beta \varpi(l,t) \quad (2.26)$$

where $f(x,t) = D_{\Phi} \frac{\partial^2 T(x,t)}{\partial x^2} + D_T \frac{\partial^2 T(l,t)}{\partial t \partial x}$ and l is also the distance from the soil surface to the impervious layer. The solution of the boundary-value problem (23) – (26) in dimensionless form, after transforming to the former variable $W(x, t)$ is

$$W(x,t) = \sum_{n=1}^{\infty} A_n \exp(-\mu_n F_o) \cos \mu_n \frac{x}{l} + W_{eq} - \frac{D_T}{\beta} \frac{\partial T(x,T)}{\partial x} \quad (2.27)$$

where μ_n is the root of the characteristic equation $ctg \mu_n = \frac{1}{B_i} \mu_n$, $F_o = \frac{D_{\Phi} t}{l^2}$ is the

Fourier criterion and $B_i = \frac{l}{\beta D_{\Phi}}$ is the Biot criterion.

The coefficients A_n are given by

$$A_n = \frac{\mu_n}{\mu_n + \sin \mu_n \cos \mu_n} \frac{2}{l} \left[\int_0^l f_o(x) \cos \mu_n \frac{x}{l} dx + \int_0^l \int_0^l f(x,t) \cos \mu_n \frac{x}{l} \exp(\mu_n F_o) dx dt \right] \quad (2.28)$$

Oduro–Afriyie (1977) studied temperature distribution with soil depth over these regions in Ghana. The results showed that the temperature gradients are small, thermal moisture conductivity may be neglected without introducing a large error, and moisture transport

may be considered as isothermal. In this case, iteration of the function $\varpi(x, 0)$ in the form

$$A_n = \frac{2}{\mu_n + \sin \mu_n \cos \mu_n} \left[\sum_{k=0}^m \left(\varpi'_k - \varpi_k \sin \frac{\mu_n}{l} x_k \right) + \frac{l}{\mu_n} \sum_{k=0}^m (\delta_k + \delta_{k-1}) \cos \frac{\mu_n}{l} x_k \right] \quad (2.29)$$

may be used; where

$$\delta_k = \frac{\varpi'_k - \varpi_k}{x_k - x_{k-1}} \quad (2.30)$$

The annual moisture – content is calculated over individual successive time interval (weeks, ten day etc); within which all the coefficient are assumed constant. The precipitation dates within the indicated small time interval are equally probable. Therefore, all the precipitation is taken as occurring at the end of the interval. It is absorbed (the absorption time is assumed negligibly small) and fills up the air pores in the upper, permeable layer, imparting to the soil a moisture content W_{\max} . The depth of wetting H_p is given by

$$H_p = \frac{\gamma l'}{P_r - W} \quad (2.31)$$

where l' is the surface equivalent of the precipitation column; γ is a coefficient representing the fraction of precipitation which infiltrates; P_r is the soil porosity; W is the upper soil layer moisture content before infiltration.

The moisture – content distribution with soil depth is found at the end of the first interval, allowing for constant moisture content (W_{\max}) in the arbitrary soil layer (which replaces the effect of the ground – water zone) and precipitation penetration to a depth H . This is taken as the value of the function $\varpi_1(x, 0)$, for the second interval, and so on. It is clear that the resulting moisture – content variation is to a certain extent averaged.

A computer program based on the above algorithm can be prepared for annual moisture – content march over depth varies levels (for example; from 2.5m to the soil surface) of say loamy soils can be calculated from known meteorological data in a region.

2.3 Hydraulic Conductivity of a Two-Phase System

The moisture flux per unit area of any cross section is given according to Darcy's law by

$$q = K_s I_h \quad (2.32)$$

where I_h is the head gradient and K_s is independent of the gradient for a Newtonian fluid and is called the saturated hydraulic conductivity.

The hydraulic conductivity is determined by the fluid viscosity and pore space geometry i.e. by the dimension and shape of the pores and pore size distribution.

Sometimes the term q is also called the Darcian flow rate. The mean water flow rate (velocity) in the soil pores is

$$v_p = q / P_r \quad (2.33)$$

where P_r is the porosity of the soil.

2.3.1 Kozeny Model

The model consists of a bundle of paralleled capillary tubes of uniform radius (Scheidegger1957).

It is assumed that the soil and the model have identical porosity P_r , specific surface A_m and water flux density q .

The mean flow rate v_p in a capillary of radius r is described by Hagen – Poiseuille's

$$\text{equation } v_p = \frac{\rho_w g r^2}{8\eta_d} I_h \quad (2.34)$$

Where g is the acceleration due to gravity, ρ_w the density of water and η_d the dynamic viscosity. When n is the number of capillaries of unit length x , the porosity of the model is.

$$P_r = \frac{n\pi r^2 x}{V_u} \quad (2.35)$$

where V_u is the unit volume and the specific surface is

$$A_m = \frac{2n\pi r x}{V_u} \quad (2.36)$$

From (2.35) and (2.36)

$$r = \frac{2P_r}{A_m} \quad (2.37)$$

From (2.33), (2.34) and (2.37) the water flux density is

$$q = \frac{\frac{1}{2} \rho_w g P_r^3 I_h}{\eta_d A_m^2} \quad (2.38)$$

Because soil pores are irregularly shaped and mutually interconnected, a shape factor c replaces $\frac{1}{2}$ in (38)

$$q = \frac{c \rho_w g P_r^3 I_h}{\eta_d A_m^2} \quad (2.39)$$

Then

$$q = \frac{K_p \rho_w g}{\eta_d} I_h \quad (2.40)$$

$$K_p = \frac{c P_r^3}{A_m^2} \quad (2.41)$$

Equation (2.40) is identical to (2.32) because the term K_p that relates to the flow of any fluid through a soil, is called the permeability. But flow channels in actual soil are tortuous compared with the capillary model. We introduce a tortuosity factor τ^* in (41) which yields the Kozeny equation.

$$K_p = \frac{c P_r^3}{\tau^* A_m^2} \quad (2.42)$$

The tortuosity τ^* , is the ratio between the real flow path length L_e and the straight distance L between the two points of the soil. Because $L_e > L$, $\tau^* > 1$. In a mono dispersed sand manifesting a value of $\tau^* = 2$, the flow path forms approximately a sinusoidal curve (Corey 1977).

Many authors have derived equations identical or of similar type to (2.42). If a model of parallel plates is used instead of capillary tubes the slits are oriented in the direction of the laminar flow, we obtain the mean flow rate as.

$$v_p = \frac{\rho_w g d^2}{3\eta_d} I_h, \text{ and } q = \frac{\rho_w g d^2 P_r}{3\eta_d} I_h \quad (2.43)$$

where $2d$ is the distance between the plates. When B is the width of the plate

$$P_r = \frac{2n d B x}{V_u} \text{ and } A_m = \frac{2n x (2d + B)}{V_u}. \text{ Taking } x = 1 \text{ and } B = 1 \text{ we obtain}$$

$$d = \frac{P_r}{A_m - 2P_r} \text{ and hence equation (2.43) becomes } q = \frac{\rho_w g}{3\eta_d} \left[\frac{P_r}{(A_m - 2P_r)} \right]^2 P_r I_h$$

$$q = \frac{\rho_w g P_r^3}{3\eta_d (A_m - 2P_r)^2} I_h = \frac{c \rho_w g P_r^3}{\tau^* \eta_d (A_m - 2P_r)^2} I_h \quad (2.44a)$$

$$q = \frac{K_p \rho_w g}{\eta_d} I_h \quad (2.44b)$$

where

$$K_p = \frac{c P_r^3}{\tau^* (A_m - 2P_r)^2} \quad (2.44c)$$

Scheidegger (1957) gave detail derivation of Kozeny – Carman equation to be

$$K_p = \frac{P_r^3}{5 A_m^2 (1 - P_r)^2} \quad (2.45)$$

From (32) and (40) the relationship between K and any formulation of K_p is

$$K_s = \frac{K_p \rho_w g}{\eta_d} \quad (2.46)$$

Equation (32) is restricted to only small rates or lamina flow, which generally occurs with flow of water in soil, when the inertia terms of the Navier-Stokes equation are

negligible. The critical value of the Reynolds number below which Darcy's law applicable is about 5. For engineering purposes the upper limit of the validity of Darcy's Equation is indicated by the critical value of Reynold's number for porous media

$$Re = \frac{q d \rho}{\eta_d} \quad (2.47)$$

Where d denotes length: In sands d is the effective pore diameter. Sometimes d is related to the permeability of the sand e.g., $d = K_p^{1/2}$.

However in all soils other than sands, d is not at all definable and hence (2.47) is not applicable. The difficulty in defining d is manifested by controversy in the literature

regarding the assignment of critical value of R_e . Most frequently, critical values of R_e have been reported to range from 1 to 100.

Saturated hydraulic conductivity, K_s is one of the principal soil characteristics and for its determination, only direct measurement is appropriate. Indirect methods, derived from soil textural characteristics, which are sometimes combined with aggregate analyses generally, do not lead to reliable values.

Measuring K_s is realized either in the laboratory on soil core samples previously taken from the field, or directly in the field without removing a soil sample.

Field methods are preferred. They provide data that better represent the reality of water flow in natural conditions. Their main disadvantage is the lack of rigorous quantitative procedures for measuring soil attributes in the majority of field tests.

For laboratory measurements the size of the REV (the representative elementary volume) should be theoretically estimated in order that an appropriate soil core sampler be selected. In order to obtain equation (2.32) inertial effects were neglected and the density and viscosity of water were assumed invariant (Bear 1972). Scheidegger (1957) showed that K_s should be considered a scalar quantity for isotropic soils and a tensor of K_s dependent upon the direction of flow. When the tensor K_s is assumed to be symmetric, its principal axes defined by six values are identical to those of an ellipsoid of conductivity. If the gradient of the potential is not in the direction of a principal axis, the direction of flow is different from that of the gradient.

2.4 Infiltration

The term infiltration denotes the entry of water into the soil through its surface.

The soil surface could be plane, concave or convex. The source of water can complete or partially cover the entire surface.

Equations describing infiltration are usually one-dimensional water flow in either the vertical or horizontal direction. A limited number of solutions exist for two- and three-dimensional infiltration processes. Hydrologically, the infiltration process separates rain into two parts. One part stored within the soil supplies water to the roots of vegetation and recharges ground water. The other part, which does not penetrate the soil surface, is responsible for surface run off. Although steady infiltration is simpler to solve and understand because only the Darcy-Buckingham equation is involved, unsteady infiltration is the dominant process in nature.

For the unsteady state we have two types of infiltration. When the soil surface is instantaneously and excessively ponded as it is in an infiltration test performed with a ring infiltrometer, we have Dirichlets Boundary Condition (DBC). When infiltration occurs under natural rainfall we meet Newman's Boundary Condition (NBC) for the full duration of the rain or for at least its initial occurrence.

2.4.1 Steady infiltration.

Steady infiltration is characterized by the condition that the flux density does not change with time nor with position in the unsaturated soil, i.e. $\partial q / \partial t = 0$ and $\partial q / \partial z = 0$ where q is water flux density and θ is water content. It follows from the equation of continuity for one – dimension that

$$\frac{\partial \theta}{\partial t} = - \frac{\partial q}{\partial z} \quad (2.48)$$

and that the soil water content does not change in time

(i.e. $\frac{\partial \theta}{\partial t} = 0$ as well as $\frac{\partial h}{\partial t} = 0$), where h is the matrix potential head. In order to satisfy

the condition $\frac{\partial h}{\partial t} = 0$, we define a non-variant hydraulic condition at the bottom of the

soil column. The simplest practical provision is a constant ground water level at its bottom. Such conditions are simply demonstrated by the following process.

A rain intensity q_R is constant in time ($\partial q_R / \partial t = 0$) and equals the infiltration rate as well as the flux density in the soil q provided that $q_R < K_s$. In this case, rainfall has been constant and infiltration has lasted long enough to allow the wetting front to reach the ground water level. We further assume that the ground water level is kept at a constant elevation by e.g. a drainage system. It is mathematically convenient to identify the origin of the z coordinate at the ground water level from which z increases positively upwards. As a result at $z = 0$, $h = 0$ and at the soil surface $z = Z$, $h = h_z$ and $q = -q_R$. Some solutions derived for steady state conditions approximate non-steady infiltration after a long time has elapsed when $\frac{\partial q}{\partial t} \rightarrow 0$.

For a solution of infiltration problem we first search for $h(z, t)$ and from it we obtain

$\theta(z, t)$ from Soil water retention curves (SWRC). Some solutions provide $\theta(z, t)$ directly.

Integration of the soil moisture profile at time t defines the cumulative infiltration at that time.

$$I_c = \int_{\theta_i}^{\theta_s} z d\theta \quad (2.49)$$

Solutions to the infiltration problems can be divided into three classes – (i) analytical and semi-analytical (ii) approximate solutions and (iii) empirical equations.

2.4.2 Analytical and Semi – Analytical Procedures.

Richard's equation in its diffusivity form for the vertical coordinate oriented positively downward from the soil surface where $z = 0$ is

$$\frac{\partial \theta}{\partial t} = \frac{\partial}{\partial z} \left[D(\theta) \frac{\partial \theta}{\partial z} \right] - \frac{dK}{d\theta} \frac{\partial \theta}{\partial z} \quad (2.50)$$

This equation sometimes denoted as the non-linear Fokker – Planck equation (Philip, 1969), is non-linear owing to the strong dependence of D and K upon θ . The first term on the right-hand-side of (2.50) describes the transport of water owing to the initial degree of unsaturation of the soil profile. Therefore as the initial water content, θ_i increases, the importance of this term decreases. The Second term on the right hand-side of (2.50) originates because of the gravitational potential. Hence, it is called the gravitational term and describes the flow of water owing to the force of gravity.

Philip's (1957) solution of (2.50) is based upon the idea of separating the infiltration into its two components – those caused by the matric potential force and those caused by the gravitational potential force. He obtained a solution for horizontal infiltration in the form $x(\theta, t)$. Here, the dependent variable was changed to that of the horizontal axis x .

Next, he assumed that the real $z(\theta, t)$ for vertical infiltration was the horizontal component $x(\theta, t)$ plus a correction term. The correction due to the gravitational force is time dependent. Here, we first look at horizontal infiltration. Our horizontal soil column, initially at an unsaturated water content θ_i has its end at $x = 0$ maintained at water saturation θ_s . Hence for

$$t = 0 \quad x > 0 \quad \theta = \theta_i \quad (2.51)$$

$$t \geq 0 \quad x = 0 \quad \theta = \theta_s \quad (2.52)$$

We solve (2.50) without the gravitational term.

$$\frac{\partial \theta}{\partial t} = \frac{\partial}{\partial x} \left[D(\theta) \frac{\partial \theta}{\partial x} \right] \quad (2.53)$$

When D is a constant (homogeneous soil) the solution according to Carslaw and Joeger (1959) is:

$$\frac{\theta - \theta_i}{\theta_s - \theta_i} = \text{erfc} \frac{x}{2\sqrt{Dt}} \quad (2.54)$$

where erfc is the error function. When D is a function of θ , we transform (2.53) into an ordinary differential equation using the Boltzmann transformation. The transformed equation has a new variable η instead of the two original variables x and t . The new variable η defined by the Boltzmann transformation

$$\eta(\theta) = xt^{-\frac{1}{2}} \quad (2.55)$$

leads to

$$\frac{\partial \eta}{\partial t} = -\frac{1}{2} xt^{-\frac{3}{2}} = \frac{\eta}{2t} \quad (2.56)$$

$$\frac{\partial \theta}{\partial t} = \frac{d\theta}{d\eta} \frac{\partial \eta}{\partial t} = -\frac{\eta}{2} \frac{d\theta}{d\eta} \quad (2.57)$$

$$\frac{\partial \eta}{\partial x} = t^{-\frac{1}{2}} \quad (2.58)$$

and

$$\begin{aligned} \frac{\partial}{\partial x} \left[D(\theta) \frac{\partial \theta}{\partial x} \right] &= \frac{\partial}{\partial \eta} \left[D(\theta) \frac{d\theta}{d\eta} \frac{\partial \eta}{\partial x} \right] \frac{\partial \eta}{\partial x} \\ &= \frac{\partial}{\partial \eta} \left[D(\theta) \frac{d\theta}{d\eta} t^{-\frac{1}{2}} \right] t^{-\frac{1}{2}} \end{aligned} \quad (2.59)$$

from the above (2.53) transforms to

$$-\frac{\eta}{2} \frac{d\theta}{d\eta} = \frac{\partial}{\partial \eta} \left[D(\theta) \frac{d\theta}{d\eta} \right] \quad (2.60)$$

The transformed initial and boundary conditions are

$$\eta = \infty \quad \theta = \theta_i \quad (2.61)$$

$$\text{and } \eta = 0 \quad \theta = \theta_s \quad (2.62)$$

The solution for which we search is simply $\theta(\eta)$. Measured soil water profiles

$\theta[x(t_1)]$, $\theta[x(t_1)]$, $\theta[x(t_2)]$, $\theta[x(t_3)]$ etc are thus transformed into the unique $\theta(\eta)$ relationship by merely dividing x by $t^{1/2}$ for first profile, $t^{1/2}$, for the second profile etc. for $t = 1$, $x \equiv \eta$. Hence, the physical reality of $\theta(\eta)$ is the soil water profile $\theta(x)$ when the infiltration time is unity.

Philip (1960) and Kutilek (1984) have shown for which analytical expression of $D(\theta)$ analytical solution of (60) subject to (61) and (62) exist.

Because it is exceptional that any of those analytical expressions accurately describe $D(\theta)$ of a real soil, an iterative procedure proposed by Philip (1955) is commonly used to calculate $\theta(\eta)$ from measured distributions of D versus θ .

With the content of infiltrated water being denoted as cumulative infiltration I_c ,

$$I_c = \int_{\theta_i}^{\theta_s} x \, d\theta \quad (2.63)$$

From (55)

$$I_c = \int_{\theta_i}^{\theta_s} \eta(\theta) t^{1/2} \, d\theta \quad (2.64)$$

Inasmuch as $\eta(\theta)$ is unique for each soil, Philip (1957)

Introduced the term sorptivity [$LT^{-1/2}$].

$$S = \int_{\theta_i}^{\theta_s} \eta(\theta) d\theta \quad (2.65)$$

and

$$I_c = St^{1/2} \quad (2.66)$$

Because the infiltration rate

$$q_0 = \frac{dI_c}{dt} \quad (2.67)$$

we have

$$q_0 = \frac{1}{2} St^{-1/2} \quad (2.68)$$

Here we note that sorptivity is physically the cumulative amount of water infiltrated at $t = 1$ and at that time, the infiltration rate has diminished to one-half the value of S .

Sorptivity depends not only upon the $D(\theta)$ function but upon θ_i . The value of S decreases with increasing θ_i and as $\theta_i \rightarrow \theta_s$, $S \rightarrow 0$.

Sorptivity is an integral part of most investigations describing vertical infiltration. As a first approximation of the solution of (2.50) subject to (2.51) and (2.52). Philip used (2.55), the solution of (2.53) for horizontal infiltration, i.e. $z_1(\theta, t)$. He corrected this approximation with the term y , i.e. $z = z_1 + y$. However, because an exact value of y cannot be obtained, its approximation y_1 defines another correction u , i.e. $y = y_1 + u$. Again, instead of an exact u we can only find still another estimate of u , etc. Hence, Philip obtained the infinite series solution.

$$z(\theta, t) = \eta_1(\theta)t^{1/2} + \eta_2(\theta)t + \eta_3(\theta)t^{3/2} + \dots + \eta_n(\theta)t^{n/2} \quad (2.69)$$

where the function $\eta_1, \eta_2, \eta_3, \dots, \eta_n$ are defined with $D(\theta)$, $K(\theta)$ and η_{n-1} . The procedure for computing terms η_n is described in detail by Kirkham and Powers (1972).

But (2.49) is cumulative infiltration.

$$I_c = \int_{\theta_i}^{\theta_s} z d\theta \tag{2.70}$$

Philip formulated the following equation analogous to the horizontal infiltration.

$$I_c = St^{1/2} + (A_2 + K_i)t + A_3t^{3/2} + \dots + A_n t^{n/2} \tag{2.71}$$

where

$$A_n = \int_{\theta_i}^{\theta_s} \eta_n(\theta) d\theta \quad n = 2, 3, \dots \text{and } K_i = K(\theta_i)$$

The series (2.69) converges for short and intermediate time of infiltration and the infiltration rate $q_o(t)$ obtained by differentiation is

$$q_o = \frac{1}{2}st^{-1/2} + (A_2 + K_i) + \frac{3}{2}A_3t^{1/2} + \dots + \frac{n}{2}A_n t^{n/2-1} \tag{2.72}$$

for large times (2.71) does not converge.

Inasmuch as the shape of the wetting front remains invariant at large times, the wetting front moves downward at a rate.

$$V = \left(\frac{K_s - K_i}{\theta_s - \theta_i} \right) \tag{2.73}$$

While the infiltration rate for $t \rightarrow \infty$ is

$$q_o = K_s \tag{2.74}$$

Equations (2.73) and (2.74) commonly called the infinite time solutions are theoretically traveling wave solutions (Philip 1969).

The times for which (2.71) and (2.72) continue to converge was found to range broadly from 0.67h for sand to 250h for light clay (Harverkamp et al; 1988). Similarly, the times

for which the infinite time solution is applicable varies widely from approximately 100 min for a silt loam (Nielsen et al., 1961) to about 10⁸min for light clay (Kunze and Nielsen, 1982).

In order to obtain an intermediate time solution Swartzendruber (1987) adjusted Philip's time series solution of q to apply between $t \rightarrow 0$ and $t \rightarrow \infty$.

Swartzendruber intuitively proposed the equation.

$$I_c = \frac{S}{A_o} \left[1 - \exp(-A_o t^{1/2} - B_o t - C_o t^{3/2} - \dots) \right] + K_s t \quad (2.75)$$

where A_o, B_o, C_o, \dots are constants depending upon the soil hydraulic functions as well as θ_i and θ_s .

The time derivative of (2.75) gives the infiltration rate

$$q_o = \frac{S}{A_o} \left[1 - \exp(-A_o t^{1/2} - B_o t - C_o t^{3/2} - \dots) \right] \left[\frac{A_o}{2} t^{-1/2} + B_o + \frac{3}{2} C_o t^{1/2} + \dots \right] + K_s \quad (2.76)$$

2.4.3 Approximate Solutions

Green and Ampt (1911) used a physical approximation to simplify a real soil water profile infiltration to a step function profile.

In their model, water penetrates into the soil like a piston, and proceeds with time to greater depths. Below the abrupt horizontal wetting front, the soil remains dry at its initial value of $\theta = \theta_i$. In the saturated upper part of the soil, flow is simply described by Darcy's equation.

If at time t the position of the wetting front is $z = L_f$ (the thickness of the soil saturated with water is also L_f). The infiltration rate is

$$q_o(t) = -K_s \left[\frac{h_f - (h_o - L_f(t))}{L_f(t) - 0} \right] = K_s \left[\frac{h_o + L_f(t) - h_f}{L_f(t)} \right] \quad (2.77)$$

where h_o is the pressure head at the soil surface (i.e. the depth of water on the surface), h_f is the soil water pressure head at the wetting front owing to the unsaturated condition of the soil below z with $h_f < 0$. L_f is time dependent.

If there were no soil below $z = L_f$ and water was freely falling out of the saturated soil column ($h = 0$, at $z = L_f$), the water flux throughout the column of thickness L_f would be:

$$q_o = q = K_s \frac{h_o + L_f(t)}{L_f} \quad (2.78)$$

Because there is dry soil below $z = L_f$ its unsaturated condition causes the flux to increase. Green and Ampt added the term h_f to the driving force to account for the extra force acting at the wetting front.

Theoretically, the procedure is based upon the expected shape and similarity of the expected shape and similarity of the $\theta(z, t)$ profiles. Philip (1957, 1973) showed that the following Green and Ampt approximation is an exact solution only if $D(\theta)$ is expressed as a Dirac δ - function.

Considering (2.77) we know $q_o = \frac{dI_c}{dt}$ and $I = L_f \Delta\theta$ where $\Delta\theta = \theta_s - \theta_i$ and hence.

$$q_o = \frac{dL_f}{dt} \Delta\theta \quad (2.79)$$

when gravity is neglected, (2.77) becomes

$$\Delta\theta \frac{dL_f}{dt} = K_s \left[\frac{L_f(t) + (h_o - h_f)}{L_f(t)} \right] \quad (2.80)$$

After separating variables and integrating between the limits $(0, t)$ and $(0, L_f)$,

was simply compared with that of an analytic function. Inasmuch as both equations and experiments were empirical, it is useless to try to physically interpret the coefficients of the equations. The coefficients have the character of fitting parameters only with no scientific merit (Haverkamp et al., 1988 and Kutilek et al., 1988). On the other hand, because of their popularity in the literature and their usage persisting, we briefly present them here.

Kostiakov's (1932) equation of $q_o(t)$ is the hyperbola

$$q_o = C_1 t^\alpha \quad (2.84)$$

with

$$I_c = \frac{C_1}{1-\alpha} t^{(1-\alpha)} \quad (2.85)$$

where C_1 and α are empirical Coefficients. The equation does not describe infiltration at large times inasmuch as $q_o \rightarrow 0$ when $t \rightarrow \infty$.

Mezencev (1948) overcame this inconvenience by shifting the q_o axis.

$$q_o = C_2 + C_3 t^{-\beta} \quad (2.86)$$

$$\text{with } I_c = C_2 t + \frac{1}{1-\beta} C_3 t^{(1-\beta)} \quad (2.87)$$

where C_2 , C_3 and β are empirical coefficients.

Horton's equation (1940) represents an exponential decay of $q_o(t)$.

$$q_o = C_4 + C_5 \exp(-\gamma' t) \quad (2.88)$$

$$\text{with } I_c = C_4 t + \frac{C_5}{\gamma'} [1 - \exp(-\gamma' t)] \quad (2.89)$$

where C_4 , C_5 and γ' are empirical coefficients.

CHAPTER THREE

3.0 MATERIALS AND METHOD

3.1 The Research Area.

Soil samples used in this study were collected from four different areas in the Cape Coast district (Figure 3.0). The soils are associated with a variety of vegetative types, under different cultivated crops and different parent materials. Cape Coast enjoys a bimodal rainfall pattern with an average annual rainfall of 1192mm (Figure 3.1). Mean maximum annual temperature varies from 28° C to 33° C and the minimum temperature from 20° C to 23° C. The hottest months are February, March and April and the coldest months are August and September.

3.1.1 Adukrom site (AK)

The soils from Adukrom form part of the Adawso-Bawjiase/ Nta-Ofin compound association. The Adawso-Bawjiase simple upland association developed directly on the underlying biotite granite. The Nta-Ofin lowland association is derived from the erosion deposition of Adawso and Bawjiase soils. The samples were taken from Adawso series. The Adawso series consists of gray-brown loamy horizons, which overlie pale yellow-brown subsoil consisting of sandy clay and containing abundant quartz gravel. The soils are found on middle and lower slopes. The Adawso series is classified as Haplic lixisol in the FAO legend of soil classification.

3.1.2 Efutu-Esiam (TT) and Jukwa Road (W and T)

The soils here are part of the Nyanao-Opimo compound association. They are confined to erosion remnants of inselberges. They are yellowish red to yellowish brown, well-drained, gravel-free clay loams and clays developed from deep colluvium on foot slopes

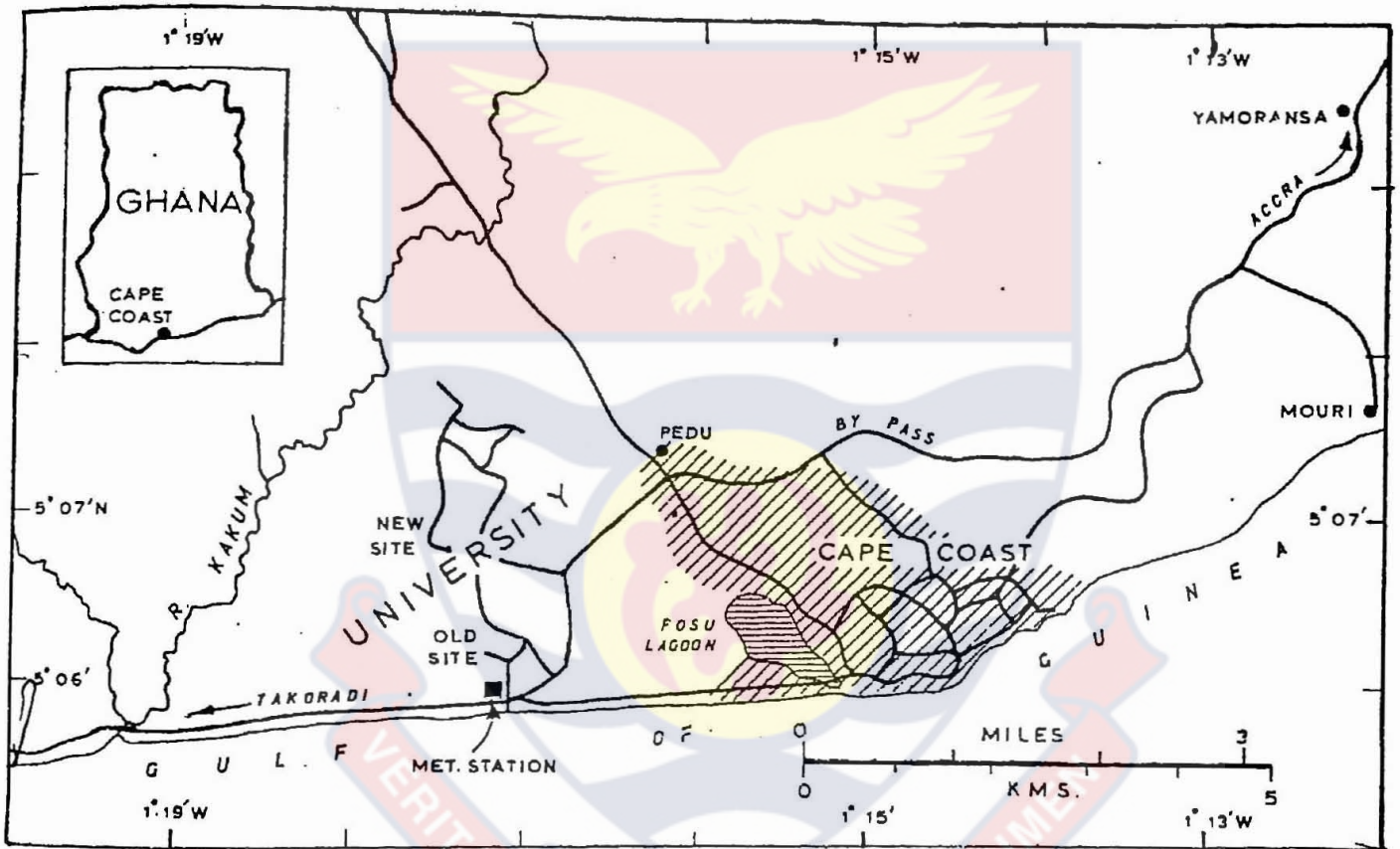


Figure 3.0: Map of Research Area

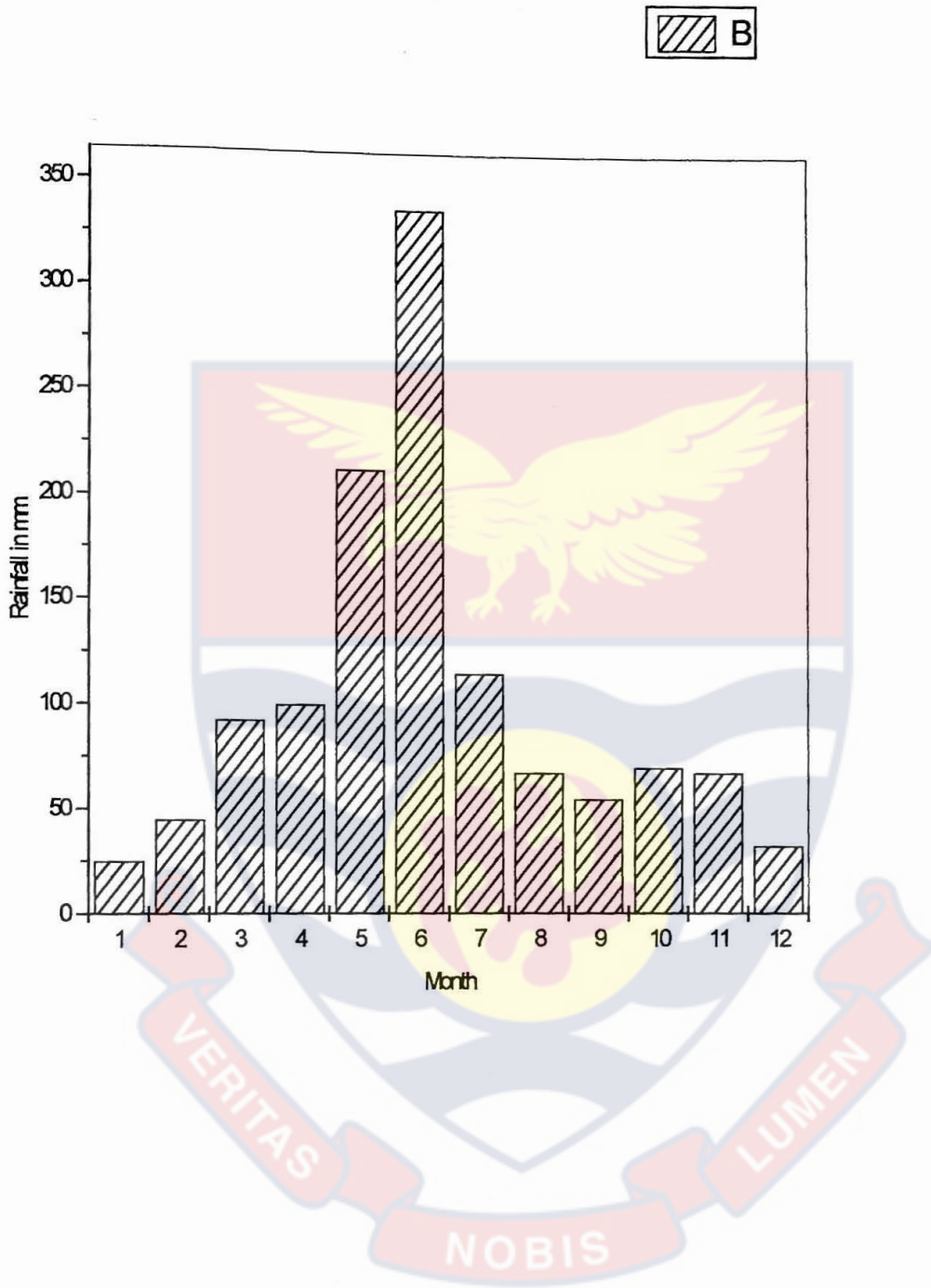


Figure 3.1: A histogram of mean monthly rainfall in Cape Coast.

sites. The surface material (0-8 cm) of Opimo is classified as Rhodic Lixisol and is dark brown, humus and loamy sand. The samples were taken from Nyanao series. The series are developed over various types of granitic rocks in which humus horizon directly overlies solid rock, rock brash or little-weathered bedrock. They are classified as Dystric Leptisol.

3.1.3. University Farm- Akotokyir Site (PO, PA, CA, VE and G).

The soils form part of Edina-Bronyibima Benya-Udu compound association. The association consists of three types of soils. We have the yellowish red to red, well to moderately well drained gravelly and concretionary clay developed over Sekondian deposits on summit to upper slope sites (Edina series). The second type is yellow to yellow brown, well to moderately well drained gravel and concretion free clay loams and clays developed from colluvium on middle to lower slope sites (Benya series). The third type is greyish to grey poorly to very poorly drained clays developed from alluvium on flat valley bottoms (Uda series).

Five sites were identified here for sampling. The sites are all in the University Farm. They are the main farm area where potatoes were grown (PO), Pasture where cattle are kept (PA), the vegetables growing plot (VE), the root and tuber growing plot where cassava was grown (CA) and the agro-forest plot where samples were taken from four sections of the hill from top to the foot of the hill (G1, G2, G3, and G4). The soils are classified as Haplic Acrisols in the FAO legend.

3.2. Particle-size Analysis and Texture.

Soil samples collected from all the twelve sites were analyzed, using the hydrometer method to find the percentage composition of sand, clay and silt in them. The soils were

then classified according to texture, using the soil – texture triangle classification chart. This type of classification is based on the grain-size distribution of soil (Kohnke, 1968). The results obtained for textural classification are given in Table 5.0

3.3 Aggregate Stability and Mechanical Ratio.

The aggregate stability of the soil was determined using the wet-sieving method. The air-dried samples were sieved through 2 mm and 0.6 mm meshes. The aggregates that remained on the 0.6 mm sieve were saved for the determination. Ten grams of each sample were poured on a mesh of 0.02 mm and wet sieved in bath water. The sieve was oscillated horizontally and rhythmically for 10 minutes to simulate the action of flowing water. The aggregates that remained on the 0.02 mm mesh were oven dried for 24 hours. The percentage aggregate stability (ζ) and the mechanical ratio (clay ratio), which relates texture to soil's susceptibility to erosion, were calculated as follows:

$$\% \zeta = \frac{\text{Oven-dried weight of aggregates after wet-sieving on 0.02mm mesh}}{\text{Oven-dried weight of 10 g sub sample}} * 100$$

$$\text{Mechanical Ratio} = \frac{\text{Sand\%} + \text{Silt\%}}{\text{Clay\%}}$$

3.4 Rainfall Simulation

The major methods used to produce simulated raindrop for erosion and hydrologic research can be grouped into two broad categories; those involving nozzles from which water is forced at a significant velocity by pressure and those where drops fall from a tip starting at essentially zero velocity (Bubenzer 1980, Mutchler and Hermsmeier 1965).

We chose the former method because nozzles produce a wide range of drop sizes, as do natural rainstorms. Three types of nozzles were used in this study. The ring spray nozzle, the oscillating spray nozzle, and the simple multi-spray nozzle.

To measure the intensities of the artificial rains, eight catch-cans (with average diameter, 85.4 mm and height of 135.0 mm) were put round a wooden box of 2 * 0.5 * 0.15 m. Water from each nozzle was allowed to fall from a height of 1.93 m under different pressures, for different durations.

The water collected in the catch-cans was measured with a measuring cylinder. The total volume of water was divided by the surface area of the can and the duration of rainfall to find the rainfall intensities in mm / h.

3.4.1 Determination of Raindrop Size

The flour pellet technique first employed by Bentley (1904) was used in this study. The method involved calibrating plain flour by dropping water drops of known mass from capillary tubes and hypodermic needles into trays containing about 25 mm- thick layer of uncompacted flour. The flour pellets formed were oven dried at 105° C for 24 hours before sieving. The calibration curve involves a plot of pellet size against the mass ratio, i.e. the mass of water drop divided by the mass of the pellet. From the graph the diameter of water drop formed by the spray nozzles were determined.

3.5 Splash Erosion.

Undisturbed core samples of soils used in this work were taken using 50 cm diameter by 50 cm deep steel cylinders. The cylinders were worked into the soil by hammering and the core samples taken carefully without disturbing the soil. The soil cores were placed in half-open cans. The soils were subjected to artificial rains after the intensities of the rains

have been determined. The Splashability experiment was repeated for each core sample at different intensities. The steel cylinders with the soil core were weighed before the experiment and then weighed again after subjecting them rain splashing and oven-drying at 105°C for 24 hrs. The correction for the water content was made.

3.6 Determination of Chemical and Mineralogical properties.

Five grams weight of soil sample was put into a 100 ml extraction bottle and 20 ml of ammonium acetate solution were added to each bottle stirred and allowed to stand overnight.

The suspensions were filtered into 100 ml volumetric flasks. The samples were leached with ammonium acetate to the 100 ml mark. An Atomic Absorption Spectrometer was used to analyse the samples.

3.7 Determination of Organic Matter Content.

Carbon is the chief element of soil organic matter that is readily measured quantitatively. Hence, estimates of organic matter frequently are based on the analysis of carbon in the soil. The method used in this study is that of Walkley and Black (1934). In this method the carbon content of the soil is determined by wet combustion.

The soil samples were sieved through a 0.5 mm sieve after which 0.5g of each of the samples were put in 500 ml conical flasks. Ten milliliters each of normal potassium dichromate ($K_2Cr_2O_7$) solution were pipetted into each flask, followed by 20 ml of concentrated sulphuric acid (H_2SO_4). The flasks were swirled vigorously for a minute and allowed to stand on asbestos sheets for about 30 minutes. Two hundred milliliters of distilled water were added, followed by one milliliter of diphenylamine indicator. The soil solutions were titrated with Ferrous Ammonia sulphate solution until the colour

changed from blue to green. A blank titration prepared in an identical way using the same reagents was done but omitting the soils. The percentage of carbon was calculated using the following formula.

$$\% \text{ Organic Carbon} = \frac{(B - S) * \text{Normality of Fe}^{++} * 0.003 * 100 * 100}{W * 77}$$

where

B = Blank titration

S = Sample titration

W = Weight of soil sample

0.003 = $12/4000$ = milliequivalent wt of carbon (gms).

$100/77$ = the factor of converting the carbon actually oxidized to total carbon and 100 is the factor to change from decimal fraction to percent.

$$\% \text{ Organic Matter} = \% \text{ organic carbon} * 100/58$$

It is assumed that soil organic matter contains 58% of carbon hence the use of the factor 100/58 to obtain the % Organic Matter.

CHAPTER FOUR

4.0 EROSION MODELS

4.1 Formulation of splash erosion Models

The capacity of rainfall to transport soil by splash is a function of a number of parameters, including slope steepness, amount of rain, soil properties, micro-topography and wind velocity (Meyer and Wischmeier 1969)

Though soil erosion is usually associated primarily with surface runoff, other studies have shown that under certain topographical conditions, soil detachment is influenced more by raindrop impact than by overland flow. Rose (1960) observed that soil loss increases ten times when water is applied as a spray in comparison with the same application rate as surface flow.

Therefore although surface runoff is usually considered the major soil-moving agent, raindrop erosion also plays an important role in not only detaching the soil particles but also causing soil movement even before the onset of runoff (Quansah 1981).

4.1.1 Splashability Coefficient

Up till now there is as yet no distinct physical scheme to the theory of raindrop erosion process. To this end one needs only to turn to studies in allied fields on the impact of drops on solid and liquid surfaces. It should however be noted that simulation of drop impact on soil involves additional difficulties because of the porous structure of soils.

It is a well-known fact that there is a relationship between the duration of erosion and the amount of soil mass left after erosion. The phenomenon behaves in the manner of a first order reaction, indicating that the rate of erosion is proportional to the amount of soil left.

Thus

$$\frac{dm}{dt} = k(m_0 - m) \quad (4.1)$$

where

dm/dt = the rate of erosion

m_0 = mass of initial soil used

m = mass of soil splashed away

t = time interval in minute

k = the Erosion Coefficient.

By separating the variables in equation 4.1 we get

$$\int \frac{dm}{m_0 - m} = \int k dt \quad (4.2)$$

Integrating both sides of equation 4.2 we obtain

$$-\log_e(m_0 - m) = kt + C \quad (4.3)$$

where C is a constant of integration. When $t=0$ and $m=0$,

$$-\log_e m_0 = C \quad (4.4)$$

By replacing C in eq 4.3 we obtain

$$-\log_e(m_0 - m) = kt - \log_e m_0 \quad (4.5)$$

Rearranging equation 4.5

$$kt = \log_e \frac{m_0}{m_0 - m} \quad (4.6)$$

$$k = \frac{1}{t} \log_e \frac{m_o}{m_o - m} \quad (4.7)$$

$$k = \frac{2.303}{t} \log_{10} \frac{m_o}{m_o - m} \quad (4.8)$$

By substituting the experimental values of t , m_o and m in eq (4.8), the erosion coefficient k , can be obtained. In this study k is referred to as splashability coefficient

4.1.2 A dynamic Splashability Model

Two processes occur simultaneously during the impact of a raindrop at a bare soil surface:

- i) A transfer of kinetic energy from the raindrop to the soil surface.
- ii) Soil imbibition

The transfer of energy, results in mechanical changes of the soil surface expressed in terms of soil compaction, particle detachment and soil splash.

Soil imbibition causes three changes to occur in the soil.

- a) it facilitates particle detachment, the amplitude of which is closely related to the physical and chemical conditions of the soil-water system
- b) it enhances the collapse of unsaturated soil aggregates, facilitated by the sudden compression of entrapped air within the aggregates.
- c) It decreases the soil resistance to destruction under subsequent striking raindrops.

Soil splashability is not dominated by rainfall alone. Some soil physico-chemical properties also affect splashability. The common aspect of these effects is the cohesive bonding between the soil particles. This bonding is related to the

mechanical, chemical and hydraulic conditions of the soil system and is also an expression of the soil susceptibility to destruction.

Now the process we are describing, depend upon the specific sizes and velocities of the impacting raindrops and the specific size and stabilities of the impacted soil aggregates. Therefore it might be relevant here to consider the results of some studies, which investigated the effect of raindrop on detachment of soil particle and aggregate destruction.

Many writers including Gradini and Payne (1977) found that aggregate destruction was related to the ratio between raindrop kinetic energy E , and its cross-section area. Reizebos and Epema(1985) found that the soil mass in the splashes resulting from raindrop impact on the soil surface was correlated to E , E/d , E/d^2 and the drop momentum. Nearing and Bradford (1987) also pointed Correlation with E/d^2 . Gilley and Finkner(1985) evaluated on a statistical basis the suitability of different rainfall characteristics to describe soil destruction. The tested factors were E , $E/\pi d$, $E\pi d$, $E\pi d^2/4$ and $E/(\pi d^2/4)$. The highest correlation was obtained for $E\pi d$.

In the following a conceptual model of the interaction between raindrops and the soil surface is formulated, leading to the prediction of the dynamic soil splashability.

Consider a bare soil of area A and an initial mass of m_i exposed to continuous rainfall intensity I . As a result of the raindrop impact splashing occurs and the mass of the initial soil decrease with time by an amount Δm_o up to a minimum $\Delta m'$ until the rains stop, depending on the soil conditions.

Let us assume that the relationship between Δm_o and t is described by

$$\frac{d\Delta m_o}{dt} = \beta - \xi \Delta m_o \quad (4.9)$$

where β represents the initial rate of change of Δm_o at the beginning of rainfall ($t=0$) and ξ is a constant related to the destruction of the soil under consideration.

$$\frac{d\Delta m_o}{dt} + \xi \Delta m_o - \beta = 0 \quad (4.10)$$

Equation (4.10) is a linear first order differential equation and has the integrating factor $e^{\xi t}$. The solution to (4.10) is

$$\Delta m_o = \frac{\beta}{\xi} + C_1 e^{-\xi t} \quad (4.11)$$

The initial condition $\Delta m(0) = 0$ at $t=0$

$$0 = \frac{\beta}{\xi} + C_1 \quad (4.12)$$

then

$$\Delta m_o = \frac{\beta}{\xi} (1 - e^{-\xi t}) \quad (4.13)$$

The specific solution of (4.11) for the initial and boundary conditions

$$\begin{aligned} \Delta m_o(t) &= 0, & t &= 0 \\ \Delta m_o(t) &= \Delta m' & t &= \infty \end{aligned} \quad (4.14)$$

$$\Delta m_o = \Delta m' (1 - e^{-\xi}) \quad \text{and} \quad \xi = \frac{\beta}{\Delta m'} \quad (4.15)$$

The rainfall of intensity I applied to a surface area, A , consists of raindrops with diameter d_i where $i=0, \dots, d_n$ and d_n is the maximum drop diameter. Every drop hits the soil surface with a velocity practically identical to the terminal velocity of the falling drop, $v_i(d_i)$. Therefore the kinetic energy, $E_i(d_i)$ of the raindrop as it reaches the soil surface is (assuming the raindrop to be spherical)

$$E_i(d_i) = \frac{\pi \rho_w d_i^3 v_i^2(d_i)}{12} \quad \text{and} \quad E(d) = \sum_{i=0}^n E_i(d_i) \quad (4.16)$$

where ρ_w is the density of water. In the case of laminar flow and according to Stoke's law, $v(d)$ is proportional to d .

When turbulent flow conditions occur $v(d)$ is related to $d^{0.5}$ (Beard, 1976) and Georgakakos and Bras (1984) assumed that $v(d)$ is proportional to d . Atlas and Ulbrich (1977) found $V(d)$ related to $d^{0.67}$. We therefore assume that

$$v(d) = R d^\alpha \quad (4.17)$$

Where R and α are constants representing the medium and the flow regime of the falling drops. Thus eq (4.16) becomes

$$E(d) = \pi \rho_w R^2 d^{2\alpha} d^3 / 12 \quad (4.18)$$

or

$$E(d) = k d^{(3+2\alpha)} \quad (4.19)$$

Where $k = \pi \rho_w R^2 / 12$

Consider now that the raindrop of diameter d , cross-sectional area $a(d)$ and kinetic energy $E(d)$ falls on an equivalent soil surface characterized by an initial mass m_i and water content θ_i . These two soil parameters joined with the specific physical-chemical characteristics of the soil-water system under consideration will determine the shear strength per unit area of the soil at the point of contact. The shear strength is proportional to the aggregate stability, ζ which is much easier to determine in the laboratory than the shear strength. As a matter of simplification we use the aggregate stability.

Let us represent the result of the collision of a drop of diameter d at a soil surface of cross-sectional area $a(d)$ by δm_o (the local change of soil mass) and as a result causing a local change of the mass. We assume that δm_o is proportional to $(\pi d E)$, and inversely proportional to $a(d)$ and ζ referring to the results of Gilley and Finkner(1985) and Nearing and Bradford(1985).

That is:

$$\delta m_o = \frac{F \pi d E(d)}{a(d) \zeta} \quad (4.20a)$$

The average change in the mass of soil of the total area A , due to the contribution of $\delta m_o(d)$ is $\Delta m_o(d)$. Thus

$$\Delta m_o(d) = \delta m_o(d) \left[\frac{a(d)}{A} \right] = \frac{F \pi d E(d)}{A a(d) \zeta} \quad (4.20b)$$

where F is a constant, representing the soil-rainfall system.

The proposed model requires

- i) the hydraulic and the physical properties of the undisturbed soil exposed to rainfall.
- ii) The initial and boundary conditions over the soil profile
- iii) The rainfall characteristics.

The undisturbed soil is defined by m_i , θ_i and ζ .

The frequency of occurrence of the raindrop with the diameter d causing Δm_o is given by the raindrop size density distribution function characterizing the rainfall $f(d, I)$. Therefore one can define the period, $T(d)$ of occurrence of a drop of a given diameter d , by the ratio between the drop volume and the part of the total rainfall volume per unit of time falling on the surface area A that is composed by drops of similar diameter.

The period of occurrence $T(d)$ is represented by

$$T(d) = \frac{\pi \left(\frac{d^3}{6} \right)}{AIf(d, I)} \quad (4.21)$$

Assume the initial rate of change of Δm_o with time for every raindrop size to be

$\frac{\Delta m_o(d)}{T(d)}$. It is possible to evaluate the initial rate of change of Δm_o with time for

the specific rainfall applied. This can be done by averaging the specific initial rates of every raindrop size over the whole range of drop diameters.

Hence the initial rate of change of Δm_o (ie β) is given by

$$\beta = d_{\max}^{-1} \int_0^{d_{\max}} \frac{\Delta m_o(d)}{T(d)} \delta d \quad (4.22)$$

Substituting equations (4.19), (4.20), and (4.21) into (4.22) we have

$$\beta = d_{\max}^{-1} \int_0^{d_{\max}} \frac{F \pi d k d^{(3+2\alpha)}}{a(d) \zeta \pi \left(\frac{d^3}{6} \right) / A I f(d, I)} \delta d \quad (4.23)$$

and

$$\xi = \frac{\beta}{\Delta m'} = \frac{6 F k I}{d_{\max} \Delta m' \zeta} \int_0^{d_{\max}} d^{(2\alpha+1)} f(d, I) \delta d \quad (4.24)$$

The value of the constant α in eq (4.24) is determined by fitting equation (4.17) to the measured velocities of drops in natural and simulated rainfall. (Gunn and Kinzer (1949), Meyer and Harmon (1979) found α to be smaller than 1 and close to 0.5, which is the theoretical value for turbulent conditions. We propose a value of 0.5 for α . As a result one can identify the integral I equation (4.24) as the second moment of the drop size density distribution which represents the variance of the drops composing the rainfall.

Thus equation (4.24) is the second moment of the drop density distribution, which represents the variance of the drops composing the rainfall. The parameter ξ can then be calculated as

$$\xi = \frac{2FkId^3}{d_{\max} \Delta m' \zeta} \quad (4.25)$$

At this point the only remaining unknown in the expression of ξ in equation (4.25) is F .

F is a constant representing soil-rainfall system. This can be determined by fitting computed infiltration rates to measured values. For the case of unsaturated flow, computed infiltration rates require the solution of the flow equation for the appropriate soil hydraulic properties and initial and boundary conditions. Bonsu (1992) concluded that in modelling hydrological processes such as infiltration in coarse-textured soils, the use of texture-based equation could be useful. Saturated hydraulic conductivity, K_s is an important hydraulic property frequently used in hydrological modelling and water flow related studies in soil such as infiltration modelling. Rawls et al (1982) estimated the values of K_s by using the following texture-based equation.

$$K_s = \frac{\frac{\alpha \phi^2}{\psi^2}}{\left[\frac{\lambda^2}{(\lambda+1)(\lambda+2)} \right]} \quad (4.26)$$

where, α is a parameter, ϕ is the total porosity minus the residual water content θ_r , ψ is the bubbling pressure (cm) and λ is the pore size distribution index. K_s is in cm s^{-1} . The parameter α is taken to be 86 when the arithmetic means of ψ and λ are used and $\alpha = 21$ when the geometric means of ψ and λ are used. Only the arithmetic means of ψ and λ are presented here since Rawls et al (1982) found

that the arithmetic means gave a slightly better estimate K_s than the geometric means.

Using the table provided K_s can be found for various texture classes. The values of θ_r , ψ and λ for different soil textual classes are given in Table 4.0

Table 4.0: Hydrological parameter of soil classified by texture according to Rawls et al (1982)

| Texture class | Sample size | Residual Saturation (θ_r) (cm^3/cm^3) | Bubbling Pressure (ψ) (cm) | Pore size Distribution index (λ) |
|-----------------|-------------|--|-----------------------------------|--|
| Sand | 762 | 0.020 | 15.98 | 0.694 |
| Loamy sand | 338 | 0.035 | 20.58 | 0.553 |
| Loam | 383 | 0.027 | 40.12 | 0.252 |
| Silt loam | 1206 | 0.015 | 50.57 | 0.234 |
| Sandy clay loam | 498 | 0.063 | 59.41 | 0.319 |
| Clay loam | 366 | 0.075 | 56.43 | 0.242 |
| Silty clay loam | 689 | 0.040 | 70.33 | 0.177 |
| Sandy clay | 45 | 0.109 | 79.48 | 0.223 |
| Silty clay | 127 | 0.056 | 76.54 | 0.150 |
| Clay | 291 | 0.090 | 85.60 | |
| Sandy loam | 666 | 0.041 | 30.20 | 0.378 |

By replacing F with K_s

Equation (4.25) then becomes

$$\xi = \frac{2K_s k l d^3}{d_{\max} \Delta m' \zeta} \quad (4.27)$$

The constant ξ may be equated with soil erodibility or splashability.

The experimental studies of splashability reveal that the phenomenon is affected by various factors associated with the mechanical, chemical and hydraulic properties of the soil, as well as the rainfall mass and kinetic energy to which the soil is exposed.

4.2 Modeling of kinetic energy of raindrops

Water has a high volumetric surface tension. It is precisely this tension which forces the falling drop of water to take on a spherical shape which offers strong resistance to

deformation. The surface layer of a water drop envelops it like an elastic shell, and gives it great strength. When the raindrop falls on the soil, it flattens out and break up, forming a crater in the soil. At the same time, the surface tension imparts to each particle of the divided raindrop, a shape corresponding to the minimum surface area, which promotes bouncing of the soil particles upward like rubber balls.

Little attention has been paid to the theory of raindrop erosion process in West Africa. There is yet no distinct physical scheme of this process despite the fact that there are some prerequisites for its construction. To this end one needs only to turn to studies in allied fields on the impact of drops on solid and liquid surfaces. It should be noted, however, that simulation of drop impact on soils involves additional difficulties because of the loose (porous) structure of soil.

As stated earlier there are two major aspects of splash erosion: destruction of the soil structure upon impact by drops and the transport of soil by splashing. The second aspect of the problem can be solved in the following manner. One must learn to determine the amount of soil splashed by the impact of a single raindrop with a given soil and drop characteristics and find the loss of soil at a given point, by determining the number of drops falling on that point of the surface of a slope, which contributes to the total transport of soil down slope. The area of this can be calculated on the basis of calculations of the soil splashed particle trajectories.

Determination of the amount of soil splashed by the impact of a single drop is directly associated with the first aspect of the problem and must be based on an analysis of the forces of impact, surface tension, cohesion etc.

The damage caused by raindrop hitting the soil at a high velocity is the first step in the erosion process. We may think of the raindrops as miniature bombs hitting the soil surface. They shatter the particles and in turn reduce the infiltration capacity of the soil. The problem with natural rainfall is how to determine the terminal velocities of the raindrops. The problem becomes compounded when we are using artificial rainfall. The distances involved with simulated rainfall, are such that the drops do not attain their terminal velocities. We are therefore faced with the problem of finding the falling velocity of the raindrop.

4.2.1 The fall velocity of raindrop.

The buoyant force of a raindrop falling at terminal velocity in a quiescent air is expressed as

$$F_B = g(\rho_w - \rho_a)V_d \quad (4.28)$$

where F_B is the buoyant force, V_d is the drop volume ($\pi d^3/6$) for spheres, ρ_w is the density of the raindrop, ρ_a is the density of air, d is the diameter of the raindrop and g is the acceleration due to gravity.

The drag force driving a raindrop at a terminal velocity is

$$F_D = C_D \rho_a A \frac{v_T^2}{2} \quad (4.29)$$

where F_D is the drag force, C_D the drag coefficient, A the projected area of the drop in a direction of fall which is πd^2 for spheres and v_T is terminal velocity of a drop.

By equating the drag force and the buoyant force at terminal velocity equation (4.32) describing the drag coefficient is obtained.

$$g(\rho_w - \rho_a)V_d = C_D \rho_a A \frac{v_T^2}{2} \quad (4.30)$$

$$g(\rho_w - \rho_a) \frac{\pi d^3}{6} = C_D \rho_a \pi d^2 \frac{v_T^2}{2} \quad (4.31)$$

$$C_D = g \left(\frac{\rho_w}{\rho_a} - 1 \right) \frac{d}{3v_T^2} \quad (4.32)$$

For the Stokes range ($R_e \leq 0.1$) Park et al (1983) computed terminal velocity by using

$$v_T = \frac{(\rho_w - \rho_a)gd}{1.8} \quad (4.33)$$

In our case the fall distance is insufficient for a terminal velocity to be achieved. In such a case the impact velocity of raindrop would be less than the terminal velocity. The forces exerted on accelerating raindrop are F_B the buoyant force, F_D the drag force and F_R designated as other resisting forces due to inertia of the air or turbulence (eddies)

To determine the fall velocity Park et al (1983) had to balance the forces exerted on an accelerating raindrop as

$$F_B - F_D - F_R = M_{eq} \frac{dv_s}{dt} \quad (4.34)$$

where F_B and F_D are buoyant force and drag force as given in (4.28) and (4.29) respectively. F_R designates other resisting forces due to inertia of air and turbulence.

M_{eq} is the equivalent mass of a raindrop which is defined as the raindrop mass plus an added mass generated by air mass for the volume of raindrop multiplied by a coefficient. v_s is the fall velocity and t is the travel time from the initial velocity v_o , to the fall velocity v_s . The equivalent mass is defined as

$$M_{eq} = (\rho_w - K_m \rho_a) V_d \quad (4.35)$$

where K_m is eddy coefficient, and ρ_a , ρ_w and V_d are defined in equation (4.28).

The added mass term $K_m \rho_a V_d$ is neglected because it is assumed that the air density ρ_a is very small compared to ρ_w .

$$M_{eq} = \rho_w V_d \quad (4.36)$$

Equation (34) becomes

$$F_B - F_D - F_R = \rho_w V_d \frac{dv_s}{dt} \quad (4.37)$$

Assuming F_R is negligible and substituting for F_B and F_D we have

$$g(\rho_w - \rho_a) V_d - C_D \rho_a \frac{v_s^2}{2} = \rho_w V_d \frac{dv_s}{dt} \quad (4.38)$$

Substituting for C_D equation (4.38) becomes

$$\rho_w V_d \frac{dv_s}{dt} = g(\rho_w - \rho_a) V_d - g \left[\left(\frac{\rho_w}{\rho_a} - 1 \right) \frac{d}{3v_s^2} \right] \rho_a A \frac{v_s^2}{2} \quad (4.39)$$

$$\frac{dv_s}{dt} = g \left(1 - \frac{\rho_a}{\rho_w} \right) \left(1 - \frac{d\pi d^2 v_s^2}{6v_T^2 \frac{\pi d^3}{6}} \right) \quad (4.40)$$

$$\frac{dv_s}{dt} = g \left(1 - \frac{\rho_a}{\rho_w} \right) \left(\frac{v_T^2 - v_s^2}{v_T^2} \right) \quad (4.41a)$$

Neglecting the term $\frac{\rho_a}{\rho_w}$ in (4.41a) we have

$$\int_0^t dt = \frac{1}{g} \int_{v_0}^{v_s} \frac{v_T^2}{(v_T^2 - v_s^2)} dv_s \quad (4.41b)$$

and solving for t, the travel time we have

$$t = \frac{v_T}{2g} \left[\ln \left(\frac{v_T + v_s}{v_T - v_s} \right) - \ln \left(\frac{v_T + v_0}{v_T - v_0} \right) \right] \quad (4.42)$$

where v_0 is the initial velocity at $t = 0$. The travel distance of a raindrop from the initial velocity v_0 to the fall velocity v_s is

$$z = \frac{v_T}{2g} \int_{v_0}^{v_s} v_s d \left[\ln \left(\frac{v_T + v_s}{v_T - v_s} \right) \right] \quad (4.43)$$

$$z = \frac{v_T^2}{4g} \ln \left(\frac{v_T^2 - v_0^2}{v_T^2 - v_s^2} \right) \quad (4.44)$$

where z is the travel distance

The fall velocity for a given distance is defined by solving equation (4.44).

$$v_s^2 = v_T^2 - (v_T^2 - v_0^2)\phi(z) \quad (4.45)$$

where $\phi(z) = e^{-4gz/v_T^2}$ with $V_0 = 0$. Equation (4.45) reduces to

$$v_s = v_T \sqrt{1 - \phi(z)} \quad (4.46)$$

Equation (4.46) was used to simulate fall velocity.

4.2.2 Numerical Modeling – Runge- Kutta Method

Soil erosion is a work process in the physical sense that work is the expenditure of energy and energy is used in all the phases of erosion- in breaking down soil aggregates, in splashing them in air, in causing turbulence in surface runoff, in scouring and carrying away soil particles. If the available sources of energy are considered we see why splash erosion is so vital in erosion process. Since the characteristics of natural rainfall were established several decades ago researchers have sought a parameter that would indicate how closely simulated rainfall attained the important characteristics of natural rainfall. There is experimental evidence that the erosive power of rainfall is related to compound parameters derived from combination of more than one physical property. The kinetic energy of the rain and its momentum are examples.

If the size of raindrops is known and also their terminal velocity, it is possible to calculate the kinetic energy by summation of the values for individual raindrops

$$E = \sum_{i=1}^n \frac{1}{2} m_i v_i^2 \quad (4.47)$$

The forces involved are so small that any instrument sufficiently sensitive to record them mechanically is liable to be swamped by wind effects.

The Kinetic energy of fall mass of raindrop from a known height is reduced to differential equation and its solution found by Runge-Kutta method by means of computer.

In many applications it is required to find the value \bar{y} of y corresponding to $x = x_0 + h$

From the particular solution of a given differential equation

$$y' = f(x, y) \quad (4.49)$$

satisfying the initial conditions $y = y_0$ when $x = x_0$, such problems have been solved by first finding primitive equation

$$y = F(x) + c \quad (4.50)$$

of (4.49), then selecting the particular solution

$$y = g(x) \quad (4.51)$$

through (x_0, y_0) and finally computing the required value $y = g(x_0 + h)$

When no method is available for finding the primitive, it is necessary to use some procedure for approximating the desired value. Integrating (49) between the limits $x = x_0, y = y_0$ and $x = x, y = y$ we obtain

$$y = y_0 + \int_{x_0}^x f(x, y) dx \quad (4.52)$$

the value of y when $x = x_0 + h$ is then

$$\bar{y} = y_0 + \int_{x_0}^{x_0+h} f(x, y) dx \quad (4.53)$$

For values of x near $x = x_0$ the corresponding value of $y = g(x)$ is near $y_0 = g(x_0)$. Thus a first approximation y_1 of $y = g(x)$ is obtained by replacing y by y_0 , that is

$$y_1 = y_0 + \int_{x_0}^x f(x, y_0) dx \quad (4.54)$$

A second approximation y_2 is then obtained by replacing y by y_1 , that is

$$y_2 = y_0 + \int_{x_0}^x f(x, y_1) dx \quad (4.55)$$

Continuing this procedure a succession of function of x ie $y_0, y_1, y_2, y_3, \dots$ is obtained each giving a better approximation of the required solution than the preceding one.

This is Picards method. In general, it is unsatisfactory as a practical means of approximation because of the difficulties, which arise in performing the necessary integration.

The Taylor's expansion of $y = g(x)$ near (x_0, y_0) is

$$y = g(x_0) + (x - x_0)g'(x_0) + 1/2(x - x_0)^2 g''(x_0) + 1/6(x - x_0)^3 g'''(x_0) + \dots \quad (4.55a)$$

From (49) $y' = g'(x) = f(x, y)$ hence, by repeated differentiation

$$y'' = g''(x) = \frac{\partial f}{\partial x} + \frac{\partial f}{\partial y} \frac{dy}{dx} = \frac{\partial f}{\partial x} + f \frac{\partial f}{\partial y} \quad (4.55b)$$

$$y''' = g'''(x) = \frac{d}{dx} \left(\frac{\partial f}{\partial x} + f \frac{\partial f}{\partial y} \right) = \left(\frac{\partial}{\partial x} + f \frac{\partial}{\partial y} \right) \left(\frac{\partial f}{\partial x} + f \frac{\partial f}{\partial y} \right) \quad (4.56a)$$

$$y''' = \frac{\partial^2 f}{\partial x^2} + \frac{\partial f}{\partial x} \frac{\partial f}{\partial y} + 2f \frac{\partial^2 f}{\partial x \partial y} + f \left(\frac{2f}{2y} \right)^2 + f^2 \frac{\partial^2 f}{\partial y^2} \quad (4.56b)$$

For convenience we write

$$p = \frac{\partial f}{\partial x}, q = \frac{\partial f}{\partial y}, r = \frac{\partial^2 f}{\partial x^2}, s = \frac{\partial^2 f}{\partial x \partial y}, t = \frac{\partial^2 f}{\partial y^2} \text{ and let } f_0, p_0, q_0 \text{ denote the values}$$

of f, p, q, \dots at (x_0, y_0) substituting in (4.55) the results of (4.56) and evaluating from $x =$

$x_0 + h$ we obtain

$$\bar{y} = y_o + hf_o + \frac{1}{2}h^2(p_o + f_o q_o) + \frac{1}{6}h^3(r_o + p_o q_o + 2f_o s_o + f_o q_o^2 + f_o^2 t_o) + \dots \quad (4.57)$$

This series may be used to compute \bar{y} . It is evident however that those additional terms will be increasingly complex.

Probably one of the most useful as well as accurate numerical procedures used in obtaining approximate solutions to differential equations is the fourth-order Runge-Kutta method. The method consists of determining appropriate constants so that a formula such as $y_{n+1} = y_n + aK_1 + bK_2 + cK_3 + dK_4$ agrees with a Taylor expansion to h^4 or the fifth term. The K_i are constant multiple of $f(x, y)$ evaluated at select points. From (4.53) and (4.57) we obtain

$$K = \bar{y} - y_o = \int_{x_o}^{x_o+h} f(x, y) dx = hf_o + \frac{1}{2}h^2(p_o + f_o q_o) + \frac{1}{6}h^3(r_o + p_o q_o + 2f_o s_o + f_o q_o^2 + f_o^2 t_o) + \dots \quad (4.58)$$

Now assume that values of y_o, y_1, y_2 of $y = g(x)$ corresponding to $x_o, x_1 = x_o + 1/2h, x_2 = x_o + h$ are known. Then by Simpson Rule

$$K = \int_{x_o}^{x_o+h} f(x, y) dx \approx \frac{h}{6} [f(x_o, y_o) + 4f(x_o + 1/2h, y_1) + f(x_o + h, y_2)] \quad (4.59)$$

Runge's method is based on certain approximations y_1 and y_2

$$y_1 \approx y_o + \frac{1}{2}hf(x_o, y_o) = y_o + \frac{1}{2}hf_o$$

$$y_2 \approx y_o + hf(x_o + h, y_o + hf_o)$$

Thus (4.59) becomes

$$K \approx \frac{h}{6} \left\{ f_o + 4f\left(x_o + \frac{1}{2}h, y_o + \frac{1}{2}hf_o\right) + f\left[x_o + h, y_o + hf(x_o + h, y_o + hf_o)\right] \right\} \quad (4.60)$$

These calculations are best made as follows:

$$K_1 = hf_0, K_2 = hf(x_0 + h, y_0 + K_1), K_3 = hf(x_0 + h, y_0 + K_2), K_4 = hf(x_0 + 1/2h, y_0 + 1/2K_1)$$

$$K \approx \frac{1}{6}(K_1 + 4K_4 + K_3)$$

The Runge-Kutta method is thus given as follows:

$$y_{n+1} = y_n + \frac{1}{6}(K_1 + 2K_2 + 2K_3 + K_4)$$

$$K_1 = hf(x_n, y_n)$$

$$K_2 = hf(x_n + 1/2h, y_n + 1/2K_1)$$

$$K_3 = hf(x_n + 1/2h, y_n + 1/2K_2)$$

$$K_4 = hf(x_n + h, y_n + K_3)$$

(4.61)

The problem with natural rainfall is how to determine the terminal velocities of the raindrops. We formulate the problem this way, if air resistance is proportional to the square of the terminal velocity; velocity v_T of mass m of raindrop from a height h is determined from

$$m \frac{dv}{dt} + kv_T^2 - mg = 0, k > 0 \quad (4.62)$$

where g is the acceleration due to gravity. We use the Runge-Kutta method to find an approximation to the velocity of the falling raindrop mass at t seconds.

The computer programme for the solution of differential equation using Runge-Kutta method is presented in Appendix A.

CHAPTER FIVE

5.0 RESULTS

5.1 Some soil physical properties

5.1.1 Soil texture

The textural classes of different samples are found in Table 5.0. Five of the samples

Table 5.0: Soil textural classification

| Sample | Sand % | Silt % | Clay % | Textural classification |
|--------|--------|--------|--------|-------------------------|
| TT | 69.40 | 2.00 | 28.60 | Sandy clay loam |
| W | 53.40 | 10.00 | 36.60 | Sandy clay |
| T | 35.40 | 12.00 | 52.60 | Clay |
| AK | 73.40 | 12.00 | 14.60 | Sandy loam |
| PA | 85.40 | 8.00 | 6.60 | Loamy sand |
| PO | 53.40 | 22.00 | 24.60 | Sandy clay loam |
| CA | 65.40 | 16.00 | 18.60 | Sandy loam |
| VE | 75.40 | 8.00 | 16.60 | Sandy loam |
| G1 | 61.40 | 18.00 | 20.60 | Sandy clay loam |
| G2 | 49.40 | 18.00 | 32.60 | Sandy clay loam |
| G3 | 59.40 | 18.00 | 22.60 | Sandy clay loam |
| G4 | 69.40 | 16.00 | 14.60 | Sandy loam |

were classified as sandy clay loam, three as sandy loam. The other samples were sandy clay, loamy sand and clay respectively. In general the percentage of silt in the samples were lower compared with the percentage of sand and clay. The silt levels ranged from 2% in sample T to 22% in sample PO. The clay levels were appreciable with sample T having the highest level of 52.6%.

5.1.2 Aggregate stability and Mechanical ratio

The Aggregate stability as determined by wet sieving method and Mechanical ratio calculated from soil texture are presented in Table 5.1. Sample TT, W and AK had the highest percentage aggregate stability in that order. Samples VE, G4 and PO had the lowest percentage aggregate stability. The samples with high Mechanical ratios were PA, G4 and AK. Samples T, W and G2 had lower Mechanical ratio. The Mechanical ratio is in the following decreasing order: T>W>G2>TT>PO>G3>G1>CA>VE>AK>G4>PA.

Table 5.1: Aggregate stability and Mechanical ratio

| Sample | Aggregate stability (%) | Mechanical ratio |
|--------|-------------------------|------------------|
| TT | 83.90 | 2.50 |
| W | 70.90 | 1.73 |
| T | 53.40 | 0.90 |
| AK | 70.40 | 5.85 |
| PA | 58.40 | 14.15 |
| PO | 48.40 | 3.07 |
| GA | 63.40 | 4.38 |
| VE | 34.90 | 5.02 |
| G1 | 57.70 | 3.85 |
| G2 | 65.10 | 2.07 |
| G3 | 59.20 | 3.42 |
| G4 | 45.60 | 5.85 |

5.2 Some chemical properties of the soil

The chemical properties of the samples are shown in Tables 5.2 and 5.3. The pH of the samples ranged from near neutral to almost acid. Sample G1 had the highest pH of 6.6 and sample PO the lowest of 4.8. The percentage Nitrogen and Organic carbon contents of the samples were relatively low. However the Phosphorus and Calcium

contents were relatively high compared with Sodium, Magnesium and K^+ . The total elemental analysis indicated that the major element was Fe. Other elements like Mn, Cds, Cu and Zn were either in very small traces or were nonexistent. Samples T, TT, PA, G2 and G3 contained higher amounts of Fe in that order.

Table 5.2: Chemical properties of soils

| Sample | pH | % N | %O.C | P μ gg $^{-1}$ | EXCHANGEABLE c mol kg $^{-1}$ | | | | Acidity | c mol kg $^{-1}$ |
|--------|------|------|------|--------------------|-------------------------------|---------|---------|------------|---------|------------------|
| | | | | | K $^+$ | Na $^+$ | Mg $^+$ | Ca $^{2+}$ | | |
| TT | 5.70 | 0.23 | 2.25 | 5.79 | 0.21 | 0.19 | 0.78 | 10.62 | 0.15 | 11.95 |
| T | 5.30 | 0.06 | 0.56 | 1.60 | 0.07 | 0.09 | 0.32 | 2.30 | 0.09 | 2.87 |
| AK | 6.60 | 0.11 | 0.80 | 11.60 | 0.35 | 0.19 | 0.39 | 40.71 | 0.11 | 5.75 |
| W | 6.00 | 0.19 | 1.81 | 3.80 | 0.23 | 0.20 | 0.40 | 6.68 | 0.14 | 7.65 |
| PA | 5.40 | 0.05 | 0.88 | 7.21 | 0.29 | 0.19 | 0.31 | 1.25 | 0.07 | 2.11 |
| PO | 4.80 | 0.09 | 0.95 | 8.36 | 0.27 | 0.17 | 0.23 | 2.31 | 0.16 | 2.87 |
| CA | 6.30 | 0.09 | 0.85 | 5.81 | 0.51 | 0.29 | 0.16 | 3.35 | 0.18 | 4.49 |
| VE | 5.60 | 0.10 | 1.10 | 14.24 | 0.42 | 0.31 | 0.08 | 3.58 | 0.10 | 4.49 |
| G1 | 6.60 | 0.21 | 2.36 | 5.03 | 0.72 | 0.43 | 1.65 | 7.68 | 0.11 | 10.59 |
| G2 | 5.90 | 0.27 | 2.42 | 5.42 | 0.73 | 0.42 | 4.39 | 7.50 | 0.16 | 13.20 |
| G3 | 6.20 | 0.19 | 2.12 | 8.74 | 0.55 | 0.33 | 0.79 | 7.69 | 0.17 | 9.53 |
| G4 | 5.80 | 0.13 | 1.10 | 8.67 | 0.16 | 0.11 | 0.16 | 1.43 | 0.11 | 1.97 |

Table 5.3: Values of some elements in percentages (determined Atomic Absorption Spectrometer)

| Sample | Fe | Mn | Cd | Cu | Zn |
|--------|------|------|------|------|------|
| TT | 8.06 | 0.00 | 0.00 | 0.01 | 0.00 |
| T | 9.55 | 0.00 | 0.00 | 0.01 | 0.00 |
| AK | 3.78 | 0.10 | 0.00 | 0.01 | 0.00 |
| W | 3.43 | 0.02 | 0.00 | 0.00 | 0.00 |
| PA | 7.92 | 0.10 | 0.00 | 0.01 | 0.00 |
| PO | 2.59 | 0.10 | 0.00 | 0.00 | 0.00 |
| CA | 5.37 | 0.01 | 0.00 | 0.01 | 0.01 |
| VE | 3.80 | 0.00 | 0.00 | 0.01 | 0.01 |
| G1 | 7.07 | 0.01 | 0.00 | 0.01 | 0.01 |
| G2 | 9.82 | 0.02 | 0.00 | 0.02 | 0.02 |
| G3 | 7.58 | 0.01 | 0.00 | 0.02 | 0.02 |
| G4 | 4.05 | 0.01 | 0.00 | 0.00 | 0.00 |

5.3 Relationship between soil splashed and rainfall intensity

Table 5.4 shows data for soil splashed at different intensities. A linear plot was used

Table 5.4: Intensity of rainfall and soil splashed in g/min

| Intensity mm/hr | Sample | Soil used (g) | Soil splashed (g/min) | Intensity mm/hr | Sample | Soil Used (g) | Soil Splashed (g/min) |
|--------------------|--------|---------------------|-----------------------------|--------------------|--------|---------------------|-----------------------------|
| 73.39 | T | 130.57 | 16.09 | 139.43 | PA | 159.94 | 36.20 |
| | TT | 146.73 | 21.67 | | PO | 123.43 | 21.86 |
| | AK | 147.93 | 29.38 | | CA | 146.14 | 27.28 |
| | W | 129.07 | 18.38 | | VE | 169.71 | 32.05 |
| 93.67 | T | 117.04 | 17.75 | 160.52 | PA | 147.30 | 39.01 |
| | TT | 149.65 | 21.70 | | PO | 129.30 | 22.75 |
| | AK | 154.08 | 29.99 | | CA | 152.37 | 34.09 |
| | W | 133.57 | 18.82 | | VE | 161.21 | 37.84 |
| 132.78 | T | 136.03 | 19.27 | 65.07 | G1 | 129.39 | 24.69 |
| | TT | 149.55 | 24.94 | | G2 | 170.90 | 18.55 |
| | AK | 150.82 | 30.77 | | G3 | 147.28 | 21.05 |
| | W | 148.04 | 21.48 | | G4 | 104.43 | 17.61 |
| 182.32 | T | 142.15 | 20.91 | 100.10 | G1 | 141.08 | 25.37 |
| | TT | 144.07 | 25.96 | | G2 | 153.57 | 20.21 |
| | AK | 154.98 | 30.84 | | G3 | 125.02 | 22.95 |
| | W | 157.53 | 22.33 | | G4 | 78.74 | 21.90 |
| 78.11 | PA | 151.41 | 31.02 | 130.38 | G1 | 141.61 | 25.53 |
| | PO | 117.04 | 17.75 | | G2 | 160.42 | 26.99 |
| | CA | 138.71 | 23.43 | | G3 | 155.41 | 25.49 |
| | VE | 180.42 | 25.83 | | G4 | 120.18 | 28.00 |
| 124.05 | PA | 157.24 | 34.90 | 161.77 | G1 | 154.15 | 26.60 |
| | PO | 132.11 | 20.44 | | G2 | 192.19 | 31.13 |
| | CA | 152.36 | 26.00 | | G3 | 136.78 | 25.75 |
| | VE | 120.18 | 28.00 | | G4 | 125.38 | 28.86 |

to establish a relationship between the soil splashed and rainfall intensity. The average soil splashed for different samples is given in Table 5.5a. The sample linear plots between the soil splashed and rainfall intensity are presented in Figures 5.0 (a-d). The relationship was observed to be approximately linear with highly significant correlation. The raw data used in establishing this relationship is given in appendix B. The regression parameters describing the relationship between soil splashed and rainfall intensity is given in Table 5.5b. The empirical slope of this relationship was used to describe the coefficient of splashability.

In the section following a relationship will be established between the empirical coefficient of splashability and the splashability coefficients derived from the physically based models. The log-log relationship was also established between soil splashed and rainfall intensity. This log-log relationship was also observed to be approximately linear. The sample plots of this log-log relationship are given in Figures (5.1 a-b). The regression parameters from these log-log relationships are given in Table 5.5c. The regression coefficients were equally highly significant and similar to the linear relationship.

The data for rainfall intensity and number of raindrops hitting the soil surface per unit time is presented in Table 5.6a. The kinetic energy values calculated from the drop mass and velocity of drops are given in Table 5.6b. The data for drop size, kinetic energy of raindrops and soil splashed are summarized in Tables 5.6c-5.6d.

Table 5.5a: Percentage of soil splashed

| Sample | Ave. soil used | Ave soil splashed | Percentage soil splashed |
|--------|----------------|-------------------|--------------------------|
| T | 131.45 | 18.51 g/min | 14.08 |
| TT | 147.50 | 23.31 | 15.80 |
| AK | 152.14 | 30.25 | 19.88 |
| W | 142.05 | 20.25 | 14.26 |
| PA | 153.97 | 35.28 | 22.91 |
| PO | 125.47 | 20.70 | 16.50 |
| CA | 147.40 | 27.70 | 18.79 |
| VE | 157.88 | 30.93 | 19.59 |
| G1 | 141.56 | 25.55 | 18.05 |
| G2 | 169.27 | 24.22 | 14.31 |
| G3 | 141.12 | 23.81 | 16.87 |
| G4 | 107.18 | 24.09 | 22.48 |

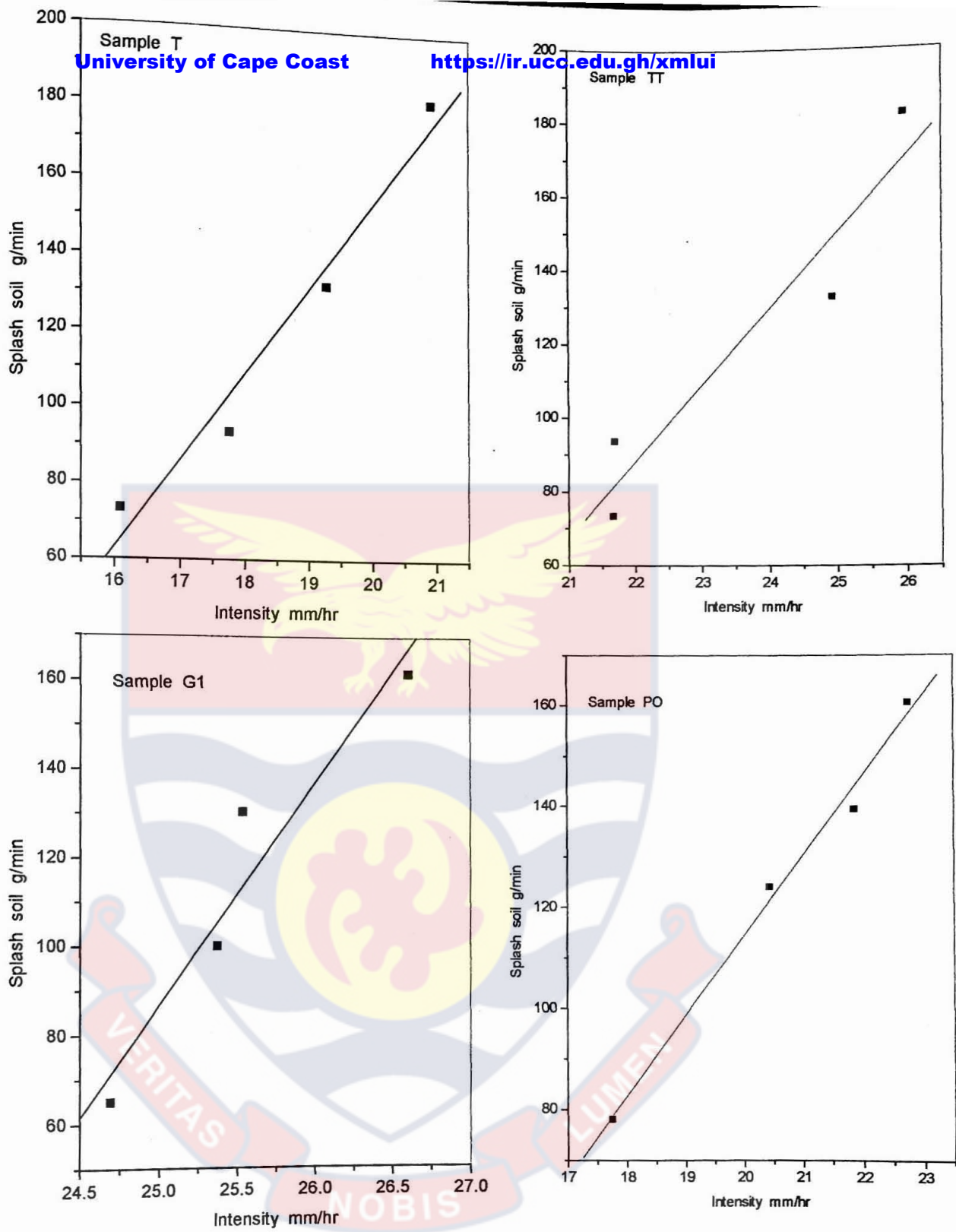


Figure 5.0 (a-d): Linear plot of soil splashed and rainfall intensity

Table 5.5b: Linear regression parameters

| Sample | A | B | r |
|--------|-------|------|------|
| PA | 23.45 | 0.09 | 0.99 |
| G4 | 9.86 | 0.12 | 0.96 |
| AK | 28.69 | 0.01 | 0.90 |
| VE | 13.70 | 0.14 | 0.91 |
| CA | 13.23 | 0.12 | 0.89 |
| G1 | 23.45 | 0.02 | 0.96 |
| G3 | 17.86 | 0.05 | 0.96 |
| PO | 12.89 | 0.06 | 0.99 |
| TT | 18.26 | 0.04 | 0.96 |
| G2 | 8.45 | 0.14 | 0.97 |
| W | 15.54 | 0.04 | 0.96 |
| T | 13.41 | 0.04 | 0.98 |

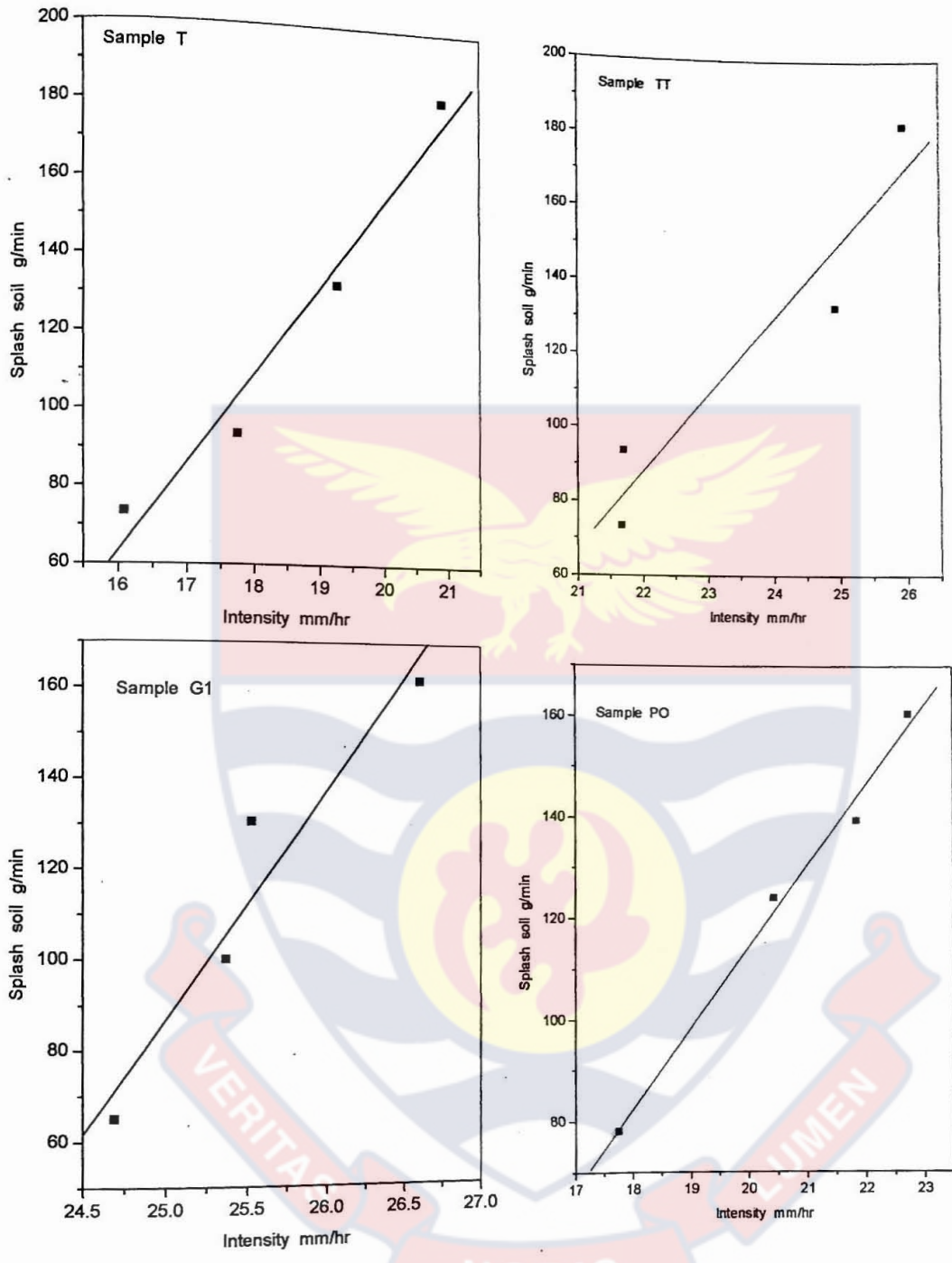


Figure 5.0 (e-h): Linear plot of soil splashed and rainfall intensity

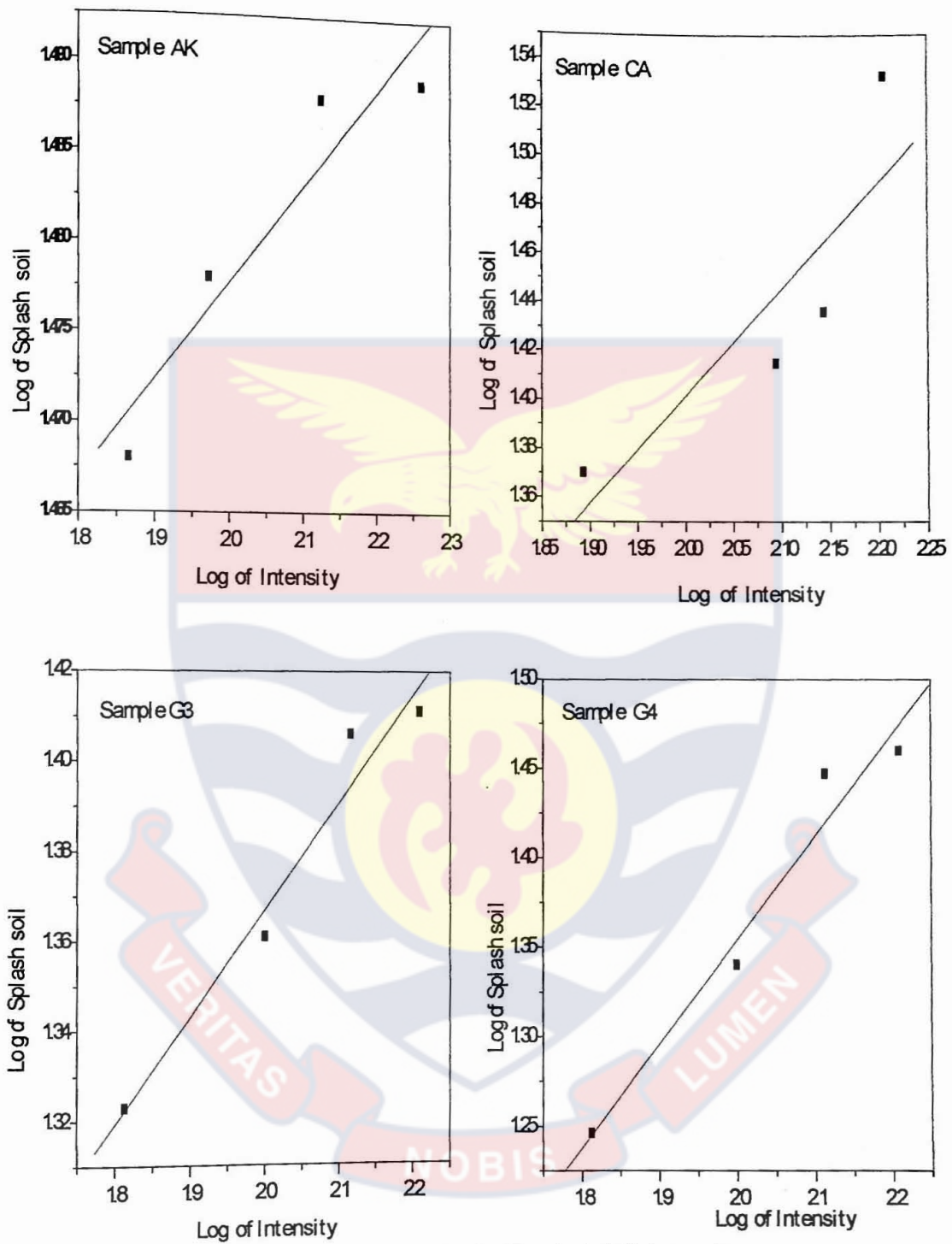


Figure 51(a-d): The log-log plot of splashed soil and rainfall intensity

Table 5.5c: Regression parameters of log- log relation

| Sample | A | B* | R |
|--------|------|------|------|
| PA | 0.92 | 0.30 | 0.99 |
| G4 | 0.19 | 0.58 | 0.98 |
| AK | 1.37 | 0.06 | 0.95 |
| VE | 0.45 | 0.50 | 0.87 |
| CA | 0.52 | 0.44 | 0.87 |
| G1 | 1.26 | 0.07 | 0.94 |
| G3 | 0.89 | 0.24 | 0.98 |
| PO | 0.59 | 0.35 | 0.99 |
| TT | 0.91 | 0.23 | 0.96 |
| G2 | 0.18 | 0.59 | 0.95 |
| W | 0.82 | 0.24 | 0.97 |
| T | 0.69 | 0.28 | 0.99 |

Table 5.6a: Rainfall intensity and number of drops hitting soil per second

| Sample | Intensity mm/hr | Drops per m ² /s | Drops hitting soil per second |
|----------------|-----------------|-----------------------------|-------------------------------|
| T, TT, AK, W | 73.39 | 1319.29 | 2.59 |
| | 93.67 | 1490.46 | 2.93 |
| | 132.78 | 1774.55 | 3.49 |
| | 182.32 | 2079.40 | 4.08 |
| PA, PO, CA, VE | 78.11 | 1361.05 | 2.68 |
| | 124.05 | 1715.22 | 3.37 |
| | 139.43 | 1818.44 | 3.57 |
| | 160.52 | 1951.13 | 3.83 |
| G1, G2, G3, G4 | 65.07 | 1242.26 | 2.44 |
| | 100.10 | 1540.77 | 3.03 |
| | 130.38 | 1758.44 | 3.45 |
| | 161.77 | 1958.77 | 3.85 |

Table 5.6b: Determination of kinetic energy of raindrop

| Drop Diameter (mm) | No of Drops (1min) | Drop Mass (mg) | Mass of all drops/kg | Vel V m/s | V^2 m^2/s^2 | MV^2 Kg m^2/s^2 | $1/2MV^2$ $*10^{-6}$ | K.E $J*10^{-6}$ | Sample |
|--------------------|--------------------|----------------|----------------------|-----------|-----------------|---------------------|----------------------|-----------------|------------------|
| 0.54 | 155 | 0.08 | 12.77 | 2.15 | 4.62 | 58.70 | 29.35 | 29.35 | T, TT, AK, W |
| | 176 | 0.08 | 14.43 | 2.15 | 4.62 | 66.64 | 33.32 | 33.32 | |
| 0.30 | 209 | 0.01 | 2.93 | 1.05 | 1.10 | 3.23 | 1.61 | 1.61 | |
| | 245 | 0.01 | 3.43 | 1.05 | 1.10 | 3.78 | 1.89 | 1.89 | |
| 0.54 | 161 | 0.08 | 13.20 | 2.15 | 4.62 | 60.97 | 30.48 | 30.48 | PA, PO, CA, VE |
| | 202 | 0.08 | 16.56 | 2.15 | 4.62 | 76.49 | 38.25 | 38.25 | |
| 0.30 | 214 | 0.01 | 2.99 | 1.05 | 1.10 | 3.31 | 1.65 | 1.65 | |
| | 230 | 0.01 | 3.22 | 1.05 | 1.10 | 3.55 | 1.78 | 1.78 | |
| 0.54 | 146 | 0.08 | 11.97 | 2.15 | 4.62 | 55.29 | 27.64 | 27.64 | G1, G2 G3, G4 |
| | 182 | 0.08 | 14.92 | 2.15 | 4.62 | 68.92 | 34.46 | 34.16 | |
| 0.30 | 207 | 0.01 | 2.89 | 1.05 | 1.10 | 3.20 | 1.60 | 1.60 | |
| | 231 | 0.01 | 3.23 | 1.05 | 1.10 | 3.57 | 1.78 | 1.78 | |

Table 5.6c: Drop-size, kinetic energy and soil splashed

| Sample | Drop-size (mm) | Kinetic energy (10^{-6}) J | Soil splashed (g/min) |
|--------|----------------|-----------------------------------|--------------------------|
| T | 0.54 | 29.35 | 16.09 |
| | | 33.32 | 17.75 |
| TT | | 29.35 | 21.67 |
| | | 33.32 | 21.70 |
| AK | | 29.35 | 29.38 |
| | | 33.32 | 29.99 |
| W | | 29.35 | 18.38 |
| | | 33.32 | 18.82 |
| PA | | 30.48 | 31.02 |
| | | 38.25 | 34.90 |
| PO | | 30.48 | 17.75 |
| | | 38.25 | 20.44 |
| CA | | 30.48 | 23.43 |
| | | 38.25 | 26.00 |
| VE | | 30.48 | 25.83 |
| | | 38.25 | 28.00 |
| G1 | | 27.64 | 24.69 |
| | | 34.16 | 25.37 |
| G2 | | 27.64 | 18.55 |
| | | 34.16 | 20.21 |
| G3 | | 27.64 | 21.05 |
| | | 34.16 | 22.95 |
| G4 | | 27.64 | 17.61 |
| | | 34.16 | 21.90 |

Table 5.6d: Drop-size, kinetic energy and soil splashed

| Sample | Drop-size (mm) | Kinetic energy (10^{-6}) J | Soil splashed (g/min) |
|--------|----------------|-----------------------------------|--------------------------|
| T | 0.30 | 1.61 | 19.27 |
| | | 1.89 | 20.91 |
| TT | | 1.61 | 24.94 |
| | | 1.89 | 25.96 |
| AK | | 1.61 | 30.77 |
| | | 1.89 | 30.84 |
| W | | 1.61 | 21.48 |
| | | 1.89 | 22.33 |
| PA | | 1.65 | 36.20 |
| | | 1.77 | 39.01 |
| PO | | 1.65 | 21.86 |
| | | 1.77 | 22.75 |
| CA | | 1.65 | 27.28 |
| | | 1.77 | 34.09 |
| VE | | 1.65 | 32.05 |
| | | 1.77 | 37.84 |
| G1 | | 1.60 | 25.53 |
| | | 1.78 | 26.60 |
| G2 | | 1.60 | 26.99 |
| | | 1.78 | 31.13 |
| G3 | | 1.60 | 25.49 |
| | | 1.78 | 25.50 |
| G4 | | 1.60 | 28.00 |
| | | 1.78 | 28.86 |

5.4 Rainfall kinetic energy and intensity relationship

Drop size remaining the same, the higher the intensity, I , the higher the number of raindrop per unit time. Park et al (1983) observed that the number of drops N_d is approximately proportional to the square root of rainfall intensity I ($N_d = 154 I^{0.5}$).

The number of drops hitting the soil per second ranged between 2.59 drops to 4.08 drops, depending on the intensity of the rainfall.

It was also observed that drop size remaining the same the higher the kinetic energy (E_i) of the drop the greater the amount of soil splashed per minute (S_d). While the relationship

between rainfall intensity (I) and soil splashed (S_d) is clearly defined, the relationship between rainfall kinetic energy E_I and soil splashed is not simple. Each subset data representing fixed rainfall intensity with different drop-size distribution and related rainfall energies tended to have a unique trend. Analyses of the general data were carried out using two empirical functions ($S_d = aE_I^b$ and $S_d = nI^m$). The parameters of the power equations and their coefficients of regression are shown in Table 5.7. The relationship of splashed soil with both rainfall intensity and

Table 5.7: Rainfall energy and intensity relationship –Regression parameters

$$S_d = aE_I^b$$

$$S_d = nI^m$$

| Sample | R^2 | a | b | R^2 | n | m |
|--------|-------|-------|------|-------|-------|------|
| T | 0.74 | 20.68 | 0.06 | 0.99 | 4.91 | 0.28 |
| TT | 0.95 | 26.22 | 0.06 | 0.91 | 8.10 | 0.23 |
| AK | 0.84 | 31.01 | 0.01 | 0.90 | 23.30 | 0.06 |
| W | 0.94 | 22.57 | 0.06 | 0.95 | 6.64 | 0.24 |
| PA | 0.59 | 38.33 | 0.04 | 0.97 | 8.27 | 0.30 |
| PO | 0.94 | 22.84 | 0.05 | 0.99 | 3.89 | 0.35 |
| CA | 0.56 | 31.52 | 0.07 | 0.75 | 3.33 | 0.44 |
| VE | 0.76 | 36.33 | 0.08 | 0.87 | 3.14 | 0.47 |
| G1 | 0.52 | 26.22 | 0.01 | 0.88 | 18.08 | 0.07 |
| G2 | 0.89 | 31.03 | 0.14 | 0.90 | 1.51 | 0.59 |
| G3 | 0.82 | 26.27 | 0.05 | 0.96 | 7.78 | 0.24 |
| G4 | 0.80 | 30.19 | 0.12 | 0.96 | 1.56 | 0.58 |

rainfall kinetic energy indicated that soil splashed was better correlated with rainfall intensity than kinetic energy. The splashability index (B) calculated from the slope of the relationship between soil splashed and rainfall intensity is presented in Table 5.10 for all the samples used.

5.5 Physical models

The splashability index (k) calculated from equation (4.8) is presented in Table 5.8. for all the samples The values of dynamic splashability index (ξ) calculated from equation (4.27) for different d_{\max} values are also presented in Tables 5.9a-b.

Table 5.8: Splashability Index (k) of soils used.

| Sample | Average soil Soil splashed g min^{-1} | Percentage soil splashed | Splashability Index (k) $*10^{-2} \text{ min}^{-1}$ |
|--------|--|-----------------------------|---|
| PA | 35.28 | 22.91 | 12.28 |
| G4 | 24.09 | 22.48 | 12.06 |
| AK | 30.25 | 19.88 | 11.09 |
| VE | 30.93 | 19.59 | 11.21 |
| CA | 27.70 | 18.79 | 10.40 |
| G1 | 25.55 | 18.05 | 9.98 |
| G3 | 23.81 | 16.87 | 9.31 |
| PO | 20.70 | 16.50 | 9.01 |
| TT | 23.57 | 15.98 | 8.72 |
| G2 | 24.22 | 14.31 | 7.71 |
| W | 20.25 | 14.26 | 7.69 |
| T | 18.51 | 14.08 | 7.59 |

Table 5.9a: Determination of Splashability Index (ξ)

| Sample | $K_s / (\text{m s}^{-1})$ $*10^{-7}$ | I (mm/hr) | $\Delta m'$ (g) | ζ (%) | $\xi (\text{m}^2 / \text{s}^4)$ $*10^{-10}$ |
|--------|---|-----------|-----------------|-------------|--|
| TT | 5.60 | 73.39 | 125.06 | 83.90 | 1.49 |
| W | 1.60 | 73.39 | 110.69 | 70.90 | 0.57 |
| T | 1.10 | 73.39 | 114.48 | 53.40 | 0.50 |
| AK | 48.90 | 73.39 | 118.55 | 70.40 | 16.30 |
| PA | 152.00 | 78.11 | 120.39 | 58.40 | 64.00 |
| PO | 5.60 | 78.11 | 99.29 | 48.40 | 3.45 |
| CA | 48.90 | 78.11 | 115.28 | 63.40 | 19.81 |
| VE | 48.90 | 78.11 | 154.59 | 34.90 | 26.84 |
| G1 | 5.60 | 65.07 | 104.70 | 57.70 | 2.29 |
| G2 | 5.60 | 65.07 | 152.35 | 65.10 | 1.39 |
| G3 | 5.60 | 65.07 | 126.23 | 59.20 | 1.85 |
| G4 | 48.90 | 65.07 | 86.82 | 45.60 | 30.47 |

$$\text{Determination of } \xi = 2 \frac{K_s k l d^3}{d_{\max} \Delta m'}$$

For $k = 2.34 * 10^6 \text{ kg/m}^2 \text{ s}^2$ when $d = d_{\max} = 0.54 \text{ mm}$

Table 5.9b: Determination of Splashability Index (ξ)

| Sample | $K_s (\text{ms}^{-1}) * 10^{-7}$ | I(mm/hr) | $\Delta m'$ (g) | ζ (%) | $\xi (\text{m}^2 / \text{s}^4) * 10^{-10}$ |
|--------|----------------------------------|----------|-----------------|-------------|--|
| TT | 5.60 | 182.32 | 118.11 | 83.90 | 0.49 |
| W | 1.60 | 182.32 | 135.20 | 70.90 | 0.15 |
| T | 1.10 | 182.32 | 121.24 | 53.40 | 0.15 |
| AK | 48.90 | 182.32 | 124.14 | 70.40 | 4.90 |
| PA | 152.00 | 160.52 | 108.29 | 58.40 | 18.52 |
| PO | 5.60 | 160.52 | 106.55 | 48.40 | 0.84 |
| CA | 48.90 | 160.52 | 118.28 | 63.40 | 5.02 |
| VE | 48.90 | 160.52 | 123.37 | 34.90 | 8.75 |
| G1 | 5.60 | 161.77 | 127.55 | 57.70 | 0.59 |
| G2 | 5.60 | 161.77 | 161.06 | 65.10 | 0.42 |
| G3 | 5.60 | 161.77 | 111.03 | 59.20 | 0.66 |
| G4 | 48.90 | 161.77 | 96.52 | 45.60 | 8.63 |

$$\text{Table: Determination of } \xi = 2 \frac{K_s k l d^3}{d_{\max} \Delta m'}$$

For $k = 0.96 \cdot 10^6 \text{ kg/m}^2 \text{ s}^2$ when $d = d_{\max} = 0.30 \text{ mm}$

Table 5.10: Splashability Indices of B, k, and ξ

| Sample | B | $k \cdot 10^{-2} / \text{min}$ | $\xi \cdot 10^{-10} (\text{m}^2/\text{s}^4)$ |
|--------|------|--------------------------------|--|
| PA | 0.09 | 12.28 | 39.04 |
| G4 | 0.13 | 12.06 | 18.87 |
| AK | 0.01 | 11.09 | 9.99 |
| VE | 0.14 | 11.21 | 16.84 |
| CA | 0.12 | 10.40 | 12.08 |
| G1 | 0.02 | 9.98 | 1.41 |
| G3 | 0.05 | 9.31 | 1.15 |
| PO | 0.06 | 9.01 | 2.11 |
| TT | 0.04 | 8.72 | 0.92 |
| G2 | 0.14 | 7.71 | 0.89 |
| W | 0.04 | 7.69 | 0.34 |
| T | 0.04 | 7.59 | 0.31 |

Table 5.11a: Coefficient Indices

| Sample | B | B^* | $k \cdot 10^{-2} / \text{min}$ | $\xi \cdot 10^{-10} (\text{m}^2/\text{s}^4)$ |
|--------|------|-------|--------------------------------|--|
| PA | 0.09 | 0.30 | 12.28 | 64.00 |
| G4 | 0.13 | 0.58 | 12.06 | 30.47 |
| AK | 0.01 | 0.06 | 11.09 | 16.30 |
| VE | 0.14 | 0.50 | 11.21 | 26.84 |
| CA | 0.12 | 0.44 | 10.40 | 19.81 |
| G1 | 0.02 | 0.07 | 9.98 | 2.29 |
| G3 | 0.05 | 0.24 | 9.31 | 1.85 |
| PO | 0.06 | 0.35 | 9.01 | 3.45 |
| TT | 0.04 | 0.23 | 8.72 | 1.49 |
| G2 | 0.14 | 0.59 | 7.71 | 1.39 |
| W | 0.04 | 0.24 | 7.69 | 0.57 |
| T | 0.04 | 0.28 | 7.59 | 0.50 |

Table 5.11b: Summary of the soil parameters

| Sample | % Soil splashed | Mech ratio | %Clay content | Sand/(clay+silt) % | % Fe | Ave $\xi^* 10^{-10}$ (m^2/s^4) | Ave $k^* 10^{-2}$ min^{-1} |
|--------|-----------------|------------|---------------|--------------------|------|------------------------------------|------------------------------|
| PA | 22.91 | 14.15 | 6.60 | 5.85 | 7.92 | 39.04 | 12.28 |
| G4 | 22.48 | 5.85 | 14.60 | 2.27 | 4.05 | 18.87 | 12.06 |
| AK | 19.88 | 5.85 | 14.60 | 2.76 | 3.78 | 9.99 | 11.09 |
| VE | 19.59 | 5.02 | 16.60 | 3.07 | 3.80 | 16.84 | 11.21 |
| CA | 18.79 | 4.38 | 18.60 | 1.89 | 5.37 | 12.08 | 10.40 |
| G1 | 18.05 | 3.85 | 20.60 | 1.59 | 7.07 | 1.41 | 9.98 |
| G3 | 16.87 | 3.42 | 22.60 | 1.45 | 7.58 | 1.15 | 9.31 |
| PO | 16.50 | 3.07 | 24.60 | 1.15 | 2.59 | 2.11 | 9.01 |
| TT | 15.80 | 2.50 | 28.60 | 2.27 | 8.06 | 0.92 | 8.72 |
| G2 | 14.31 | 2.07 | 32.60 | 0.98 | 9.82 | 0.89 | 7.71 |
| W | 14.26 | 1.73 | 36.60 | 1.15 | 3.43 | 0.34 | 7.69 |
| T | 14.08 | 0.93 | 52.60 | 0.55 | 9.55 | 0.31 | 7.59 |

5.5.1 Relationship between soil splashed and some soil properties

The regression plot of percent soil splashed versus mechanical ratio is presented in Figure 5.2. The plot was approximately linear with positive and significant correlation coefficient ($r = 1.00$). The regression plot of percent soil splashed against clay content was approximated by a negative linear relationship with a significant negative correlation ($r = -1.00$) (Figure 5.3a). The regression plot for the relationship between soil splash and values of sand/(clay + silt) was also linear with a highly significant and positive correlation coefficient ($r = 0.99$) (Figure 5.3b). However iron content showed a strong negative correlation with soil splashed ($r = -0.99$) (Figure 5.4). Even though organic carbon and calcium showed an apparent negative relationship with

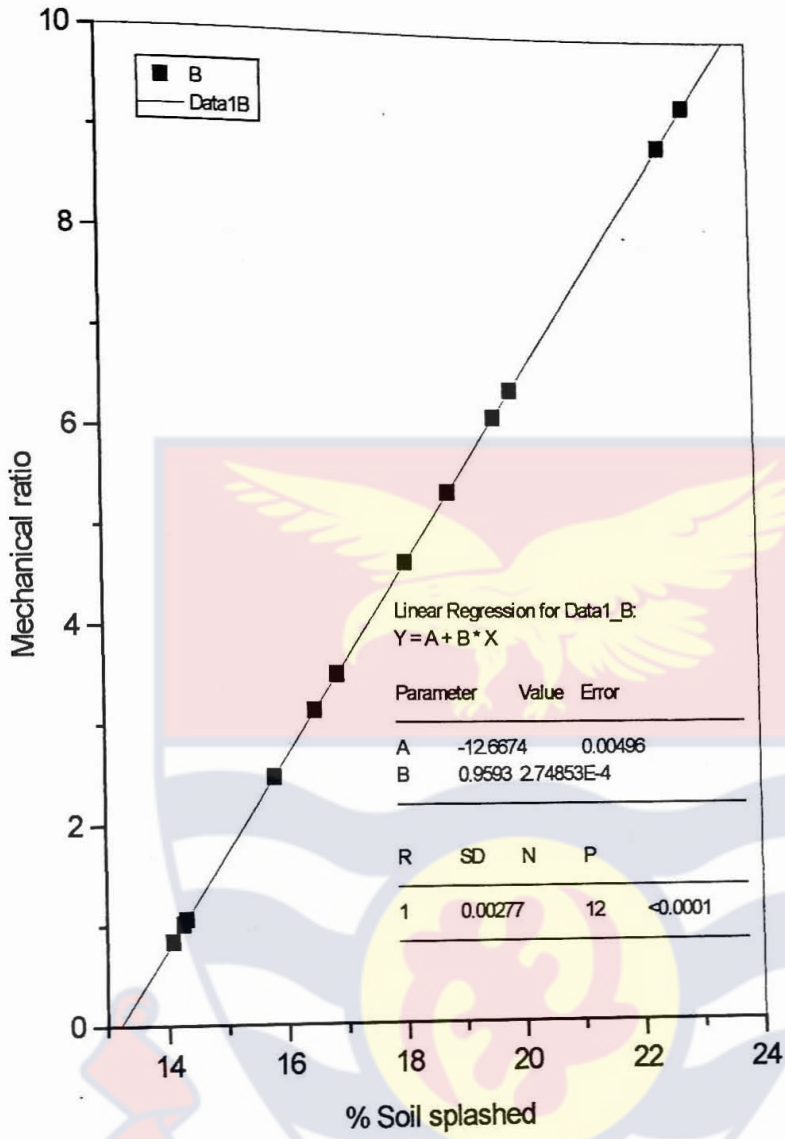


Figure 5.2: Plot of Mechanical ratio versus percentage soil splashed

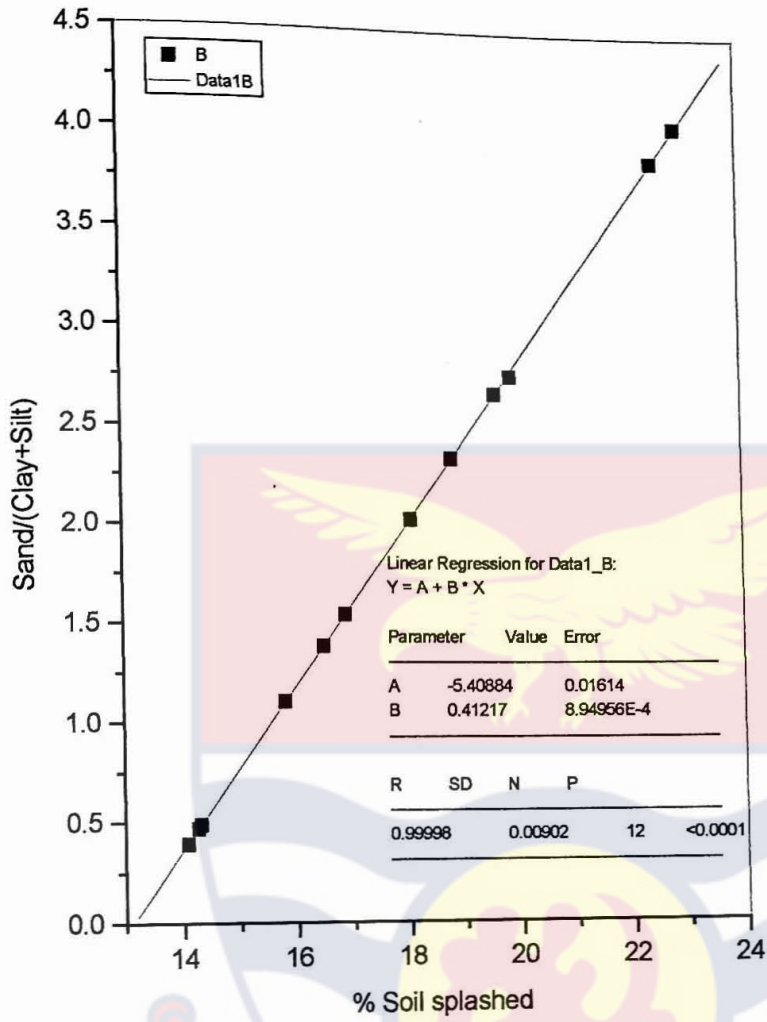


Figure 5.3b: Plot of sand/(clay+ silt)and percentage soil splashed

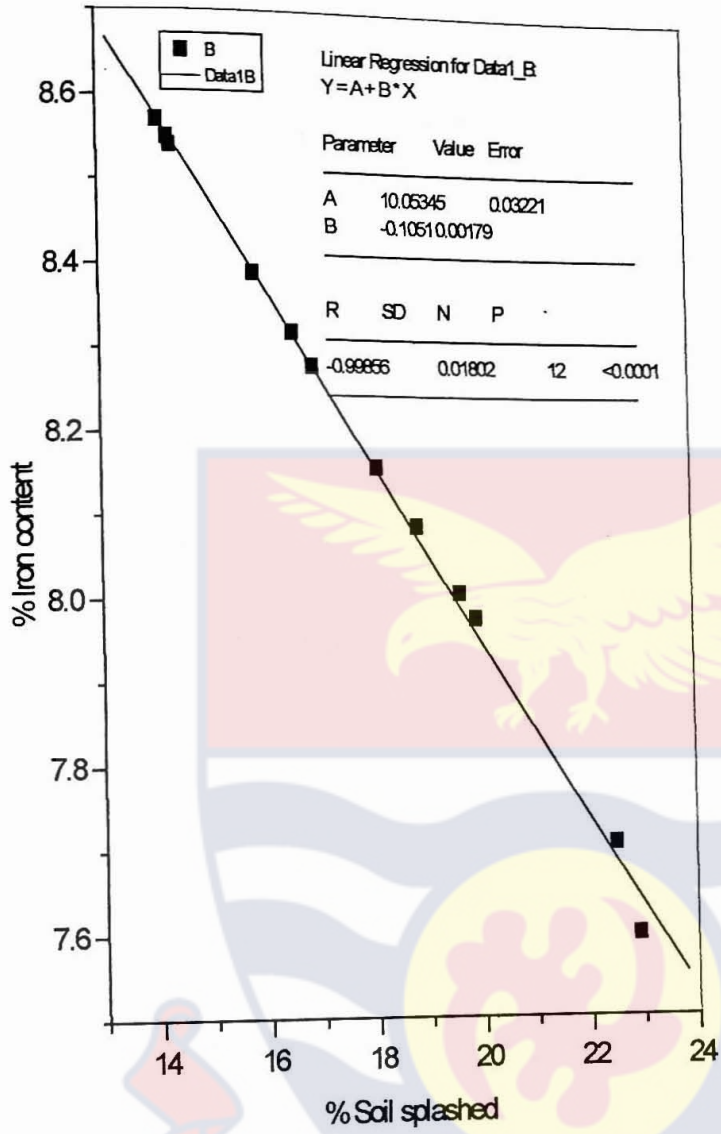


Figure 5.4: Plot of % iron against % soil splashed

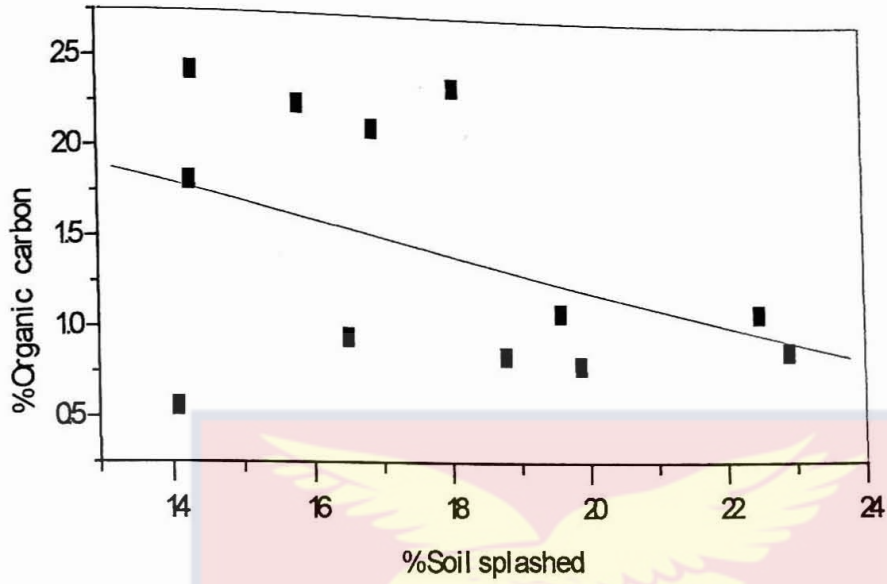


Figure 55: Plot of soil splashed against percentage carbon content

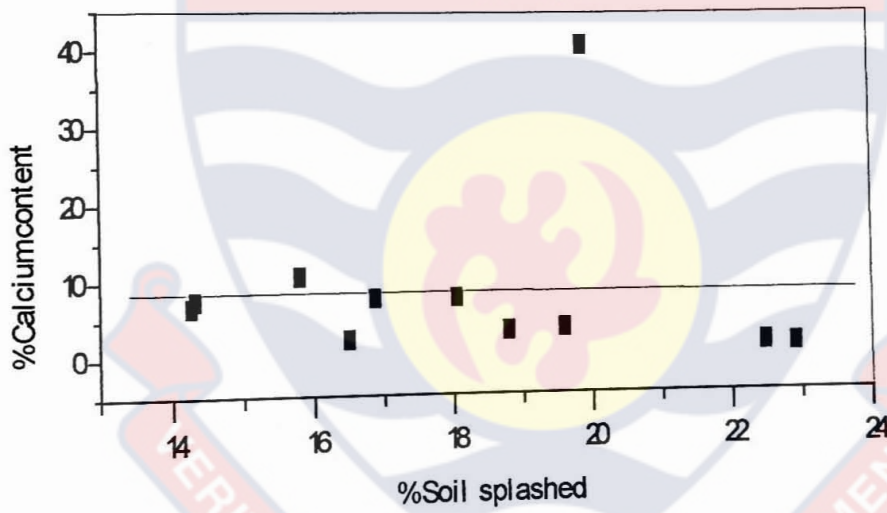


Figure 56: Plot of soil splashed against calcium content

5.5.2 Relationship between soil splashability indices, soil splash and some soil properties

As was expected soil splash increased as the kinetic energy increased (Figure 5.7). The splashability index (k) (see eq 4.8) was strongly linearly related with soil splash with a highly significant positive correlation coefficient ($r = 0.99$) (Figure 5.8a). A similar

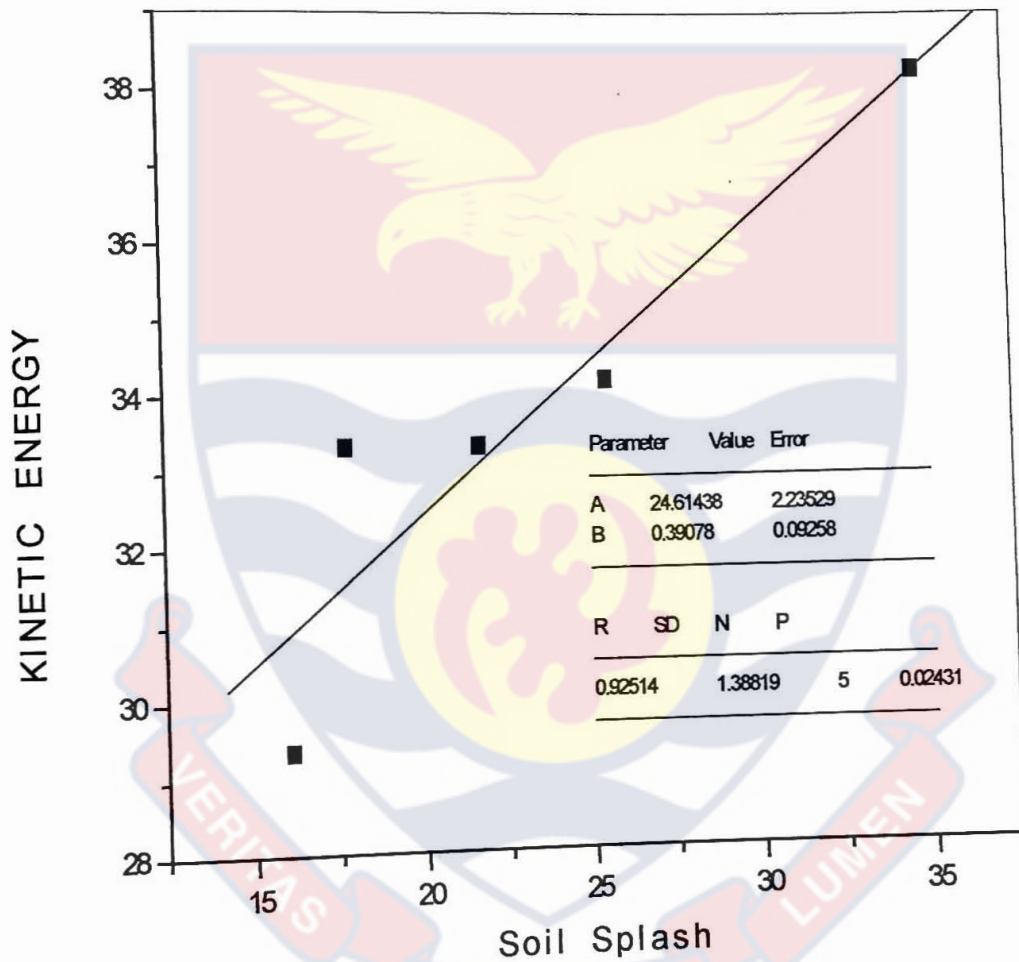


Figure 5.7: Plot of Soil splash against Kinetic energy

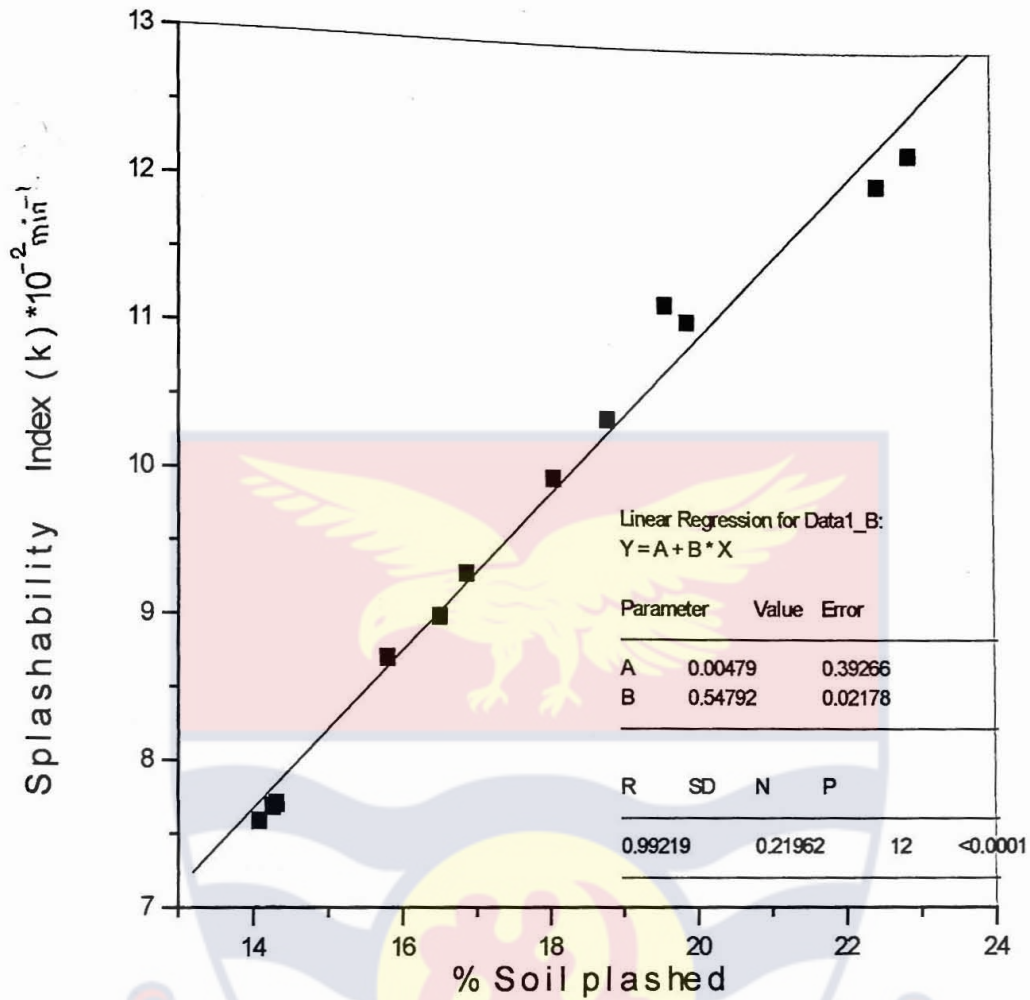


Figure 5.8 a : Plot of Splashability Index (k) against soil splashed

positive linear relationship existed between the splashability index (k) and mechanical ratio ($r = 0.97$) (Figure5.8b), like soil splash the splashability index(k) was also

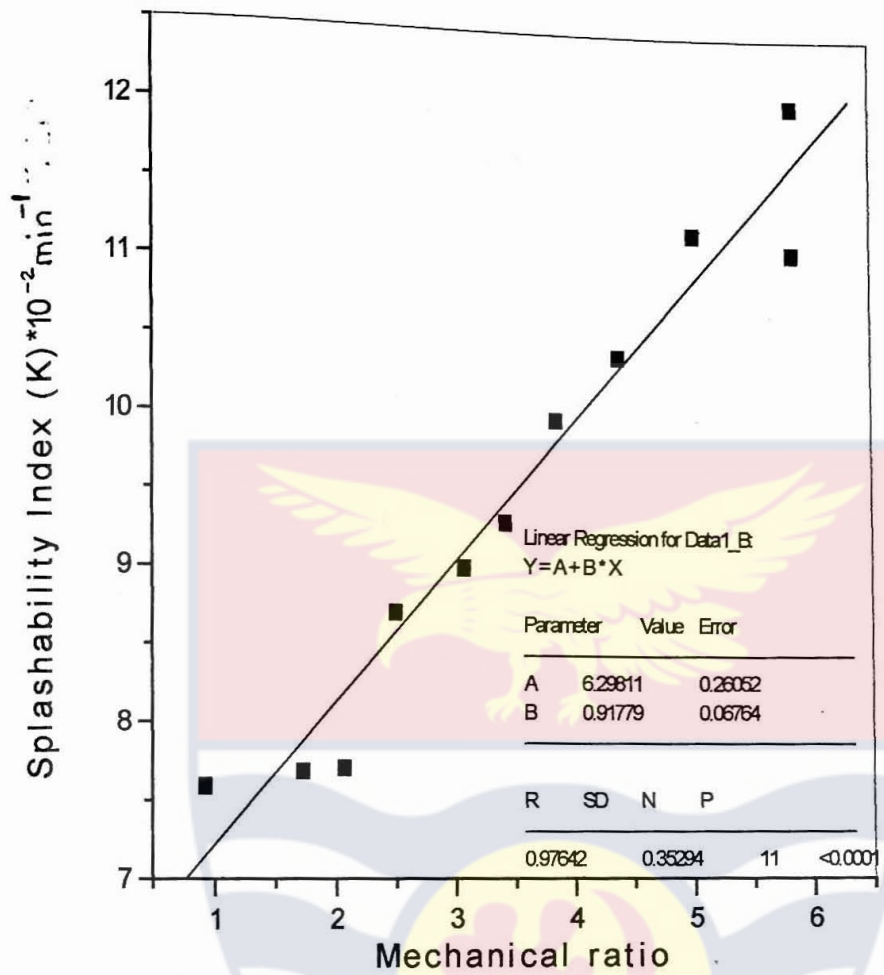


Figure 58b: Plot of Splashability index (k) against mechanical ratio

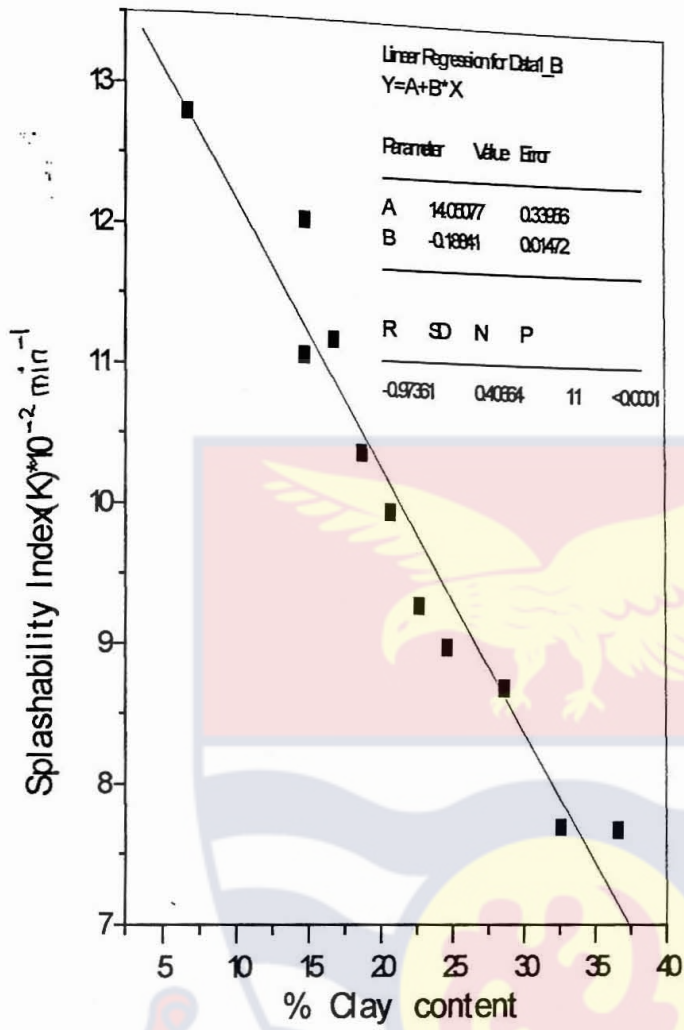


Figure 58c: Plot of Splashability Index (k) against Clay content

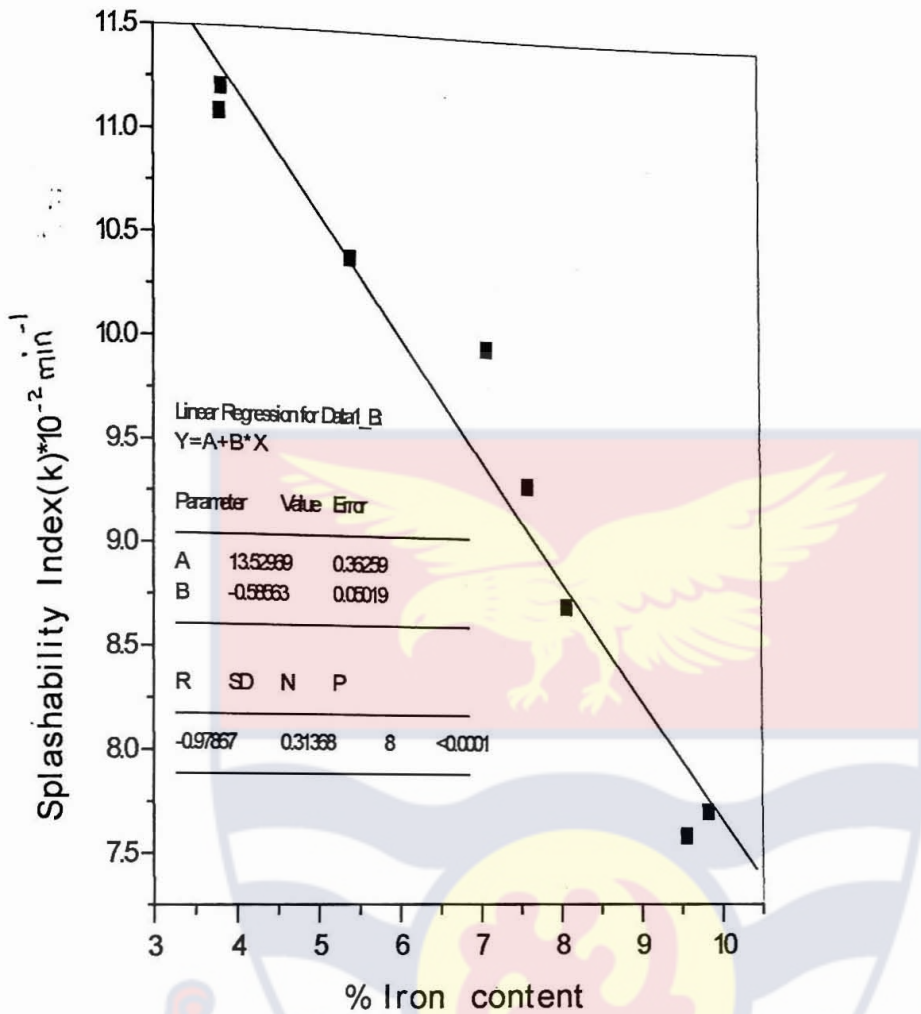


Figure 5.8d: Plot of Splashability Index(K) against Iron content

negatively related with clay content and iron content (Figures 5.8c and 5.8d) respectively. As with soil splashed, a positive linear relationship existed between the splashability index (k) and the factor sand/(clay + silt).

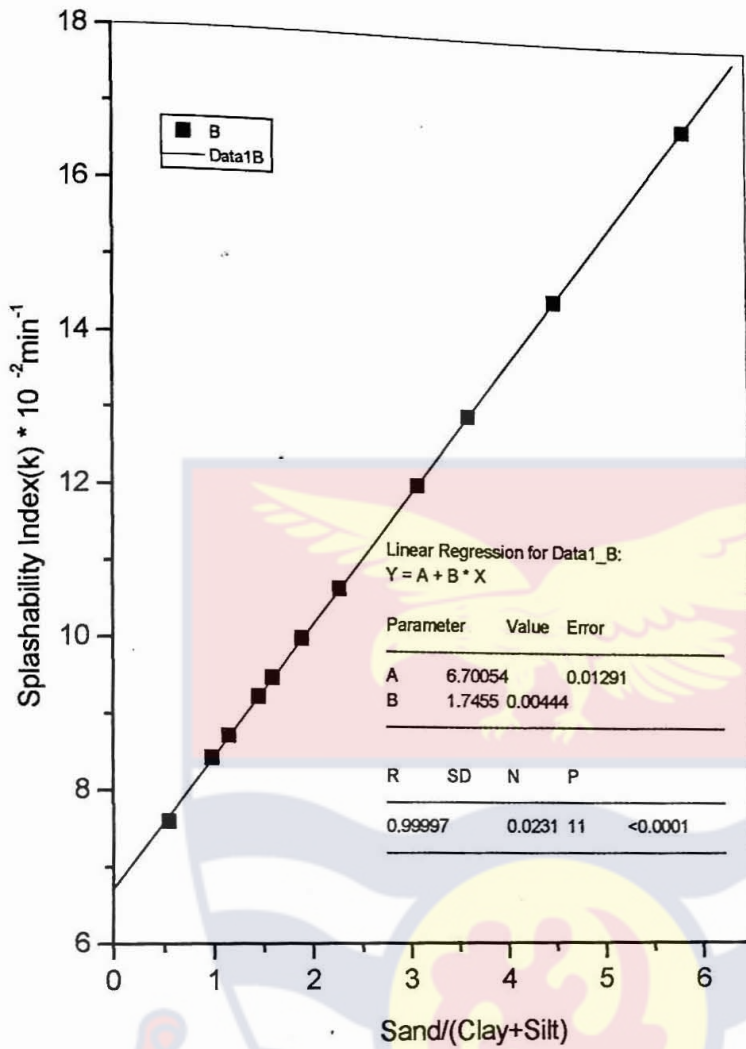


Figure 5.8e: Plot of Splashability index(k) against sand/(clay+silt)

The dynamic splashability index (ξ) (eq. 4.27) similarly behaved as the splashability index (k)(eq 4.8) with respect to their relationships with soil splash, mechanical ratio, clay content, and iron content (see Figures 5.9a-d). The similarity and behaviour of these two splashability indices (k and ξ) was demonstrated by a significant linear positive relationship between the two indices ($r = 1.00$) (Figure5.10)

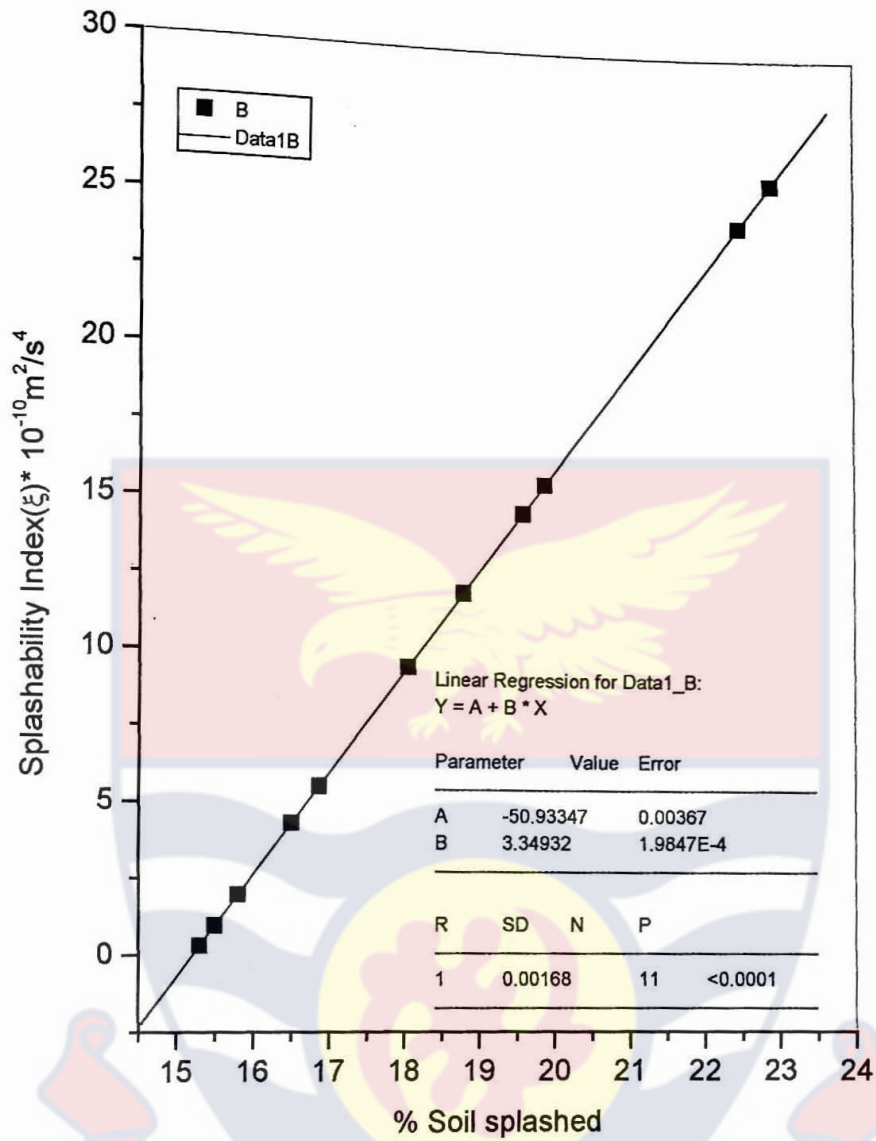


Figure 5.9a: Splashability Index(ξ) against % soil splashed

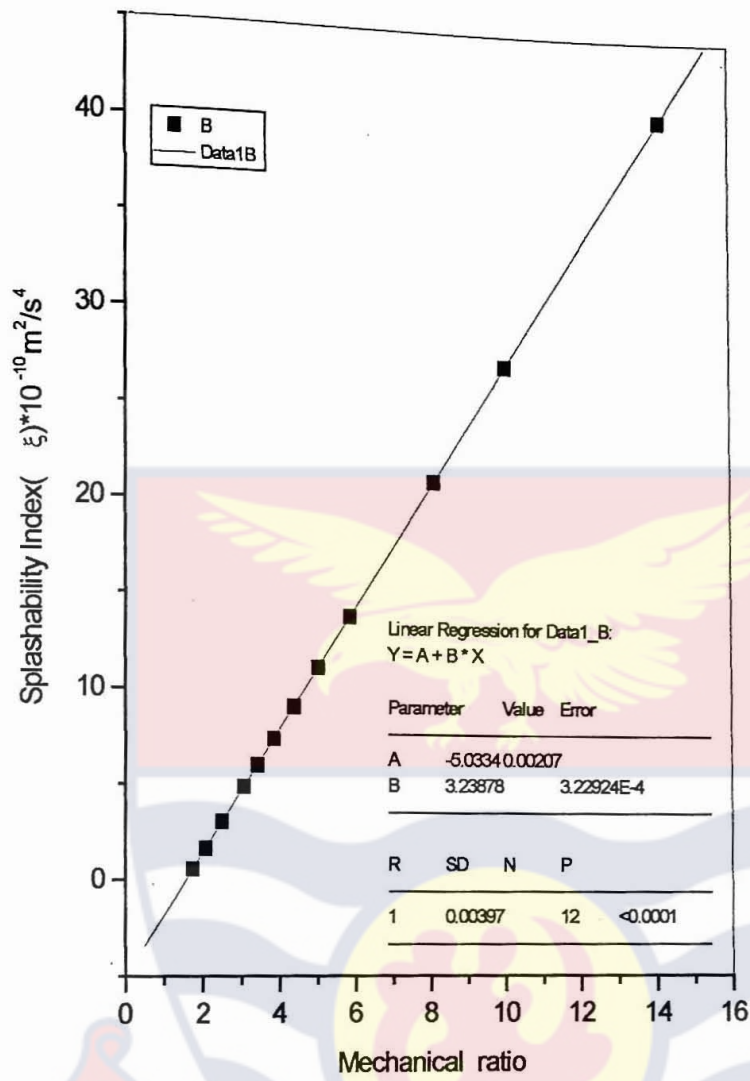


Figure5.9b: Splashability Index(ξ)against Mechanical ratio

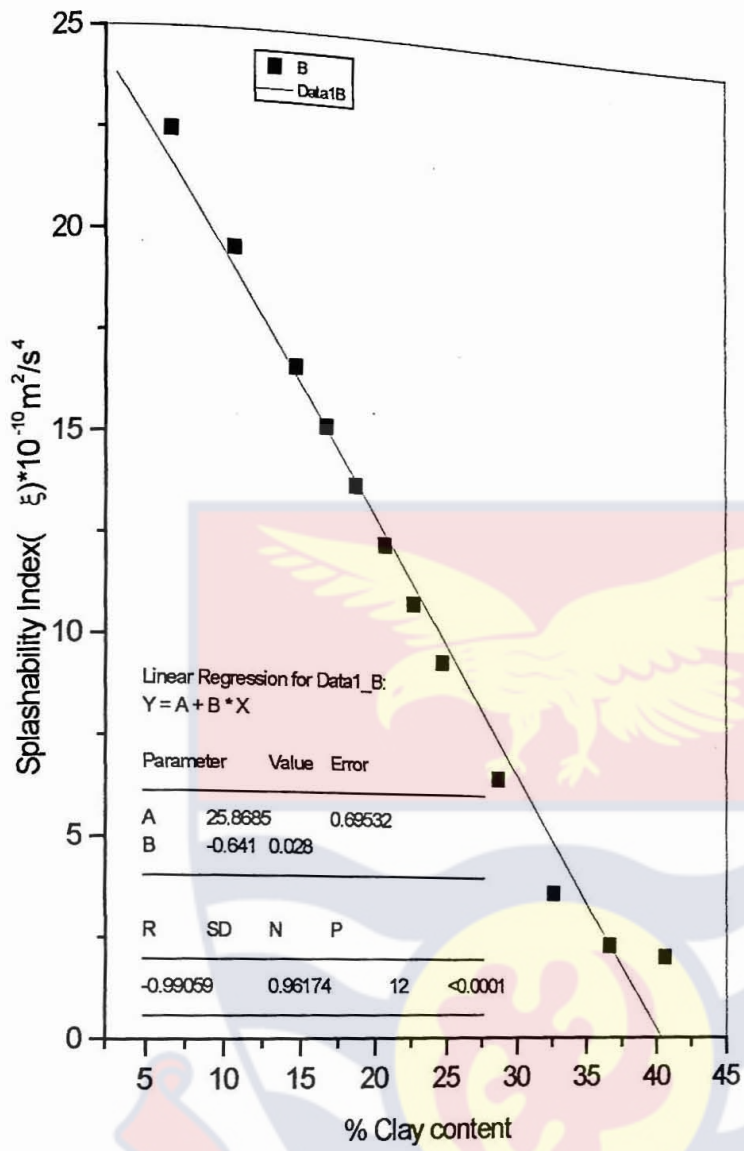


Figure 5.9c : Plot of splashability against % clay content

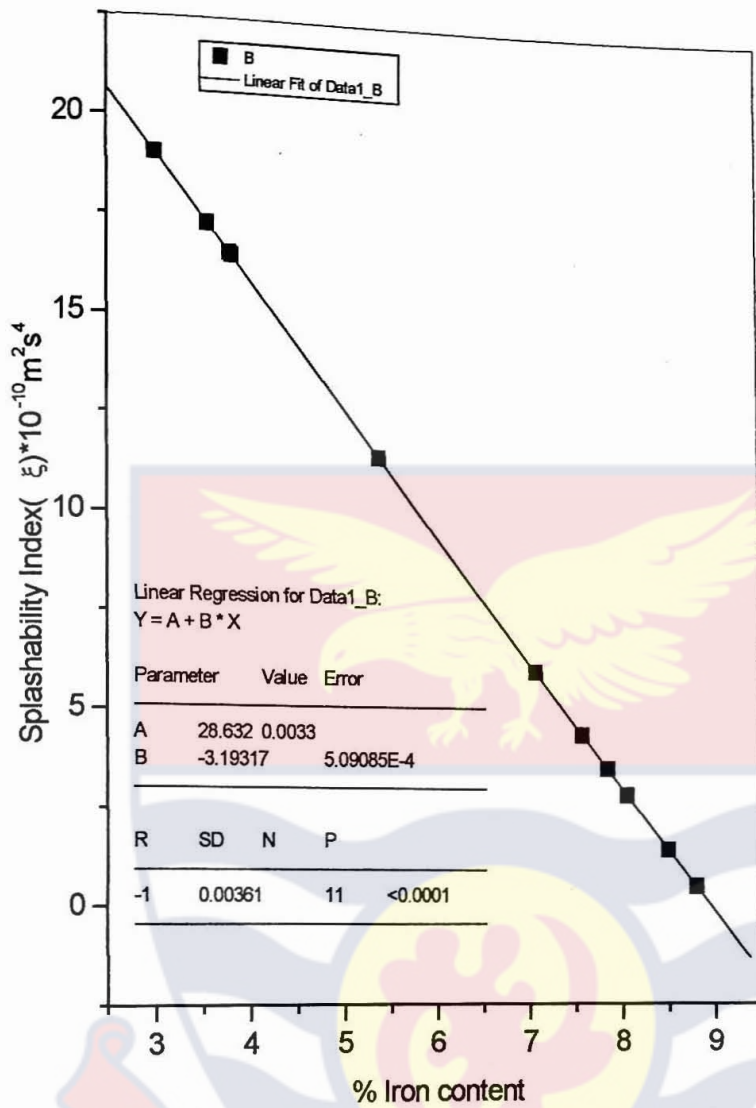


Figure 5.9d : Splashability Index(ξ) against % Iron content

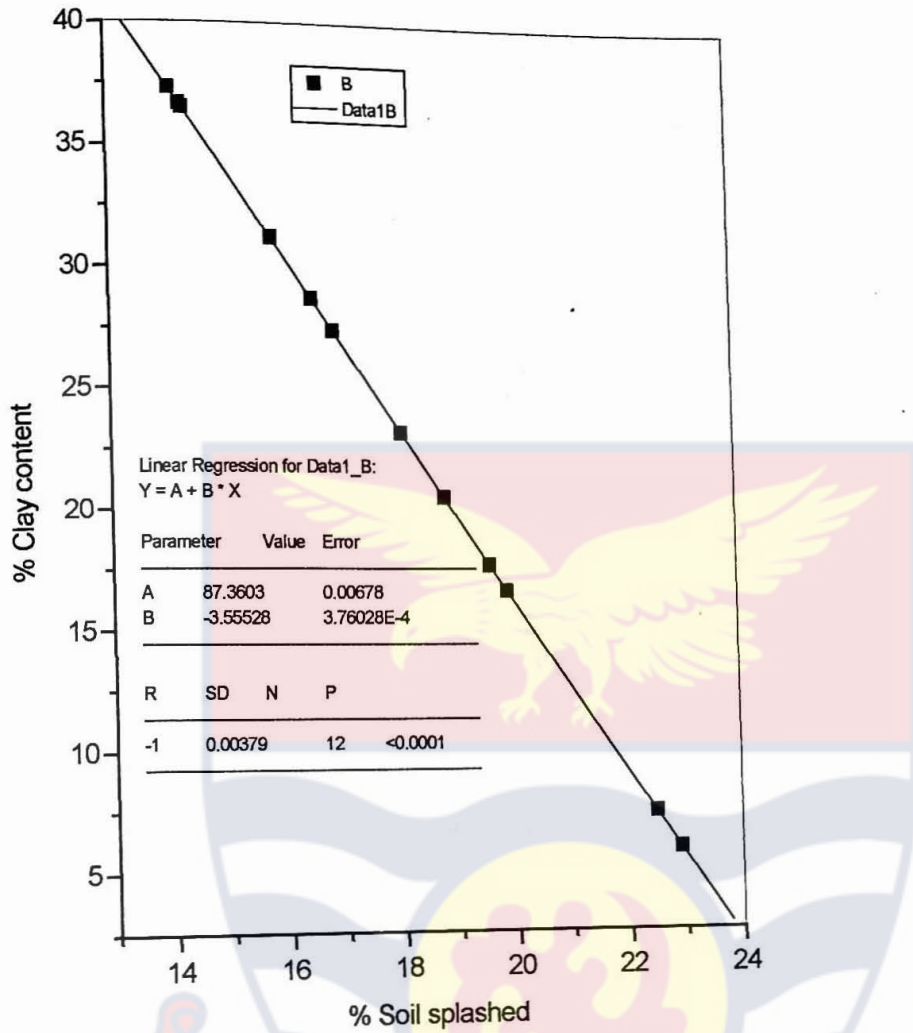


Figure 5.3a: Percentage clay content against soil splashed

soil splashed, the correlation coefficients were not significant ($r = -0.237$ and -0.238) respectively (Figures 5.5 and 5.6).

CHAPTER SIX

6.0 DISCUSSION

6.1 Splashability versus soil properties

The soil samples ranged in texture from sandy clay loam to clay. Generally soils that are high in fine sand and silt and low in clay were most erodible. Soil containing low amount of clay were easily dispersed. The results appeared to indicate that splashability of soils decreased as the sum of the percentage of sand and silt decreased (Table 5.0 and 5.8). The sample PA, containing 6.6% of clay had the highest splashability rate. The sample with the lowest splashability rate was sample T, which had almost 53% of clay. Organic carbon content of the samples was very low, and because of this no meaningful relationship could be established between soil splashed on one hand and organic carbon content on the other hand. However De Vleeschauwer et al (1978) and Vanelslande et al (1984,1985) observed that the organic carbon content of some Nigerian soils was significantly negatively related to the soils' susceptibility to erosion. Both clay and soil organic carbon are important soil colloids required for soil structure stabilization.

Aggregate stability did not correlate with soil splashed. There may be several reasons for this discrepancy. The greatest problem in determining aggregate stability by wet sieving is achieving a consistent method of pre-wetting the sample for analysis. In addition, rapid wetting of dry soil samples tend to destroy large aggregates. During

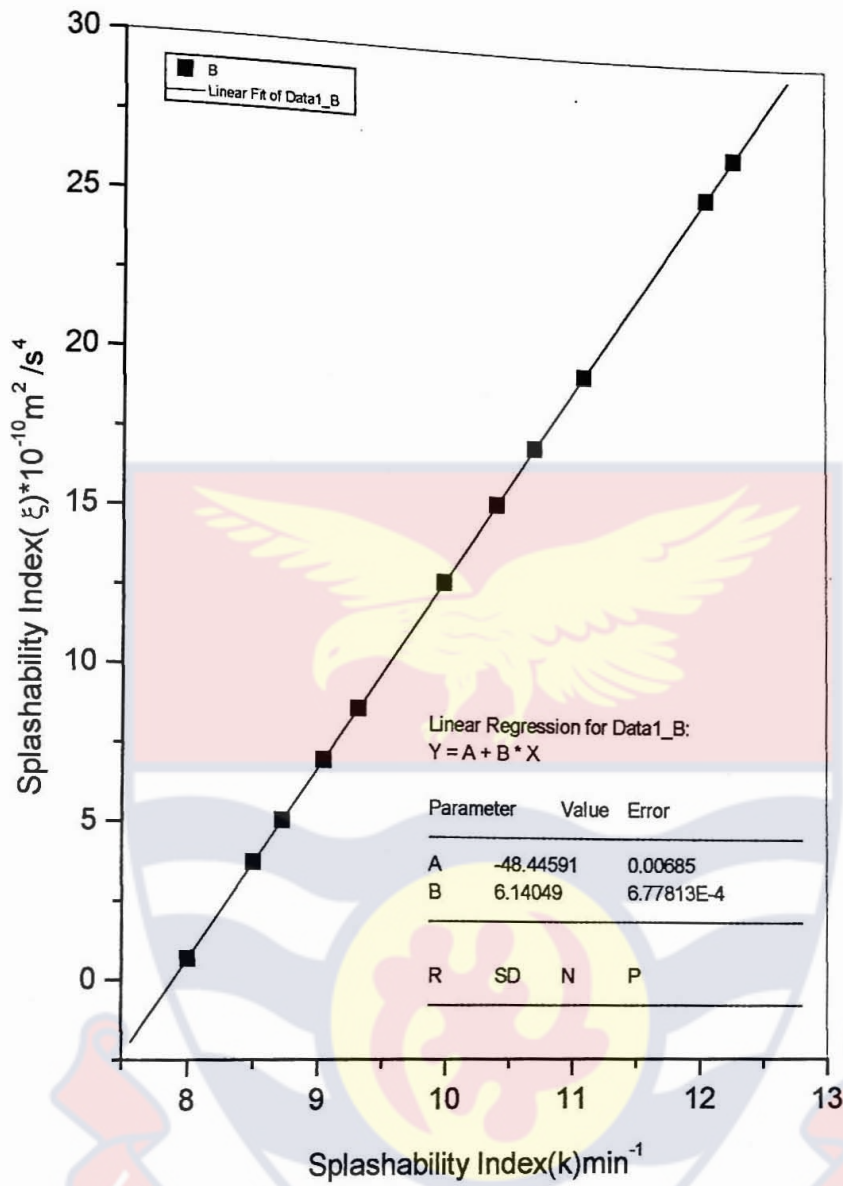


Figure 5.10 : Plot of ξ against k

splash smaller particles, which are clay and silt turn to be splashed away quicker than the larger particles. In general an inverse correlation exists between the percentage of water-stable aggregates and soil splashed (Woodburn and Kozachyn 1956, Adam et al 1958, Young and Onstad 1982). However Sahi et al. (1976) observed that the degree of aggregation alone is not a sufficient index of soil's ability to resist erosion.

Mechanical ratio correlated well with soil splashed (Figure 5.2). The soil with greater amount of soil splashed had the higher mechanical ratio. Sample T that contained high percentage of clay had lower mechanical ratio. Because of the importance of soil texture, susceptibility of soil to erosion has been related to texture-based indices for many soils from different part of the world. In India mechanical ratio has been related to the extent of erosion measured in the field (Chibber et al 1961, Sahi et al 1977, Jha and Rathore 1981, Bhatia and Vadani 1982).

The samples contained more bivalent cations (Ca^{2+} and Mg^{2+}) than the monovalent cations (Na^+ and K^+) (Table 5.2). The soils with least amount of splash contained more Ca^{2+} than those that had greater amount of splash. The charge of cation on the exchange complex influences the soil structure type. A soil containing bivalent cations has more stable structure than those containing monovalent cations. The presence of Na^+ on the exchange complex normally increases soil dispersibility.

The plot of soil splashed against percentage iron content revealed that soil splashed decreased with an increased percentage iron content (see Figure 5.4). The iron content gave the soils their stable structure. It has been noted that in tropical soils iron content is among the important soil properties responsible for the stabilization of the soil, especially the sub-soil (Baver et al 1972). Samples of plots between the soil splashed

and rainfall intensity (Fig 5.0 a-d) revealed that soil splash increased with rainfall intensity. For a given amount of rainfall, high-intensity rain produces more splash than low intensity rain. Many researchers have shown that rainfall intensity is more important than rainfall amount (Nichols and Saxton 1932, Foster and Meyer 1972 and Meyer 1981). Inoue (1985) observed a logarithmic relation between intensity and splash.

6.2 The splashability indices

The splashability indices were subjected to tests with other erosion indices and other properties of soil indicative of erodibility.

The slope of the relationship between soil splashed and rainfall intensity was used as empirical coefficient of splashability. This coefficient was used to compare two splashability indices derived from the physically based models in equation (4.8) and equation (4.27). The correlations were highly positive and significant for two groups of samples (AK, TT, W, T) where ($r = 0.964$) and for (PA, VE, CA, PO) where ($r = 0.801$). However for samples (G4, G3, G2, G1) the correlation was very poor ($r = 0.056$). The reason for this may be due to the fact that while the eight samples were taken from different locations the G samples were taken from the same location on different gradients with similar properties.

Higher kinetic energies produced higher splash rates for the same constant drop size. Increase in drop size also increased the splash rates (Table 5.6c,d). Kinetic energy strongly and positively correlated with soil splash (Fig 5.7). It is widely accepted that kinetic energy of impacting raindrops is the key factor responsible for soil splash (Ekern 1950, Mihara 1951, Bubenzer and Jones 1971). Some researchers have argued

that soil splash is related more to the momentum of raindrops than to the kinetic energy. The controversy regarding the relative importance of kinetic and momentum seems trivial because both are considered when collision problems which splashability is a part is under consideration. The two physically based splashability indices from equations (4.8) and (4.27) all correlated well with the soil parameters such as mechanical ratio, percentage iron and clay contents. However there were poor correlations between the indices and organic carbon content, calcium content and aggregate stability. Measurement of organic carbon content and aggregate stability should enable us to assess the risk of structural degradation. However, such measurements are sometimes inconsistent with erosion measurements and runoff (Wischmeier et al., 1971; Boiffin, 1984; Trott and Singer 1983; Ekwne, 1990; Loch and Foley, 1994). This may be because organic carbon and calcium contents are not the only soil properties influencing structure within any one of these types of soils.

Sahi et al (1976) observed that the degree of aggregation alone was not a sufficient index of soil ability to resist erosion. Attempts to use aggregate stability to predict soil susceptibility to erosion have yielded conflicting results. Aggregate stability has been reported to correlate with soil erodibility positively (Bryan, 1968; Elwell, 1986; Amezketa et al., 1996), negatively (Bajracharya et al., 1992) and nonsignificantly (Miller and Baharuddin, 1987). These incongruities could be attributed, at least in part, to the large variety of methods used to determine aggregate stability.

From the results we observed that soil splashability is related to three rainfall characteristics: rainfall intensity, raindrop-size, and kinetic energy. This could not be fortuitous since this is a well-known fact in soil erosion studies.

The indices derived from equations (4.8) and (4.27) were similar in their performance as soil splashability index. However, since the index derived from equation (4.8) was simpler, its use in describing soil splashability should be encouraged.

For all the samples the rates of soil splashed due to rainfall detachment increased with increasing rainfall rates. Soils in tropical regions are generally more prone to erosion by water than those in the temperate regions. It is also generally believed that erodibility factor of soils of the tropics is low (Roose 1977). Therefore, high risks of soil erosion in the tropics must play a larger part related to rainfall erosivity. Hudson (1995) argued that high intensity tropical rains might have a high-energy load than those in the temperate regions.

Our data show that splash erosion is a time-dependent process and is influenced primarily by rainfall energy and to a lesser extent by interaction with antecedent soil moisture status. Data of this type are essential for incorporation into state-of-the-art erosion prediction models if they are to be truly universal.

The lack of substantial increase in splash rate at higher rainfall intensity is similar to many results described in the literature. Several researchers have suggested that such a pattern reflects soil seal development (Remley and Bradford 1989, Luk and Cai 1990). Thus, formation of surface seal usually coincides with substantial reduction in splash detachment and increase in soil strength (Remley and Bradford 1989). It is not clear from the present study whether a seal formed, but it cannot be ruled out as suggested by El-Swaify (1980) for certain Oxisols. However, soil dispersion is a precursor to seal formation (Baver et al; 1972)

Raindrops also play a more significant role in runoff formation. The flow of water plays a transporting role. A drop generally prepares the soil material for transportation i.e. breaks soil aggregates. The products of dispersion seal the soil pores, reducing the water intake (infiltration) as a result of which runoff increases with associated erosion. Information on the relative significance of rainfall detachment (splash) and runoff entrainment as erosion processes has practical application since management methods differ in their effectiveness in protecting the soil against either erosion mechanism. For example, the interception of raindrops by plant canopies will reduce rainfall detachment (splash), but canopy cover does little in protecting soil against entrainment by overland flow. Surface contact cover, such as mulch, which interrupts overland flow and bears some fraction of the shear stress exerted on the surface by overland flow, is effective against both erosion mechanism. Vegetation protects the soil from splash erosion by intercepting the raindrops and absorbing their kinetic energies and thus reduces the splash detachment and the subsequent transport.

From the dynamic model we found that samples with high splashability index (ξ) had the high rate of splash. The application of a rainfall kinetic energy term is warranted since this allows direct comparison between simulated rainfall and natural rainfall. Rainfall intensities are not directly comparable between non-terminal velocity simulators and natural rainfall, since 100 mm/hr for example from a natural storm has a different energy than a 100-mm/hr storm from most commonly used rainfall simulators. Detailed process-based investigations of splash erosion, and its control are necessary for continued refinement of splash erosion prediction models. This is

particularly true for tropical soils, because there is a dearth of data available for even remedial model parameterisation.

We also found that splash process is influenced by many other factors including aggregate stability. Since splash erosion on cultivated soils result mainly from aggregate breakdown and detachment of fragments by raindrops, it seems likely that the measurement of aggregate stability with an improved method will effectively measure the soils susceptibility to erosion. The methodological framework for such measurement of aggregate stability should take into account the various mechanisms of aggregate breakdown, the way in which the water acts on soil, and the soil physical and chemical properties that influence breakdown.

The application of soil physics theory to practical soil conservation problems offer prospects of substantial progress in the area of determining the erodibility of soils and the monitoring of the physical effects on the soil of various forms of land management practices. The end product of such application should be quantitative evidence for choosing the better land management and soil conservation practices.

On the whole the two physically based splashability indices k and ξ corrected well with soil splashed, mechanical ratio, percentage iron content, percentage clay content and the factor defined as $\text{sand}/(\text{clay} + \text{silt})$. But correlated poorly with organic carbon content percentage calcium content and aggregate stability.

CHAPTER SEVEN

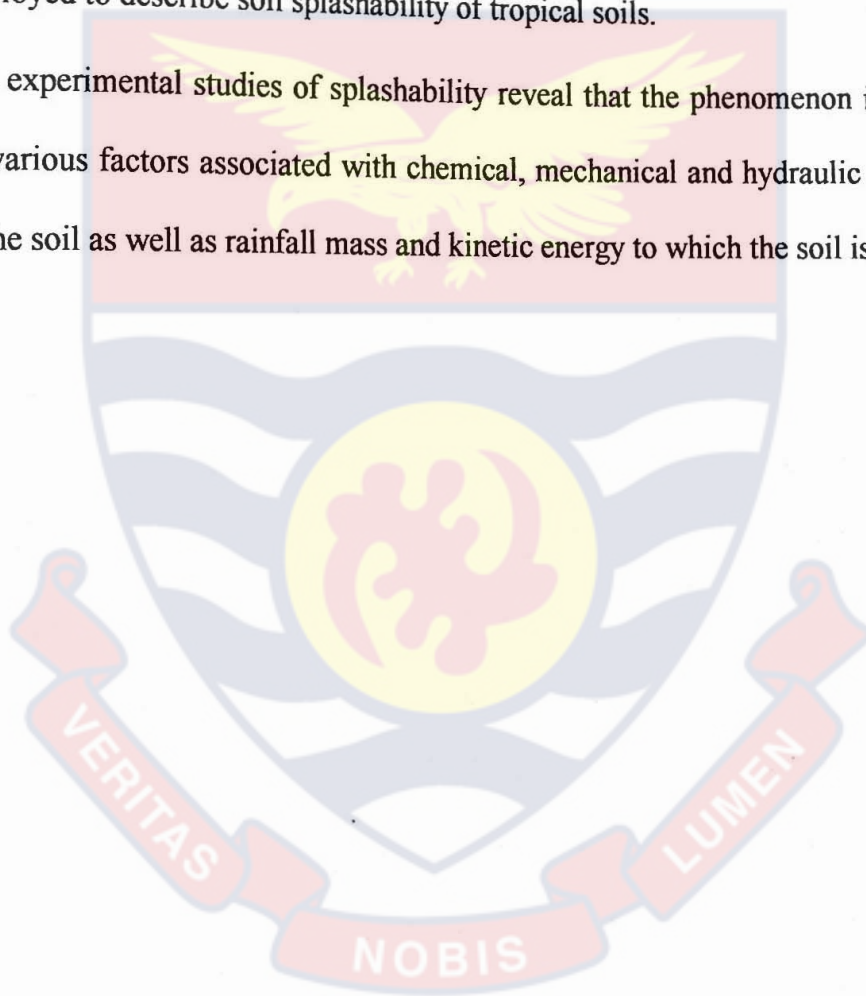
7.0 CONCLUSIONS

It is concluded from this study that:

- The splashability of soil decreases as the sum of percentage of sand and silt decreases. Soils with high percentage of clay have lower splashability rate. This is also confirmed by the fact that regression plot of percentage soil splashed against clay content is approximately negatively linearly correlated.
- The major element in the soils is iron, and this impacted negatively on soil splashability.
- The relationship between soil splashed and rainfall intensity is linear with highly significant correlation. The study confirms that rainfall drop size remaining the same, the higher the kinetic energy of the raindrops the greater the amount of splashed soil per minute.
- The splashability index (k) is linearly correlated with soil splashed, mechanical ratio and the factor defined as $\text{sand}/(\text{clay}+\text{silt})$. The Index (k) is also negatively correlated linearly with percentage clay content, and percentage iron content confirming the significance of clay and iron contents on stability of tropical soils.
- The dynamic splashability index (ξ) is similarly positively correlated with soil splashed, mechanical ratio and the factor defined as $\text{sand}/(\text{clay}+\text{silt})$. The index (ξ) is however negatively correlated with percentage clay content and percentage iron content, showing a similar behaviour as the splashability index (k). The similarity in behaviour of the two splashability indices is demonstrated by a high significant linear relationship between them. However, since the index (k) was

derived from a simpler equation its use in describing soil splashability should be encouraged.

- For the soils studied the two splashability models can also predict their erodibility values.
- It is demonstrated clearly that the models derived from either soil properties deleterious to soil stability or those derived from rainfall characteristics can be employed to describe soil splashability of tropical soils.
- The experimental studies of splashability reveal that the phenomenon is affected by various factors associated with chemical, mechanical and hydraulic properties of the soil as well as rainfall mass and kinetic energy to which the soil is exposed.



CHAPTER EIGHT

8.0 RECOMMENDATIONS AND SUGGESTION FOR FURTHER WORK

8.1 Recommendations

Splash erosion can be a problem to both agriculture and urban erosion.

On the basis of the outcome of this study the following recommendations are made:

- i) Vegetative cover and mulch intercept raindrops and provide excellent protection of the soil from rain splash. Therefore sustainable land clearing methods must be employed to ensure protective soil cover during the onset of the rainy season. In addition mulch should be left on soil surfaces to protect them from being splashed.
- ii) Splash erosion also causes the base of urban mud houses to be exposed. It is recommended that proper landscaping be done(ie by planting grass) to mitigate splash erosion.
- iii) The coastal belt along the central region of Ghana is covered by coastal shrub and grassland (coastal savanna). The soil here ranges from loamy to coastal sandy soil with patches of clay. Most of these soils types are highly susceptible to splash erosion. One common cash crop along the coast is coconut. The coconut trees seem to thrive well on the sandy coastal soil. The dense root system binds the soil and provides additional strength against the shearing force of runoff. But it is doubtful whether the canopy of the trees is able to prevent splash erosion. The coconut tree canopy 10 to 20 m above the ground surface losses its effectiveness because the coalescing drops falling from the canopy are generally big, attain terminal velocity and have high impact energy. Thus splash erosion is common along the coast even though coconut trees are plentiful. One solution would be to introduce *Pueraria* as

cover crops below the coconut trees. Another solution to this problem would be the introduction of dwarf coconut varieties to reduce raindrop impact and splash erosion since the tree canopy is close to the ground.

- iv) Physically based erosion simulation models are much more sophisticated, which in theory allow them to better, describe the influence and interaction of many and various factors that influence erosion. A limitation of current erosion models is their deterministic nature and the physical models may have greater potentials compared to the empirical models in moving from deterministic frame to a probabilistic one. In future more research effort should be put in this direction.
- v) It is further recommended that our models be used to classify and map out the erodibility of major soils in the country to plan for their sustainable use.

8.2 Suggestions for further work

- i) Since soil aggregates influence soil splashability, it will be interesting to investigate the rate of splash of different aggregates of the same soil in Cape Coast area.
- ii) Erosion stability is evaluated from the amount of soil splashed. It is suggested that erosion stability be determined under dynamic conditions taking into account the characters of the protective cover, energy of raindrop and soil properties. It is further suggested that the index of splashability be characterized by taking into account the particle-size, state of aggregation, land form, land slope, soil's rheologic properties, and soil strength like resistance to penetration and shear strength.
- iii) The kinetic energy of raindrops is vital to any calculation involving rainfall splashability. But the forces involved in raindrop impact are so small that any instrument sufficiently sensitive to record them mechanically is liable to be swamped

by wind effects. However, today it is possible to build equipment sensitive enough to measure forces due to raindrop. It will be useful to design pressure transducers that could be used to sense the raindrop impacted in microprocessors to grade, sort and store data generated during rainfall.

- iv) Rainfall simulators provide the possibility to quickly investigate different aspect of erosion processes. Any rainfall simulator used to reproduce natural conditions should be capable of approximating the natural rainfall. However accurate simulation of natural conditions requires understanding of wind effect on falling raindrops. It would therefore be useful to study the splashability of wind-driven rainfall and compare with the splashability of rainfall without the wind.
- v) During rainfall the physical properties of the soil surface change significantly. Some of these changes are surface sealing, variation in infiltration rate, water suction, bulk density and surface roughness. Investigation should be made to find out how these surface changes affect splash erosion.
- vi) It would be interesting as a follow up work to assess how different soil management strategies affect k and ξ .

REFERENCES

1. Adams, J. E., Kirkham, D., and Scholtes, W.H. 1958. Soil erodibility and other physical properties of some Iowa soils. Iowa st. Coll. J. Sci 32:485-540.
2. Agassi, M., Shainberg, I., and Morin, J. 1981. Effect of electrolyte concentration and soil sodicity on infiltration rate and crust formation. Soil Sci. Soc. Am. J. 45:848-851.
3. Agassi, M., Morin, J., and Shainberg, I. 1985. Effect of raindrop energy and water salinity on infiltration rates of sodic soils. Soil Sci. Soc. Am. J. 49:186-190.
4. Al-Durrah, M.M., and Bradford, J.M. 1982a. The mechanism of raindrop splash on surfaces. Soil Sci. Soc. Am. J. 46: 1086-1090
5. Al-Durrah, M.M., and Bradford, J.M. 1982b. Parameters for describing soil detachment due to single water drop impact. Soil Sci. Soc. Am. J. 46 (4): 836-840.
6. Amezketa, E., Singer, M.J., and Le Bissonnais, Y. 1996. Testing new procedure for measuring water-stable aggregates. Soil. Sci. Soc. Am. J. 60:888-894.
7. Atlas, D., and Ulbrich, C.W. 1977. Path and area-integrated rainfall measurements by microwave attenuation and radar methods. J. Rech. Atmos. 8, 275-298.
8. Bajracharya, R.M., Elliot, W.J., and Lal, R. 1992. Interrill erodibility of some Ohio soils based on field rainfall simulations. Soil. Sci. Soc. Am. J. 56:267-272.
9. Barry, P. V., Stott, E.E., Turco, R.R., and Bradford, J.M. 1991. Organic polymers' effect on soil shear strength and detachment by single raindrops. Soil Sci. Soc. Am. J. 55:799-804.

10. Baver, L.D. 1939. Ewald Wollny. A pioneer in soil and water conservation research. *Soil Sci. Soc. Am. J.* 3:330-333.
11. Baver, L.D., Gardner, W.H., and Gardner, W.R. 1972. *Soil Physics* 4th Edition. John Wiley and Sons, Inc., New York
12. Bear, J. 1972. *Dynamics of fluids in porous media*. Elsevier Science. New York.
13. Beard, K.V. 1976. Terminal velocity and shape of cloud and precipitation drops aloft. *Journal of Atmos Sci.* 33: 851-864.
14. Beare, M.H., Hendrix, P.R., and Coleman, D.C. 1994. Water-stable aggregates and organic matter fractions in conventional and no-tillage soils. *Soil Sci. Soc. Am. J.* 58:777-786.
15. Bentley, W.A. 1904. Studies of raindrops phenomena. *Monthly Weath. Rev.* 32: 450-456.
16. Best, A. 1950. The size distribution of raindrops. *Q. J. Roy Meteorol. Soc.* 76:16.
17. Bhatia, K. S., and Vardani, B. 1982. Physicochemical and erosional behaviour of red and black soils of Bundelkhaud region of Uttar Pradesh. *J. Indian Soc Soil Sci.* 30(4): 523-527.
18. Blanchard, D.C. 1950. Behaviour of water drops at terminal velocity. *Trans. Am. Geophys. Union.* 31:836-842.
19. Bonsu, M. 1992. A study of a texture-based equation for estimating the saturated hydraulic conductivity of an alfisol in the Sudan Savannah ecological zone Ghana. *Hydrological Sciences-Journal.* 37:599-606.

20. Boiffin, J. 1984. La degradation Structurale des conches superficielles du sol sous l'action des pluies. These de Docteur-Ingenieur. Institut National Agronomique Paris- Grignon.
21. Bradford, J.M., Ferris, J.E., and Remley, P.A. 1987. Interrill soil erosion processes: II Relationship of splash detachment to soil properties. *Soil Sci. Soc. Am. J.* 51:1571-1575.
22. Bradford, J.M., and Huang, C. 1992. Mechanisms of crust formation physical components :In: *Soil crusting: Physical and Chemical processes* (eds. M.E. Sumner and B.A. Stewart), pp.55-72. Lewis, Boca Raton, Florida.
23. Bruce-Okine, E., and Lal, R. 1975. Soil erodibility as determine by raindrop Technique. *Soil Sci.* 119 (2): 149-157.
24. Bryan, R.B. 1968. Development, use and efficiency of indices of soil erodibility. *Geoderma.* 2: 5-26.
25. Bubenzer, G. D., and Jones, A. B., Jr. 1971. Drop size and impact velocity effects on the detachment of soils under simulated rainfall. *Trans. ASAE* 14 625-628.
26. Bubenzer, G.D. 1980. An overview of rainfall simulators page No 80-2033. American Society of Agricultural Engineers. St. Joseph Michigan.
27. Carslaw, H.S., and Jaeger, J.C.1959. *Conduction of Heat in Solids.* 2nd ed. Oxford University Press, London
28. Chiang, S.C., West, L.T., and Radcliffe, D.F. 1994. Morphological properties of surface seal in Georgia soils. *Soil Sci. Soc. Am. J.* 58: 901-910.
29. Chenu, C. 1989. Influence of a fugal polysaccharide, sclerogluean, on clay microstructures. *Soil Biology and Biochemistry*, 21: 299-305.

30. Chibber, R.K., Ghos, P. C., Satyahasrayana, K. V. S. 1961. Studies on the physical properties of some of the Himadral Pradesh soils formed on different materials in relation to their erodibility. *J. Indian Soc Soil Sci.* 9:187-192.
31. Churchman, G.J., and Tate, K.R. 1987. Stability of aggregates of different size grades in allophonic soils from volcanic ash in New Zealand. *J. Soil Sci.* 38: 19-27.
32. Corey, A.T. 1977. *Mechanics of Heterogeneous Fluids in Porous Media.* Water Resour. Publ. Fort Collins, Colorado.
33. Cruse, R.M., and Larson, W.E. 1977. Effects of soil shear strength on soil detachment due to raindrop impact. *Soil Sci. Soc. Am. J.* 41: 777-781.
34. De Ploey, J., and Poesen, J. 1985. Aggregate stability, runoff generation and interrill erosion. In: *Geomorphology and soils* (ed. K.S. Richards, R.R. Arnet and S. Ellis. Allen and Unwin. pp. 99-120.
35. De Vleeschauwer, D., Lal, R., and De Boodt, M. 1978. Comparison of detachability indices in relation to soil erodibility for some important Nigerian soils, *Pedologie* 28(1): 5-20
36. Ekern, P.C. 1950. Rainfall intensity as a measure of storm erosivity. *Soil Sci. Soc. Am. Proc.* 18: 212-216.
37. Ekwue, E.I. 1990. Effect of organic matter on splash detachment and the process involved. *Earth. Surf. Process and Landforms.* 15:175-181.
38. El-Swaify, S.A. 1980. Physical and mechanical properties of oxisols. In: B.K.G. Theng (editor), *soils with variable charge.* New Zealand Soc. Of Soil Sci. Offset Publication, Palmerston North, New Zealand. Pp. 303-324.

39. Ellison, W.D. 1944. Studies of Raindrop Erosion. *Agricultural Engineering*. 25: 131-136, 181-182.
40. Ellison, W.D. 1945. Some effects of raindrop and surface flow on soil erosion and infiltration. *Transaction of American Geophysical Union*. 24: 452-459.
41. Ellison, W.D. 1947. Soil erosion studies. Part II. *Agric Eng.* 197-201.
42. Ellison, W.D. 1947a. Soil erosion studies. II soil detachment hazard by raindrop splash. *Agric. Eng.* 28: 197-201.
43. Ellison, W.D. 1947b. Soil erosion. V. Soil transportation in the splash process. *Agric. Eng.* 28: 349-351.
44. Elwell, H. A. 1986. Determination of erodibility of subtropical clay soil: A laboratory rainfall simulation experiment. *J. Soil. Sci.* 37:345-350.
45. Emerson, W.W. 1967. A classification of soil aggregates based on their coherence in water. *Australian Journal of Soil Research*. 5: 47-57.
46. Emerson, W.W., and Greenland, D.J. 1990. Soil aggregates-formation and stability. In: *Soil colloids and their associations in aggregates* (eds. M. De Boodt, M. Hayes, and A. Herbillon), Plenum Press, New York pp. 485-511.
47. Emmett, W. W. 1970. The hydraulic of overland flow on hill slopes. *U.S. Geol. Surv. Prof paper* 662-A.
48. Farres, P.J. 1987. The dynamics of rain splash erosion and the role of soil aggregate stability. *Catena* 14,119-130
49. Flanagan, D.C., Foster, G.R., and Moldenhauer, W.C. 1988. Storm pattern effect on infiltration, runoff and erosion. *Trans. Am Soc. Agric. Eng.* 31: 337-350.

50. Foster, G.R., and Meyer, L.D. 1972. A closed-form soil erosion equation for upland areas. In. Sedimentation (H. W. Shen, ed), pp1-12, 19 Colorado State University, Fort Collins
51. Foster, G.R., and Meyer, L.D. 1975. Mathematical Simulation of upland erosion by fundamental erosion mechanics: In Present and Prospective Technology for predicting Sediment Yields and Sources. AR-S-40, USDA, Washington. Pp. 190-207.
52. Foster, G.R, Lane, L.T., Nowlin, J.D., Laflen, J.M., and Young, R.A. 1977. An erosion equation derived from basic erosion principles. Trans ASAE. 24: 1253-1262
53. Fournier, F. 1967. Research on soil erosion and soil conservation in Africa. African Soils. 12: 53-96.
54. Frenkel, H., Goertzen, J.O., and Rhoades, J.D. 1978. Effects of clay type and content, exchangeable sodium percentage and electrolyte concentration on clay dispersion and soil hydraulic conductivity. Soil Sci. Soc. Am. J. 42: 32-39.
55. Gal, M., Arcan, L., Shaiberg, I., and Kereen, R. 1984. The effect of exchangeable Na and phosphogypsum on the structure of soil crust-SEM observations. Soil Sci. Soc. Am. J. 48: 872-878.
56. Georgakakos, K.P., and Bras, R.L.1984. A hydrological useful station precipitation model, I, Formulation. Water Resources Res. 20:1585-1596.
57. Ghadiri, H., Payne, D. 1977. Raindrop impact stress and the breakdown of soil crumbs. Soil. Sci. 28:257-258

58. Gilley, J.E., and Finkner, S.C. 1985. Estimating soil detachment caused by raindrop impact. *Trans. ASAE*. 28:140-146.
59. Gimenez, D., Dirksen C., Eppink, L.A.A.J., and Schoonderbeck, D. 1992. Surface sealing and hydraulic conductance under varying-intensity rains. *Soil Sci. Soc. Am. J.* 56: 234-242.
60. Green, W.H., and Ampt, G.A. 1911. Studies on soil physics. I. Flow of air and water through soil. *J. Agric. Sci.* 4 {1-24.
61. Gunn, R., and Kinzer, G.D. 1949. Terminal velocity of water droplets in stagnant air. *Journal of meteorology.* 6: 243-248.
62. Hamblin, A.P., and Davies, D.B. 1977. Influence of organic constituents and complexed metal ions on aggregate stability of some East Anglian soils. *J. Soil Sci.* 28: 410-416.
63. Harris, R.F., Chesters, G., and Allen, O.N. 1966. Dynamics of soil aggregation. In N.C. Brady (Ed.), *Advance in Agronomy*. Academic Press, New York, NY. 18.pp. 107-169.
64. Haverkamp, R., Kutilek, M., Parlange, J.Y., Rendon, L., and Mrejca, M. 1988. Infiltration under ponded conditions: 2. Infiltration equations tested for parameter time-dependence and predictive use. *Soil Sci.* 145: 317-329.
65. Haynes, R.J., and Swift, R, S. 1990. Stability of soil aggregates in relation to organic constituents and soil water content. *J. Soil Sci.* 41:73-83.
66. Henin, S. 1938. *Etude physico-chimique dela stabilite structurale des terres*. These de Doctorat, Universite de Paris.

67. Hinkle, S.E., Heerman, D.F., and Blue, M.C. 1987. Falling water drops at 1570 m elevation. *Transaction of American Society of Agricultural Engineers*. 30 (1): 94-100.
68. Horton, R. E. 1940. An approach toward a physical interpretation of infiltration-capacity. *Soil Sci Soc. Am. Proc.* 5,399-417.
69. Hudson, N.W. 1964. Bearing and incidence of sub-tropical convective rainfall. *Quarterly Journal of the Royal Meteorological Society*. 90, 385,325-328.
70. Hudson, N.W. 1965. The influence of rainfall on the mechanics of soil erosion with particular reference to Southern Rhodesia. MSc. Thesis, University of Cape Town.
71. Hudson, N.W. 1971. *Soil Conservation*. B.T. Batsford. Limited London. 320 pp.
72. Hudson, N.W. 1981. Instrumentation for studies of the Erosive Power of Rainfall, pp.383-390, *IAHS Bull.* 133. IAHS. Washington. .
73. Hudson, N.W. 1995. *Soil Conservation*. Third Edition. B.T.Batsford Limited London.
74. Hutchinson, J., Manning, H.L., and Earbrother, H.G. 1958. On the characterization of tropical rainstorms in relation to runoff and percolation. *Quarterly. Journal of the Royal Meteorological Society*. 84: 250-258.
75. Inoue, S. 1985. Mechanism of soil erosion by raindrop impact. *International Symposium on Erosion, Debris Flow and Disaster Prevention*, Tsukuba, Japan. *Erosion Control Engineering Society*, pp 35-39.
76. Jha, M. N., and Rathore, R. K. 1981. Erodibility of soil in shifting cultivation ares of Tripura and Orissa. *Indian Forester* 107(5): 310-313.

77. Jouany, C., Chenu, C., and Chassin, P. 1992. Determination de la mouillabilite des constituents du sol a partir de mesures d'angles de contacts: revue bibliographique. *Science du sol*, 30, 33-47.
78. Kazman, Z., Shainberg, I., and Gal, M. 1983. Effect of low levels of exchangeable sodium and applied phosphogypsum on infiltration rate of various soils. *Soil Sci.* 135: 184-192.
79. Kemper, W.D., and Kock, E. 1966. Aggregate stability of soils from Western United States and Canada. U.S. Department of Agriculture Technical Bulletin, No 1355.
80. Kereen, R. 1990. Water-drop K.E. effect on infiltration in sodium –calcium-magnesium soils. *Soil Sci. Soc. Am. J.* 54: 983-987.
81. Kinnell, P.I.A. 1973. The problem of assessing the erosive power of rainfall from meteorological observations. *Soil Sci. Am. Proc.* 37: 617-621.
82. Kinnell, P.I.A. 1981. Rainfall intensity – kinetic energy relationships for soil loss prediction. *Soil Sci. Am. Proc.* 45: 153-155.
83. Kirkham, D., Powers, W. L. 1972. *Advanced Soil physics*, Wiley- Interscience, New York
84. Kohnke, H. 1968. *Soil Physics*. McGraw-Hill, Inc., New York
85. Kostiakov, A.N. 1932. On the dynamics of coefficient of water-percolation in soil and on the necessity of studying it from a dynamic point of view for purposes of amelioration. *Trans. Sixth comm. intl. Soc. Soil Sci*, part A: 17-21.
86. Kowal, J.M., Kijewski, w, and Kassam, A.H. 1973. A simple device for analyzing the energy loaded intensity of rainstorms. *Agricultural meteorology* 12: 271-280.

87. Kowal, J.M., and Kassam, A.H. 1976. Energy and instruments intensity of rainstorms at Samaru, Northern Nigeria. *Trop. Agric.* 53: 185-198.
88. Kowal, J.M., and Kassam, A.H. 1978. *Agricultural Ecology of Savanna: A study of West Africa*, Clarendon Press. Oxford, England.
89. Kutilek, M. 1984. Some theoretical and practical aspects of infiltration in clays (ILRI) Publication 37, Wageningen. p. 114-128.
90. Kutilek, M., Krejca, M., Haverkamp, R., Rendon, L.P., and Parlange, J.Y. 1988. An extrapolation of algebraic infiltration equation. *Soil Tech.* 1: 47-61.
91. Kunze, R.J., and Nielsen, D.R. 1982. Finite-difference solutions of the infiltration equation. *Soil Sci.* 134: 81-88.
92. Lal, R. 1973. Soil erosion and shifting agriculture FAO/SIDA Regional Seminar on shifting cultivation and soil conservation in Africa. Ibadan, Nigeria. July 2-21, 1972.
93. Lal, R. 1987. Soil degradation in relation to climate. Paper delivered at International symposium on climate and food security. 6-9. February 1987. New Delhi, India.
94. Laws, J.O. 1941. Measurement of fall velocity of water drops and raindrops. *Trans. Am. Geophys. Union* 22: 709-721.
95. Laws, J.O., and Parsons, D.A. 1943. The relationship of raindrop size to intensity. *Trans. Am. Geophys. Union.* 24: 452-460.
96. Levy, G.J., and Miller, W.P. 1997. Aggregate Stabilities of some Southeastern U.S. Soils. *Soil Sci. Soc. Am. J.* 61: 1176-1182.

97. Le Bissonnais, Y. 1996. Aggregate stability and assessment of soil crustability and erodibility: I. Theory and methodology. *European Journal and Soil Science*, 47,425-437.
98. Le Bissonnais, Y., and Singer, M.J. 1993. Seal formation, runoff and interrill erosion from seventeen Californian soils. *Soil Sci. Soc. AM. J.* 57: 224-229.
99. Loch, R. J., and Foley, J. L. 1994. Measurement of aggregate breakdown under rain: comparison with tests of water stability and relationships with field measurements of infiltration. *Australia Journal of Soil Research*. 32:701-720.
100. Lowrance, R., and Williams, R.G. 1988. Carbon movement in Runoff and Erosion under simulated Rainfall conditions. *Soil Sci. Soc. Am. J.* 52: 1445-1448.
101. Luk, S. -H., and Cai, Q.G. 1990. Laboratory Experiments on crust development and rain splash erosion of loess soils. *China. Catena*. 17: 261-276.
102. Luk, S.H., Dubbin, W.E., and Mermut, A.R. 1990. Fabric analysis of surface crust developed under simulated rainfall on loess soil. *China. Catena Suppl.* 17:29-40.
103. Lynch, J.M., and Bragg, E. 1985. Microorganisms and soil aggregate stability. *ADV. Soil Sci.* 2: 133-171.
104. McGhie, D.A., and Posner, A.M. 1980. Water repellence of a heavy- textured Western Australian surface soil. *Australian Journal of Soil Science*. 18: 309-323.
105. McIntyre, D.S. 1958. Soil splash and the formation of surface crust by raindrop impact. *Soil Sci.* 85: 261-266.
106. Meyer, L.D., and Wischmeier, W.H. 1969. Mathematical simulation of process of soil erosion by water. *Trans. ASAE*. 12: 754-758, 762.

107. Meyer, L.D., and Harmon, W.C. 1979. Multiple-intensity Simulator for erosion research on row side slopes. *Trans. ASAE*. 22: 100-103
108. Meyer, L.D., and Harmon, W.C. 1990. Inter-rill runoff and erosion: Effects of row side slope shape, rain energy, and rain intensity. *Trans. ASAE*. 35: 1199-1203.
109. Meyer, L.D. 1981. How rain intensity affect interrill erosion. *Trans. ASAE*. 24: 1472-1475.
110. Mezencev, V. J. 1948. Theory of formation of the surface runoff (in Russian). *Meteorologia I Hidrologia* 3:33-40
111. Mihara, Y. 1951. Raindrops and Soil Erosion. National Institute of Agricultural science, Tokyo, Japan, series A.
112. Miller, W. P., and Baharuddin, M. K. 1986. Relationship of soil dispersibility to infiltration and erosion of southeastern soil. *Soil. Sci.* 142:235-240.
113. Miller, W.P. 1987. Infiltration and soil loss of three gypsum-amended Ultisols under simulated rainfall. *Soil Sci. Soc. Am. J.* 51: 1314-1320.
114. Moldenhauer, W.C., and Kemper, W.D. 1969. Interdependence of water drop energy on clod size on infiltration and clod stability. *Soil Sci. Soc. Am. Proc.* 33: 297-301.
115. Monnier, G. 1965. Action des matieres organiques sur la universite de Paris. VII.
116. Morgan, R.P.C. 1977. Soil Erosion in United Kingdom field studies in Silsoe area 1973-75, National College of Agricultural Engineering. Occasional paper 4.
117. Morin, J., and Benyamini, Y. 1977. Rainfall infiltration into bare soils.

Water Resource Res 13: 813-817

118. Moss, A.J., and Walker, P.H. 1978. Particle transport by continual water flows in relation to erosion deposition, soils and human activities. *Sediment. Geol.* 20: 81-139.
119. Moss, A.J., Mutchler, C.K., and Morin, J., and Benyamini, Y. 1977. Rainfall infiltration into bare soils. *Water. Resource. Res.* 13: 813-817.
120. Moss, A.J., Walker, P.H., and Hutka, J. 1979. Simulated transportation in shallow water flows: an experimental study. *Sediment. Geol.* 22: 165-184.
121. Moss, A.J., and Green, P. 1983. Movement of solids in air and water by raindrop impact. Effects of drop-size and water depth variations. *Aust J. Soil. Res.* 21: 257-269.1
122. Moss, A.J. 1988. Effects of flow-velocity variation on rain-driven transportation and the role of rain impact in the movement of soil. *Aust. J. Soil. Res.* 26: 443-450.
123. Mutchler, C.K., and Hermsmeier, L.F. 1965. A review of rainfall simulators. *Transactions American Society of Agricultural Engineers.* 8: 63-65.
124. Mutchler, C.K., and Young, R, A. 1975. Soil Detachment by raindrops. U.S. Dept. Agric, Agric. Res. Serv (ARS-S-40).
125. Nearing, M.A., and Bradford, J.M. 1985. Single water drop splash detachment and mechanical properties of soils. *Soil Sci. Soc. Am. J.* 49: 547-552.
126. Nearing, M.A., and Bradford, J.M. 1987. Relationship between water drop properties and forces of impact. *Soil Sci. Am. J.* 51: 425-430.
127. Nearing, M.A., and Bradford, J.M., and Holtz, R.D. 1987. Measurement of

- water drops impact pressure on soil surfaces. *Soil Sci. Soc. Am. J.* 51: 1302-1306.
128. Nerpin, S. V. 1970. *Physics of the Soil*. Translated from Russian by IPST Staff. Israel Program for Scientific Translation, Jerusalem pp 157.
129. Nichols, M.L., and Saxton, H.D. 1932. A method of studying soil erosion. *Agric. Eng.* 13: 101-103.
130. Nielsen, D.R., Kirkham, D., and Van Wijk, W.R. 1961. Diffusion equation calculations of field soil water infiltration profiles. *Soil Sci. Soc. Am. J.* 25:165-168.
131. NSESPRPC (National Soil Erosion- Soil Productivity Research Planning Committee). 1981. Soil erosion effect on soil productivity. A research perspective. *Journal of soil and water conservation* 36 (2): 82-90.
132. Oades, J.M. 1984. Soil organic matter and structural stability mechanisms and implications for management. *Plant Soil.* 76,319-337.
133. Oduro-Afriyie, K. 1977. Analyses of the time series of soil temperature recorded at different depths at three locations in Ghana. MSc. Thesis. Dept of Physics. University of Cape Coast, Ghana.
134. Olson, O.C., and Wischmeier, W.H. 1963. Soil erodibility evaluations for soils on the runoff and erosion stations. *Soil Sci. Soc. Am. Proc.* 27: 590-592.
135. Olson, K.R., Lal, R., and Norton L.D. 1994. Evaluation of methods to study soil erosion – productivity relationship. *J. Soil and Water Conservation* 49 (6) 586-590.

136. Onofio, K.O., and Singer, M.J. 1984. Scanning electron microscope studies of surface crusts formed by simulated rainfall. *Soil Sci. Am. J.* 48: 1137-1143.
137. Palmer, R.S. 1963. The influence of a thin water layer on water drop impact forces. Pp. 141-148, IAHS, Publication No. 65, Washington.
138. Park, S.W., Mitchell, J.K., and Bubenzer, G.D. 1982. Splash erosion modeling: Physical analyses. *Trans. ASAE.* 25: 357-361.
139. Park, S.W., Mitchell, J.K., and Bubenzer, G.D. 1983. Rainfall characteristic and their relation to splash erosion. *Trans. ASAE* 26:795-804.
140. Paulimo, L.A. 1986. Food in the Third world. IFPRI. Res. Ppt52. Washington.
141. Philip, J.R. 1955. Numerical solution of equations of the diffusion type with diffusivity concentration-dependent. *Trans. Faraday Soc.* 51: 885-892
142. Philip, J.R. 1957. Theory of infiltration: 4 Sorptivity and algebraic infiltration equation. *Soil Sci.* 84: 257-264
143. Philip, J.R. 1960. General method of exact solution of the concentration-dependent diffusion equation. *Aust. J. Phys.* 13: 1-12.
144. Philip, J.R. 1969. Hydrostatics and hydrodynamics in swelling soil. *Water. Resource. Res.* 5: 1070-1077.
145. Philip, J. R. 1973. On solving the unsaturated flow equation: I. The flux concentration relation. *Soil Sci* 116: 328-335
146. Poesen, J. 1981. Rain wash experiments on the erodibility of loose sediments. *Earth Surface Processes Landforms* 6: 285-307.

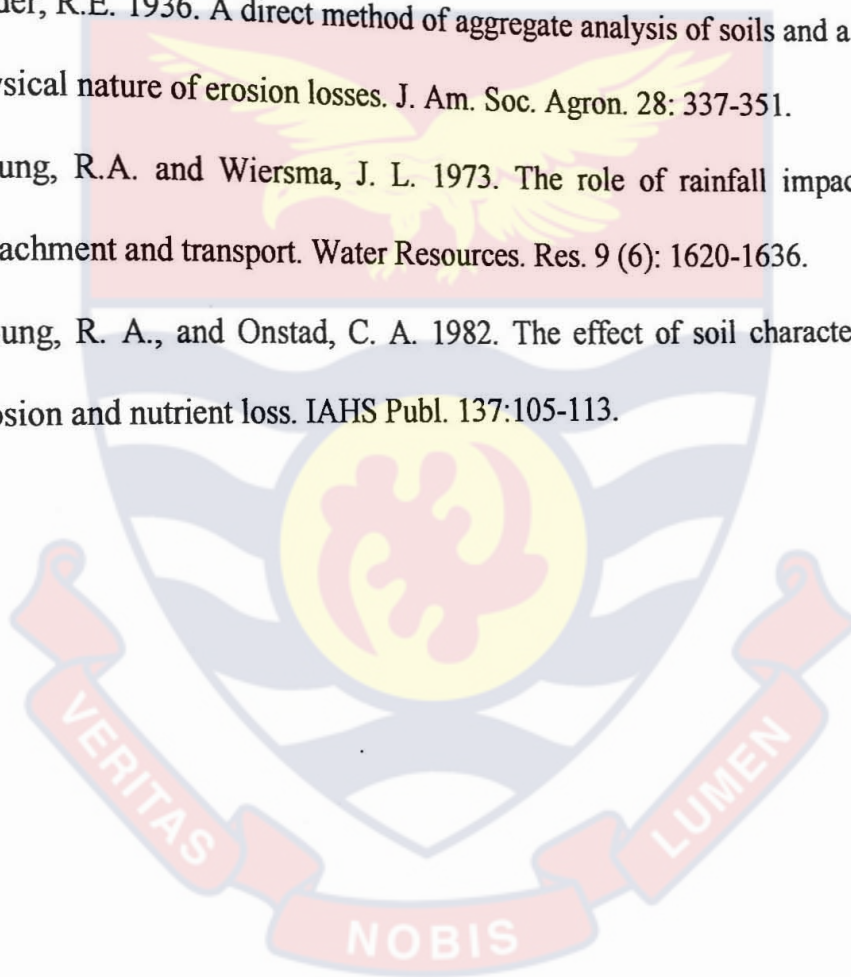
147. Poesen, J., and Savat, J. 1981. Detachment and transportation of loose sediments by raindrop splash .II. Detachability and transportability measurements. *Catena* 8: 19-41.
148. Quansah, C. 1981. The effect of soil type, slope, rain intensity and their interactions of splash detachment and transport. *J. Soil Sci.* 32: 215-224.
149. Quirk, J.P., and Panabpkke, C.R. 1962. Pore volume-size distribution and swelling of natural soil aggregates. *J. Soil Sci.* 13: 71-81.
150. Rawls, W.J., Brakensiek, R.L., and Saxton, K.E. 1982. Estimation of soil water properties. *Trans. Am. Soc. Agric. Engrs.* 25: 1316-1320.
151. Remley, P.A., and Bradford, J. M. 1989. Relationship of soil crust morphology inter-rill erosion parameters. *Soil Sci. Soc. Am. J.* 53: 1215-1221.
152. Richardson, E.G. 1950. *Dynamics of Real Fluids*. Edward Arnold, Lt. London.
153. Riezebos, H.T., and Epema, G.F. 1985. Drop shape and erosivity, II, splash detachment and erosivity indices. *Earth surf Processes Landforms.* 10:69-74.
154. Roels, J.M. 1981. Cited by J.M.Eigel and I.D. Moore (1983), p.1079.
155. Romken, M.J.M., Roth, C.B., and Neilson, D.W. 1977. Erodibility of selected clay subsoil in relation to physical and chemical properties. *Soil Sci. Soc. Am.* 41: 954-960.
156. Romken, M.J.M., Prasad, S.N., and Parlange, J.Y. 1991. Surface seal development in relation to rainstorm intensity. *Catena Suppl.* 17: 1-11.
157. Roose, E.J. 1977. Application of Universal Soil Loss Equation of Wischmeier and Smith in West Africa. In: *Conservation and soil Management in the*

- Humid Tropics (D.J.Greenland and R. Lal, eds.), pp.177-187, Wiley, Chichester, U.K.
- 158.Rose, C.W. 1960. Soil detachment caused by rainfall. *Soil Sci.* 89: 28-35.
- 159.Roth, C.H., Helming, K. 1992. Surface properties, runoff formation and sediment concentration as related to rainfall characteristics and presence of already formed crust. *Soil Technology.* 5: 359-368.
- 160.Rubin, J. 1967. Numerical method of analyzing hysteresis-affected, post-infiltration redistribution of soil moisture. *Soil Sci. Soc. Am, Proc.* 31: 13-20.
- 161.Sahi, B. P., Pandey, R. S., and Singh, S. N. 1976. Studies on water stable aggregates in relation to physical constants and erosion indices of alluvial and sedentary soils of Bihar. *J. Indian Soc Soil Sci.* 24(2): 123-128.
- 162.Sahi, B. P., Singh, S. N., Sinha, A. C., and Acharya, B. 1977. Erosion index- A new index of soil erodibility. *J. Indian Soc Soil Sci.* 25(1): 7-10.
- 163.Scheidegger, A.E. 1957. *The Physics of flow through porous Media.* Second edition, 1960. Univ. Toronto Press. Toronto.
- 164.SCSA. 1982. *Resource Conservation Glossary*, Soil Conservation Society of America, Ankeny Iowa.
- 165.SCSA. 1996. *Glossary of Soil Science Terms.* Soil Science Society of America.
- 166.Shainberg, I., Levy, G.J., Rengasamy, P., and Frenkel, H. 1992. Aggregate stability and seal formation as affected by drops impact energy and soil amendments. *Soil Sci.* 154: 113-119.
- 167.Shainberg, I., Levy, G.J., Goldstein, D. 1997. Aggregate size and seal properties. *Soil Sci.* 16 2: 470-478.

168. Stein, R., Ben-Hur, M., and Shainberg, I. 1991. Clay mineralogy effect on rain infiltration, seal formation and soil losses. *Soil Sci.* 152: 4556-462.
169. Sullivan, L.A. 1990. Soil organic matter, air encapsulation and water-stable aggregation. *Journal of soil science*, 41: 529-534.
170. Swartzenduber, D. 1987. A quasi-solution of Richard's equation for the downward infiltration of water into soil. *Water Resour. Res.* 23: 809-817.
171. Tamhane, R.V., Biswas, T.D., and Das, B. 1959. Effects of intensity of rainfall on soil loss. *J. India. Soc. Soil Sci.* 7: 231-235.
172. Thompson, A.L., Gautzer, C.J., and Anderson, S.H. 1991. Topsoil depth, fertility, water management and weather influence on yield. *Soil Sci, Soc. Am J.* 5: 1085-1091.
173. Tisdall, J.M., and Oades, J.M. 1982. Organic matter and water-stable aggregates in soils. *Journal of Soil Science.* 33: 141-163.
174. Trott, K.E., and Singer, M.J. 1983. Relative erodibility of 20 California range and forest soils. *Soil Sci, Soc. Am J.* 47:753-759.
175. Truman, C.C., Bradford, J.M., and Ferris, J.E. 1990. Antecedent water content and rainfall-energy influence on soil aggregate breakdown. *Soil Sci. Soc. Am. J.* 54: 1385-1390.
176. Vaneland, A., Rousseau, P., Lal, R., Gabriels, D., and Ghuman, B.S. 1984. Testing the applicability of a soil erodibility Monogram for some Tropical soils. IAHS. Publication 144, Washington, pp.463-473.

177. Van Oost, A., Lal, R., and Gabriels, D. 1985. Erodibility of some Nigerian soils. Proc. Int. Symp on Erosion Debris, Flow and Disaster Prevention. Tsukuba, Japan. Erosion control Engineering Society, pp. 51-56.
178. Van Vliet, L.J.P., Wall, G.J., and Dickson, W.T. 1976. Effect of agricultural land use on potential sheet erosion losses in Southern Ontario. Canadian Journal of Soil Science 56: 443-751.
179. Walkely, A. and Black, I.A. 1934. An examination of Degtjareff method for determining soil organic matter and a proposed modification of the chromic and acid titration method. Soil Sci. 37:29-38
180. Wang, P.K., Pruppacher, H.R. 1977. Acceleration to terminal velocity of cloud and raindrops. J. Appl. Met. 16: 275-280.
181. Wilkinson, G.E. 1975. Rainfall characteristics and soil erosion in the forest area of Western Nigeria. Exp. Agric. 11: 247-255.
182. Wischmeier, W.H., and Mannering, L.V. 1969. Relation of soil properties to its erodibility. Soil Sci. Soc. Am. J. Proceedings 33: 131-137.
183. Wischmeier, W.H., and Smith, D.D. 1958. Rainfall energy and its relationship to soil loss. Trans. Am. Geophys. Union. 39: 285-291.
184. Wischmeier, W.H., Johnson, C. B., and Cross, B.V. 1971 Soil erodibility monograph for farmland and construction sites. Journal of soil and Water Conservation 20:150-152.

185. Wischmeier, W.H. 1976. Use and misuse of Universal soil loss equation. *J. Soil Water Conserv.* 31: 5-9.
186. Woodburn, R., and Kozachyn, J. 1956. A study of relative erodibility of a group of Mississippi gully soils. *Trans. Am. Geophys. Union* 37:749-753.
187. Yariv, S. 1976. Comments on the mechanism of soil detachment by rainfall. *Geoderma.* 15: 393-399.
188. Yoder, R.E. 1936. A direct method of aggregate analysis of soils and a study of physical nature of erosion losses. *J. Am. Soc. Agron.* 28: 337-351.
189. Young, R.A. and Wiersma, J. L. 1973. The role of rainfall impact in soil detachment and transport. *Water Resources. Res.* 9 (6): 1620-1636.
190. Young, R. A., and Onstad, C. A. 1982. The effect of soil characteristics on erosion and nutrient loss. *IAHS Publ.* 137:105-113.



APPENDIX A
Computer program

APPENDICES

SOLUTION OF DIFFERENTIAL EQUATION USING RUNGE-KUTA A METHOD

DEFINE THE FUNCTION

REAL J, N, M, P, K1, K2, K3, K4, K5

$F(V) = G - Q * (V^{**2})$

G = 9.8

Q = ?

PRINT* 'ENTER H'

READ*, H

PRINT* 'SOLN TO DIFF. EQN.'

PRINT*, TIME', ' ', 'VELOCITY'

PRINT*, '(SEC)', ' ', '(M/SEC)'

V = 0.0

T = 0.0

a. IF (T.LE.5.0) THEN

P = V

K1 = H*F (P)

J = V+K1/2.0

$$N = V + K2 / 2.0$$

$$K3 = H * F (N)$$

$$M = V + K3$$

$$K4 = H * F (M)$$

$$K5 = (K1 + 2 * K2 + 2 * K3 + K4) / 6.0$$

$$V = V + K5$$

PRINT *, T, V

$$T = T + 1.0$$

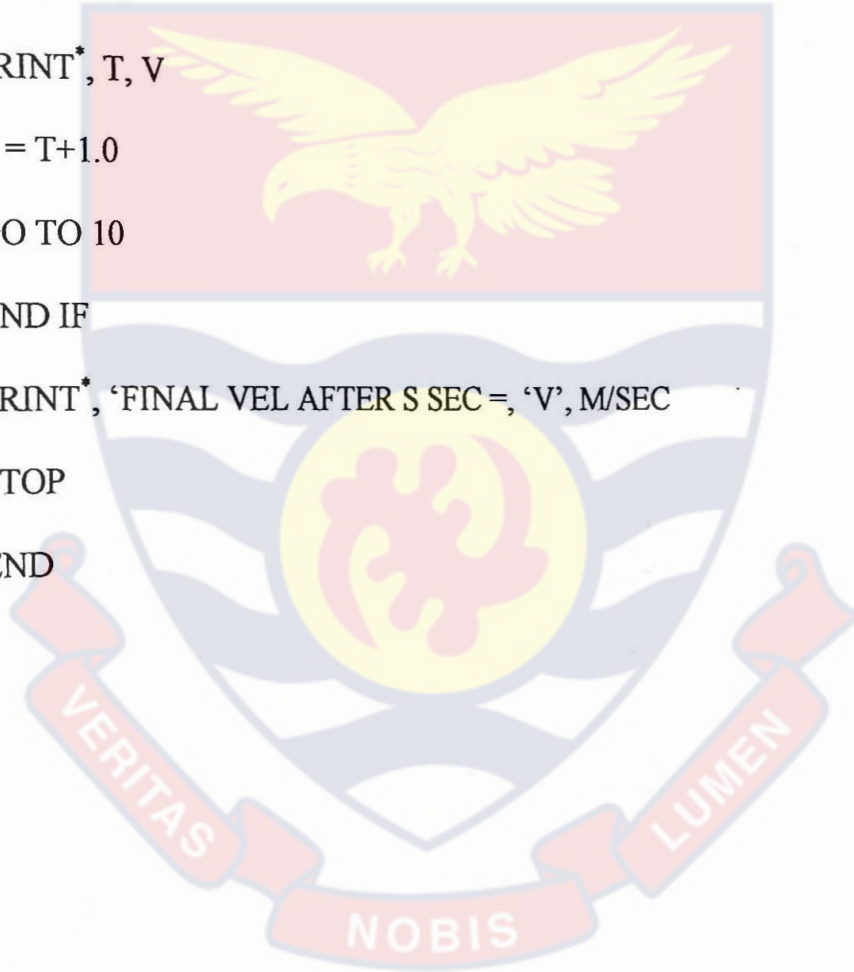
GO TO 10

END IF

PRINT *, 'FINAL VEL AFTER S SEC =', 'V', M/SEC

STOP

END



APPENDIX B

Table1: Intensity and soil splashed per minute

| Intensity | Sample | Soil used in experiment | | Soil splashed during Experiment | |
|--------------------------------------|--------|-------------------------|--------|---------------------------------|-------|
| | | m_o | m_o' | m | m' |
| 73.39 mm/h Duration 2 minutes | T | 155.25 | 130.57 | 19.13 | 16.09 |
| | TT | 169.47 | 146.73 | 25.03 | 21.67 |
| | AK | 163.17 | 147.93 | 32.41 | 29.38 |
| | W | 147.79 | 129.07 | 21.05 | 18.38 |
| 93.67 mm/h Duration 2 minutes | T | 139.16 | 117.04 | 21.11 | 17.75 |
| | TT | 172.85 | 149.65 | 25.06 | 21.70 |
| | AK | 166.35 | 150.82 | 33.94 | 30.77 |
| | W | 152.94 | 133.57 | 21.55 | 18.82 |
| 132.78 mm/h Duration 2 minutes | T | 161.74 | 136.03 | 22.91 | 19.27 |
| | TT | 166.40 | 144.07 | 29.98 | 25.96 |
| | AK | 170.79 | 154.84 | 33.09 | 29.99 |
| | W | 180.37 | 157.53 | 25.57 | 22.33 |
| 182.32 mm/h Duration 2 minutes | T | 169.02 | 142.15 | 24.86 | 20.91 |
| | TT | 172.73 | 149.55 | 28.81 | 24.94 |
| | AK | 170.94 | 154.98 | 34.02 | 30.84 |
| | W | 169.51 | 148.04 | 24.60 | 21.48 |
| 78.11 mm/h Duration 2 minutes | PA | 173.06 | 151.41 | 35.46 | 31.02 |
| | PO | 124.06 | 117.04 | 18.82 | 17.75 |
| | CA | 152.44 | 138.71 | 25.75 | 23.43 |
| | | | | | |

| | | | | | |
|--------------------------------------|--------------------------------------|--------|--------|--------|-------|
| 124.05 mm/h Duration 2 minutes | VE | 206.40 | 180.42 | 29.55 | 25.83 |
| | PA | 179.73 | | | |
| | PO | 140.04 | 157.24 | | |
| | CA | 167.44 | 132.11 | 39.89 | 34.90 |
| | VE | 137.49 | 152.36 | 21.67 | 20.44 |
| 139.43 mm/h Duration 2 minutes | | | 120.18 | 32.03 | 28.00 |
| | PA | 182.81 | | | |
| | PO | 130.84 | 159.94 | 41.38 | 36.20 |
| | CA | 160.61 | 123.43 | 23.17 | 21.86 |
| | VE | 194.15 | 146.14 | 29.98 | 27.28 |
| 160.52 mm/h Duration 2 minutes | | | 169.71 | 36.67 | 32.05 |
| | PA | 168.36 | 147.30 | 44.59 | 39.01 |
| | PO | 137.06 | 129.30 | 24.12 | 22.75 |
| | CA | 167.45 | 152.37 | 37.47 | 34.09 |
| | VE | 184.42 | 161.21 | 43.29 | 37.84 |
| 65.07 mm/h Duration 2 minutes | G1 | 150.22 | 129.39 | 28.43 | 24.49 |
| | G2 | 194.83 | 170.90 | 21.15 | 18.55 |
| | G3 | 170.40 | 147.28 | 24.36 | 21.05 |
| | G4 | 119.78 | 104.43 | 20.20 | 17.61 |
| | 100.10 mm/h Duration 2 minutes | G1 | 163.79 | 141.08 | 29.46 |
| G2 | | 175.07 | 153.57 | 23.04 | 20.21 |
| G3 | | 144.65 | 125.02 | 26.55 | 22.95 |
| G4 | | 90.32 | 78.74 | 25.12 | 21.90 |
| 130.38 mm/h Duration 2 minutes | | G1 | 164.41 | 141.61 | 29.64 |
| | G2 | 182.88 | 160.42 | 30.77 | 26.99 |
| | G3 | 179.81 | 155.41 | 29.49 | 25.49 |
| | G4 | 137.85 | 120.48 | 32.112 | 28.00 |
| | 161.77 mm/h Duration 2minutes | G1 | 178.97 | 154.15 | 30.88 |
| G2 | | 219.10 | 192.19 | 35.49 | 31.13 |
| G3 | | 158.26 | 136.78 | 27.55 | 23.81 |
| G4 | | 143.81 | 125.38 | 33.10 | 28.86 |

m_o = weight of soil used

m_o' = weight of soil used after correction for water content University of Cape Coast <https://ir.ucc.edu.gh/xmlui>

m = weight of soil splashed

m' = weight of soil splashed after correction for water content

APPENDIX C

Table 2: Soil Textural Classification

| Sample | 40 sec | | 5 hours | | % Sand | % Silt | % Clay |
|---------|------------|---------|------------|---------|--------|--------|--------|
| | Hydrometer | | Hydrometer | | | | |
| | Reading | Temp | Reading | Temp | | | |
| TT | 14 | 27.3 °C | 13 | 27.3 °C | 69.4 | 2.0 | 28.6 |
| W | 22 | 26.3 °C | 17 | 27.2 °C | 53.4 | 10.0 | 36.6 |
| T | 31 | 27.3 °C | 25 | 27.2 °C | 35.4 | 12.0 | 52.6 |
| AK | 12 | 27.3 °C | 6 | 27.3 °C | 73.4 | 12.0 | 14.6 |
| PA | 6 | 26.3 °C | 2 | 27.3 °C | 85.4 | 8.0 | 6.6 |
| PO | 22 | 27.3 °C | 11 | 27.2 °C | 53.4 | 22.0 | 24.6 |
| CA | 16 | 26.3 °C | 8 | 27.2 °C | 65.4 | 16.0 | 18.6 |
| VE | 11 | 26.3 °C | 7 | 27.1 °C | 75.4 | 8.0 | 16.6 |
| G1 | 18 | 27.2 °C | 9 | 27.3 °C | 61.4 | 18.0 | 20.6 |
| G2 | 24 | 26.4 °C | 15 | 27.1 °C | 49.4 | 18.0 | 32.6 |
| G3 | 19 | 27.2 °C | 10 | 27.3 °C | 59.4 | 18.0 | 22.6 |
| G4 | 14 | 26.3 °C | 6 | 27.1 °C | 69.4 | 16.0 | 14.6 |
| Blank 1 | -1 | | | | | | |
| Blank 2 | -1 | | | | | | |

APPENDIX D**Table 3: Aggregate Stability**

| Sample | Mass before dispersion (g) | Mass after dispersion (g) | Aggregate stability % |
|--------|----------------------------|---------------------------|--------------------------|
| TT | 9.7140 | 6.3192 | 65.1 |
| W | 9.7170 | 6.8893 | 70.9 |
| T | 9.7507 | 8.1515 | 83.9 |
| AK | 9.8500 | 4.7651 | 48.4 |
| PA | 9.9106 | 3.4611 | 34.9 |
| PO | 9.9360 | 6.2946 | 63.4 |
| CA | 9.7751 | 5.6377 | 57.7 |
| VE | 9.6866 | 5.1819 | 53.4 |
| G1 | 9.9352 | 5.8018 | 58.4 |
| G2 | 9.8976 | 6.9681 | 70.4 |
| G3 | 9.7798 | 5.7933 | 59.2 |
| G4 | 9.9088 | 4.5207 | 45.6 |

APPENDIX E**Table 4: Mechanical ratio and Water content of Samples**

| Sample | Mechanical ratio (%) | Water content (%) |
|--------|----------------------|-------------------|
| T | 53.50 | 15.90 |
| TT | 84.00 | 13.41 |
| AK | 70.00 | 9.36 |
| W | 71.00 | 12.69 |
| PA | 58.40 | 12.52 |
| PO | 48.40 | 5.63 |
| CA | 63.40 | 9.08 |
| VE | 34.90 | 12.60 |
| G1 | 57.70 | 13.90 |
| G2 | 65.00 | 12.27 |
| G3 | 59.20 | 13.54 |
| G4 | 45.20 | 12.79 |

Mechanical ratio = (Sand + Silt) / Clay

APPENDIX F

Table 5: Flour Pellet experiment

| Diameter of Water drop (mm) | Mass of water drop (mg) | Mass of flour Pellet (mg) | Mass ratio Water / Pellet |
|--------------------------------|----------------------------|------------------------------|------------------------------|
| 0.30 | 0.014 | 0.105 | 0.133 |
| 0.54 | 0.082 | 0.220 | 0.373 |
| 0.65 | 0.148 | 0.304 | 0.487 |
| 0.69 | 0.172 | 0.307 | 0.560 |
| 0.87 | 0.345 | 0.487 | 0.708 |
| 1.53 | 1.875 | 2.018 | 0.929 |
| 2.23 | 5.807 | 5.390 | 1.077 |
| 2.50 | 8.181 | 7.422 | 1.102 |
| 2.63 | 9.525 | 8.574 | 1.111 |
| 2.86 | 12.249 | 10.908 | 1.123 |
| 3.42 | 20.945 | 17.357 | 1.141 |
| 4.03 | 34.270 | 29.777 | 1.151 |

APPENDIX G

Table 6: Weight of soil used, soil splashed and their Splashability indices (k)

| Sample | Soil used (m_o') / g | Soil splashed (m') g/min | Splashability index (k) |
|--------|--------------------------|------------------------------|-------------------------|
| T | 130.57 | 16.09 | 0.06577 |
| | 117.04 | 17.75 | 0.08220 |
| | 136.03 | 19.27 | 0.07639 |
| | 142.15 | 20.91 | 0.07957 |
| TT | 146.73 | 21.67 | 0.079915 |
| | 149.65 | 21.70 | 0.07834 |
| | 149.55 | 24.94 | 0.091237 |
| | 144.07 | 25.96 | 0.099359 |
| AK | 147.93 | 29.38 | 0.110722 |
| | 154.84 | 29.99 | 0.107659 |
| | 150.82 | 30.77 | 0.1141099 |
| | 154.98 | 30.84 | 0.1109228 |
| W | 129.07 | 18.38 | 0.076825 |
| | 133.57 | 18.82 | 0.075949 |
| | 148.04 | 21.48 | 0.078397 |
| | 157.53 | 22.33 | 0.076444 |
| | 151.41 | 31.02 | 0.114648 |
| PA | 157.24 | 34.90 | 0.125507 |
| | 159.94 | 36.20 | 0.128331 |

| | | | |
|----|--------|-------|-----------|
| | 147.30 | 39.01 | 0.3077139 |
| PO | 117.04 | 17.75 | 0.082250 |
| | 132.11 | 20.44 | 0.0840586 |
| | 123.43 | 21.86 | 0.0974801 |
| | 129.30 | 22.75 | 0.096779 |
| CA | 138.71 | 23.43 | 0.092527 |
| | 152.36 | 26.00 | 0.093572 |
| | 146.14 | 27.28 | 0.103380 |
| | 152.37 | 34.09 | 0.126651 |
| VE | 180.42 | 25.83 | 0.0772694 |
| | 120.18 | 28.00 | 0.1326476 |
| | 169.71 | 32.05 | 0.1046710 |
| | 161.21 | 37.84 | 0.1337840 |
| G1 | 129.39 | 24.49 | 0.1058851 |
| | 141.08 | 25.37 | 0.0991379 |
| | 141.61 | 25.53 | 0.0994165 |
| | 154.15 | 26.60 | 0.0947260 |
| G2 | 170.90 | 18.55 | 0.0574594 |
| | 153.57 | 20.21 | 0.0705648 |
| | 160.42 | 26.99 | 0.0921256 |
| | 192.19 | 31.13 | 0.088405 |
| G3 | 147.28 | 21.05 | 0.0771288 |
| | 125.02 | 22.95 | 0.1014257 |

| | | | |
|----|--------|-------|-----------|
| | 155.41 | 25.49 | 0.089590 |
| | 136.78 | 25.75 | 0.1041958 |
| G4 | 104.43 | 17.61 | 0.0923866 |
| | 78.74 | 21.90 | 0.126597 |
| | 120.18 | 28.00 | 0.1326476 |
| | 125.38 | 28.86 | 0.130820 |

$$\frac{dm}{dt} = k(m'_o - m)$$

$$\int \frac{dm}{m'_o - m'} = \int k dt$$

where

$$\frac{dm}{dt} = \text{Rate of splashability}$$

m'_o = weight of soil used after correction for water content

m' = weight of soil splashed after correction for water content

k = Splashability index

